CHAPTER 4: VECTOR CONSTRUCTION AND DEVELOPMENT OF TRANSGENIC PLANTS

4.1 Introduction

Precise control of transgene expression and gene silencing in plants is a desired goal of the plant science research community. Constitutive overexpression of transgenes has been the method used to study the effects of various genes in plants for approximately 20 years. Promoters such as the CaMV35S, rice actin 1 and maize ubiquitin promoters are commonly used across most plant species to drive expression of transgenes. While these promoters are described as strong, constitutive promoters which provide high levels of transgene expression in all cell-types and growth stages of the plant, there is evidence that this may not be entirely accurate. There appears to be some variation in expression patterns of these promoters based on the plant species, cell/tissue/organ type and the growth stage of the plant. For example Battraw and Hall (1990) report transgene expression using the CaMV35S promoter in rice is primarily localised to the vascular tissues.

Another potential problem with the classic constitutive overexpression model for transgenic plant production is that this type of expression can lead to false assumptions about the function of a particular transgene. Constitutive overexpression of a transgene is unlikely to mirror the spatial and temporal expression pattern of the native gene. Thus, to determine the function of a particular gene it may be necessary to have control over the expression of the gene in space and time. Additionally, constitutive expression may not provide maximum benefit to the transport process being studied. For instance, expressing a transporter which is responsible for influx of a particular nutrient into a cell in the epidermal cells of the root tissue may improve uptake of the nutrient by the plant roots. However, if the transporter is also expressed in the stelar cells of the root it may actually prevent the transport of the nutrient to the xylem stream, thus working against the increased influx gained from expressing the gene in the epidermal cells. Tissue specific promoters have been used to provide cell-type specific control of transgene expression, but there are a limited number of tissue

specific promoters available and they often only function correctly within their species-of-origin due to complex upstream regulatory cascades.

A similar story exists for gene expression over time. Expressing a particular transporter at all growth stages could be wasteful of a plant's energy resources. For instance, if a transporter is expressed constitutively within a plant, the plant will be forced to produce the transgenic protein over its entire life span regardless of whether the protein is actually required by the environmental conditions it is facing. Expression of the same transgene at particular points-in-time when beneficial to the plant's growth would be a better choice from an energy standpoint. Several stress-inducible promoters have been identified to provide temporal control over transgene expression, but these are limited in number and their function is unknown in other plant species. Chemical-inducible gene expression systems are routinely used to explore the effect that induction of gene expression at specific points in the life cycle will have on plant function or development. Several studies have combined chemical-inducible systems with tissue specific promoters to control gene expression both spatially and temporally, but the general applicability is limited by the availability of suitable tissue specific promoters (e.g. Maizel and Weigel 2004).

The GAL4-GFP enhancer trapping resources in *Arabidopsis* and rice provide the tools to drive transactivation of a transgene in a diverse array of cell-type specific patterns where a suitable line is available. This allows transgene expression in many specific patterns for tissue-specific promoters are not available. The GAL4 lines may also be screened by applying stress to the individual lines and examining the plants for changes in GFP fluorescence, thereby identifying stress-responsive enhancer elements. These elements would enable transactivation of genes in a stress-responsive and (potentially) cell-type specific manner.

Subsequent to the start of this project, the GAL4-GFP system was combined with the 'Ethanol Switch' to provide both spatial and temporal control over gene expression. The trapped enhancer element drives expression of GAL4 which binds to the GAL4-UAS. This drives expression of the first component of the ethanol switch, the transcription factor 'AlcR', which undergoes a conformational change when exposed to ethanol and binds to the promoter 'alcA' and drives expression of the

transgene which is fused to it. Thus, expression of the transgene is spatially controlled by the trapped enhancer element and temporally controlled by the induction via ethanol. This system was used successfully to control gene expression in space and time in *Arabidopsis* (Sakvarelidze *et al.* 2007, Jia *et al.* 2007). The 'Ethanol Switch' was chosen because ethanol is relatively innocuous compared to other chemical-inducers, like the dexamethasone, which has been shown to produce growth defects (Amirsadeghi *et al.* 2007). Also, most of the hormone driven gene induction systems incorporate a section of GAL4, thus it is likely that these systems would be 'short-circuited' by GAL4 expressed in the GAL4-GFP enhancer trap lines.

In this study, vectors were built to combine the GAL4-GFP and 'Ethanol Switch' systems to regulate gene expression in rice GAL4 enhancer trap lines (Figure 4.1). Vectors were constructed to overexpress transgenes in specific cell-types, silence native genes in specific cell types, induce transgene expression constitutively and induce transgene expression in specific cell types with ethanol application. Several of these vectors were transformed into rice and *Arabidopsis* to study the function of AtHKT1;1, a Na^+ transporter from *Arabidopsis*, and PpENA1, a Na^+-ATPase from the moss *Physcomitrella patens*.

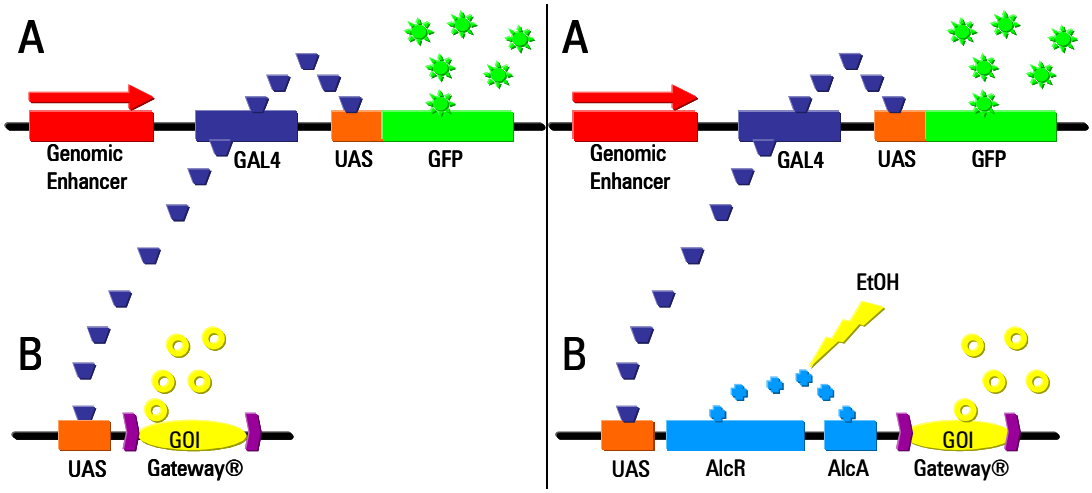

Figure 4.1: Diagrammatic representation of GAL4 transactivation of a gene of interest (GOI) (left) and GAL4 transactivation combined with the ethanol switch (right). Both vector systems have appropriate selectable markers for use in the rice and *Arabidopsis* GAL4-GFP enhancer trap lines. GAL4-GFP enhancer trap (A) contains *gal4* gene (GAL4); five tandem repeats of the upstream activation sequence element GAL4 binding site (UAS); and green fluorescent protein (GFP). Transactivation construct (B, left) contains UAS and Gateway® recombination cassette. UAS::ethanol switch construct (B, right) contains UAS; ethanol switch [comprised of AlcR transcription factor (AlcR) and alcA promoter (AlcA)]; and Gateway® recombination cassette and is induced by ethanol (EtOH).

4.2 Materials and Methods

4.2.1 General materials and methods for vector construction

4.2.1.1 PCR conditions

Unless stated otherwise PCR were performed in 25 µl reaction volumes using 100 ng of plasmid DNA as template. Elongase enzyme mix and 2.5 µl of Buffer A and of B (Invitrogen) were used with 200 µM of each dNTP and 400 nM of primers (all primers listed in Appendix I). A pre-amplification step of 94ºC for 30s was conducted prior to 35 cycles of 94ºC for 30 sec, 55-65ºC for 30 sec (dependant on primer T_m), 68ºC for 15 sec-5 min (dependant on length of expected product).

4.2.1.2 Restriction digests

Restriction digests were conducted in 20 µl reaction volumes containing 1X reaction buffer (supplied), 1-3 µg of DNA and 1-10 Units of restriction enzyme. Reactions were routinely left overnight at the enzymes optimal temperature (generally 37°C). Restriction enzymes were heat inactivated at 65°C for 15 min.

4.2.1.3 Ligations

Ligations were performed in 10 µl reaction volumes containing 1 µl of 10X T_4 DNA ligase buffer, 100 ng of vector DNA, sufficient insert DNA to create a 1:1 molar ratio of vector to insert and 1 Weiss unit of T_4 DNA ligase (Promega). Reactions were incubated overnight at 15°C.

4.2.1.4 Dephosphatasing

Vectors digested with one enzyme were dephosphorylated to prevent self-ligation. To heat inactivate restriction enzymes, restriction digests were heated to 65°C for 15 min. Dephosphorylating was conducted in 10 µl reactions using 1 µg of restricted DNA, 1 µl (5 units) of Antarctic Phosphatase (New England Biolabs), and 1 µl of 10X Antarctic Phosphatase Buffer. Reactions were incubated at 37°C for 15 min for 5' extensions and blunt-ended restrictions or 60 min for 3' extensions, then at 65°C for 5 min to heat inactivate the enzyme.

4.2.1.5 Agarose gel electrophoresis and gel extraction of DNA

PCR products and restriction digests were electrophoresed on 1% agarose gels containing ethidium bromide (0.5 µg ml^{-1}). DNA fragments of the expected size were excised from the gel and DNA was purified using a gel extraction kit (Nucleo-Spin Extract II, Macherey-Nagel, Germany). Gel slices were weighed in Eppendorf tubes and 200 µl of buffer NT was added for each 100 mg of gel. Samples were dissolved at 50°C for 5 – 10 min. Dissolved samples were loaded into a NucleoSpin Extract II column and centrifuged for 1 min at 11,000 x g. The bound DNA was washed with 600 µl of buffer NT3 by centrifuging for 1 min at 11,000 x g, then for a further 2 min at 11,000 x g to remove all traces of buffer NT3. DNA was eluted from the column by adding 20 µl of RO water (pH 8.5) and centrifuging at 11,000 x g for 1 min.

4.2.1.6 Cloning

Chemically competent *E. coli* cells were prepared by culturing 10 µl of either DB3.1 or DH5α cells (Invitrogen) in 50 ml of LB media at 37°C overnight on a shaker (100 rpm). A 20 ml aliquot was added to 500 ml of LB media and was grown at 37°C on a shaker (100 rpm) until reaching an OD_{600} of 0.68. The culture was centrifuged at 5,000 x g for 10 min and the pellets were resuspended in 200 ml of sterile water at 4°C. This process was repeated and cells were resuspended in 40 ml of sterile water, then 10

ml of sterile water , then 10 ml of sterile 10 % glycerol, and finally in 3 ml of 10 % glycerol. Aliquots of 50 µl per tube were prepared, snap frozen in liquid nitrogen and stored at -80°C.

Restriction enzyme digested and purified PCR fragments and vectors were ligated directly. Plasmid DNA from ligation reactions was used to transform chemically competent *E. coli.* Transformation reactions were performed by adding 2 µl of ligation mixture to 50 µl of chemically competent *E. coli* cells on ice and mixing. After 20 min the cells were transferred to a 42°C water bath for 45 s and quickly back to ice. The cells were incubated on ice for 2 min, then 300 µl of room temperature liquid LB media (10 g l^{-1} tryptone, 5 g l^{-1} yeast extract, 5 g l^{-1} NaCl, pH 7.5) was added to the cells and the mixture was shaken at 37°C for 1 h. The mixture was then spread on LB medium-agar plates (LB medium + 15 g l^{-1} bactoagar) containing kanamycin (50 µg ml^{-1}), spectinomycin (100 µg ml^{-1}) or ampicillin (100 µg ml^{-1}) depending on the antibiotic selection gene located in the plasmid DNA. Plates were sealed with Parafilm and incubated inverted at 37°C overnight.

E. coli colonies were picked from plates using sterile pipette tips into liquid LB media containing the appropriate antibiotic and cultures were grown overnight at 37°C on a shaker (150 rpm). Plasmid DNA was purified from 2 ml of *E. coli* cultures using a QIAprep Spin Miniprep Kit (Qiagen). Cultures were centrifuged for 20 s to pellet *E. coli* on the bottom of an Eppendorf tube. The pellet was resuspended in 250 µl of Buffer P1. Cells were lysed under alkaline conditions by adding 250 µl of Buffer P2 and mixing. Lysate was neutralized and denatured proteins, chromosomal DNA, cellular debris and SDS were precipitated by adding 350 µl of Buffer N3. This mixture was centrifuged to pellet the debris and the supernatant was transferred to a QIAprep spin column. Plasmid DNA was bound to the column by centrifuging for 30 s. The bound DNA was washed with 750 µl of Buffer PE and centrifuging to remove the extra wash buffer. DNA was eluted from the column with 50 µl of RO water (pH 7.5). Plasmid DNA (1 ul) was digested with an appropriate diagnostic restriction enzyme and analysed via agarose gel electrophoresis to locate correctly ligated plasmid DNA. The inserts and ligation junctions of plasmids were sequenced at the Australian Genome Research Facility (AGRF) in Adelaide to ensure sequence integrity. The

original *E. coli* cultures which contained correctly ligated plasmids were prepared for long-term storage at -80°C by adding 750 µl of the culture to 750 µl of 50 % glycerol in an Eppendorf tube and snap freezing in liquid nitrogen.

Ligations (not including Gateway® recombination reactions) involving vectors containing the Gateway® recombination cassette (e.g. pMDC100) were transformed into the *E. coli* strain DB3.1 as they are resistant to the ccdB protein which interferes with the *E. coli* DNA gyrase and inhibits growth of most *E. coli* strains. All other ligations were transformed into the *E. coli* strain DH5α.

4.2.2 Cloning of *AtHKT1;1*, *PpENA1*, *GUS*, *GFP* and *RFP* and Gateway® recombination

AtHKT1;1 was PCR amplified from pGreen-UAS-*AtHKT*-nos (Table 4.1) using primers HKT1Fwd and HKT1R (Appendix I) and was cloned into the vector pCR8/GW/TOPO TA (Invitrogen) (Figure 4.2). The 6 µl TOPO cloning reaction contained 2 µl of PCR product, 1 µl of the Salt Solution (diluted 1 in 4 with sterile RO water), 0.5 µl of the TOPO Vector/Enzyme and 2.5 µl sterile RO water. This mixture was incubated at room temperature for 30 min and transferred to ice. The entire 6 µl reaction was transformed into DH5α cells and plasmid DNA was isolated as described in section 4.2.1.6 and sequenced. *GUS*, *GFP* and *RFP* were received in the pCR8/GW/TOPO TA vector (Table 4.1) and *PpENA1* was received in the pENTR/D-TOPO (similar to pCR8/GW/TOPO TA) courtesy of Dr. Andrew Jacobs (ACPFG).

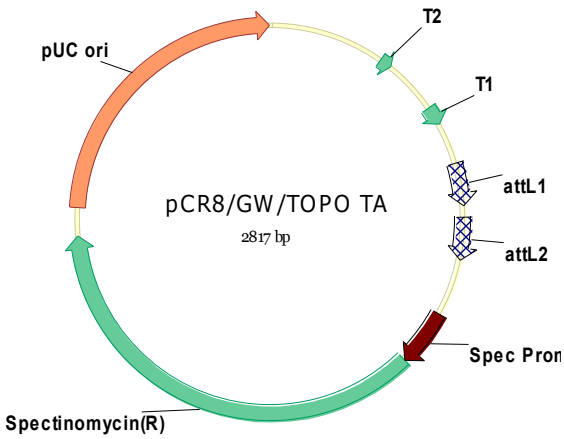

Figure 4.2: The pCR8/GW/TOPO TA Gateway® entry vector used to clone PCR amplified products. Cloned products are flanked by Gateway® recombination sites (*attL1*, *attL2*) to enable Gateway® LR recombination into Gateway® Destination vectors. Vector contains pUC origin of replication (pUC ori), Gateway® recombination sequences (*attL1, attL2*), spectinomycin promoter (Spec Prom) and spectinomycin resistance gene [Spectinomycin (R)].

Table 4.1: Summary of entry vectors used to construct all binary vectors used in rice transformation. Information includes the vector source, species the vector is used to transform, the antibiotic resistance gene for plant transformation, the antibiotic resistance gene for bacteria transformation, the intended purpose of the vector and whether the vector is compatible with the Gateway® cloning system.

Vector	Source	Species	Plant	Bact	Intended Purpose	Gateway®
pCR8/GW/TOPO TA	Invitrogen	*E. coli*	n/a	spec	Gateway Entry Vector	Yes
pGreen229-UAS-HKT1-nos	Inge Moller - University of Cambridge	Plants	basta	kan	Cell-specific expression of *AtHKT1;1* in *Arabidopsis*	No
pCR8/GW/TOPO TA + HKT1	Darren Plett - ACPFG	*E. coli*	n/a	spec	Gateway entry vector for *AtHKT1;1*	Yes
pCR8/GW/TOPO TA + *PpENA1*	Andrew Jacobs - ACPFG	*E. coli*	n/a	spec	Gateway entry vector for *PpENA1*	Yes
pCR8/GW/TOPO TA + *RFP*	Andrew Jacobs - ACPFG	*E. coli*	n/a	spec	Gateway entry vector for *RFP*	Yes
pCR8/GW/TOPO TA + *GFP*	Andrew Jacobs - ACPFG	*E. coli*	n/a	spec	Gateway entry vector for *GFP*	Yes
pCR8/GW/TOPO TA + *GUS*	Andrew Jacobs - ACPFG	*E. coli*	n/a	spec	Gateway entry vector for *GUS*	Yes

Genes were recombined from TOPO entry vectors into Gateway® Destination vectors (Table 4.1) using LR Clonase II (Invitrogen). The LR recombination reaction contained 0.5 µl of purified TOPO entry vector, 0.5 µl of purified Gateway®

Destination vector, 2 µl of Tris-EDTA (pH 8.5) and 1 µl of LR Clonase II enzyme. This mixture was incubated at 25°C for 1 h and the reaction was stopped by adding 1 µl of proteinase K (Invitrogen) and incubating at 37°C for 20 min. The entire 6 µl reaction was transformed into DH5α *E. coli* cells and plasmids were purified as in sections 4.2.1.6.

4.2.3 Vector construction starting material

The following vectors in Table 4.2 were used as starting material for construction of all vectors described in this chapter. Several vectors not shown in this chapter are summarised in Appendix II.

Table 4.2: Summary of vectors used as starting material for vector construction. Information includes the vector source, species the vector is used to transform, the antibiotic resistance gene for plant transformation, the antibiotic resistance gene for bacteria transformation, the intended purpose of the vector and whether the vector is compatible with the Gateway® cloning system.

Vector	Source	Species	Plant	Bact	Intended Purpose	Gateway
pMDC32	University of Zurich	Plants	hyg	kan	35Sx2 OEX	Yes
pMDC99	University of Zurich	Plants	hyg	kan	Large fragment cloning	Yes
pMDC100	University of Zurich	Plants	*nptII*	kan	Large fragment cloning	Yes
pMDC123	University of Zurich	Plants	basta	kan	Large fragment cloning	Yes
pHELLSGATE 8	Peter Waterhouse - CSIRO	Plants	*nptII*	spec	35Sx2 RNAi	No
pJH0022-pSRNA	Syngenta - UK	Plants	*nptII*	kan	35Sx2 Ethanol Inducible OEX	No
pGreen229-UAS-nos	Inge Moller - University of Cambridge	Plants	basta	kan	Empty vector for cell-specific expression in *Arabidopsis*	No

4.2.4 *Agrobacterium* transformation

Agrobacterium aliquots were prepared by starting an overnight culture in 10 ml of TYNG medium containing rifampicin (50 µg ml-1) shaking (150 rpm) at 28°C. The following morning 1 ml of the culture was added to 30 ml of the same media in a 50 ml centrifuge tube. Cultures were incubated shaking at 28°C for 4 h until the culture was slightly cloudy. The culture was chilled on ice for 10 min and were centrifuged at

4500 rpm for 10 min at 4°C. The supernatant was discarded and the pellet was resuspended in 500 µl of ice-cold 20 mM $CaCl_2$. Cells were aliquoted (100 µl) into chilled 1.5 ml Eppendorf tubes and frozen in liquid nitrogen and stored at -80°C.

The AGL1 or AGL0 strains of *Agrobacterium* were transformed via the 'freeze-thaw' transformation protocol (Weigel and Glazebrook 2006). Aliquots of *Agrobacterium* were thawed at room temperature and 1 µg of plasmid DNA was added to each aliquot and mixed. The cells were frozen in liquid nitrogen for 1 min, then thawed in a 37°C water bath for 5 min. The cells were incubated at 28°C for 1-2 h on a shaker (150 rpm) after adding 500 µl of TYNG medium (10 g l^{-1}, 5 g l^{-1} yeast extract, 5 g l^{-1} NaCl, 200 mg l^{-1} MgSO4*7H2O; pH 7.5). The cells were spread on LB medium-agar plates containing rifampicin (50 µg ml^{-1}) and kanamycin (50 µg ml^{-1}) and colonies appeared after 2 d.

Plasmid DNA was extracted from *Agrobacterium* to ensure the colonies contained the correct plasmid. The QIAprep Spin Miniprep Kit protocol described in section 4.2.1.6 was used to extract DNA with minor modifications. Colonies were picked into 10 ml of liquid YEB medium (5 g l^{-1} beef extract, 1 g l^{-1} yeast extract, 5 g l^{-1} peptone, 5 g l^{-1} sucrose; pH 7.2) with kanamycin (50 µg ml^{-1}), rifampicin (50 µg ml^{-1}) and $MgSO_4$ (2 mM) and grown overnight at 28°C on a shaker (200 rpm). The cultures were centrifuged for 15 min at 1,500 x g to pellet the bacteria and the pellet was processed as in section 4.2.1.6.

4.2.5 Rice transformation

Agrobacterium-mediated transformation of scutellum-derived callus was used to produce transgenic rice lines (Sallaud *et al.* 2003).

Seed was sterilised by immersion in 70 % ethanol for 1 min in 50 ml sterile tubes. Ethanol was decanted and 30 ml of sodium hypochlorite (30% of the purchased product – e.g. White King – which generates about 1% available chlorine) plus 0.5 ml Tween20 was added to the seeds with vigourous mixing for 30 minutes. Finally, seeds were rinsed 5 times with RO water to remove the bleach.

Callus was induced by placing 10 seeds on plates of NB medium (Appendix III) using sterile forceps. Plates were dried under sterile air flow hoods, sealed with Parafilm and placed in the dark at 28°C for 28 d.

Scutellum-derived callus was propagated by placing 50 embryonic units (small-medium-sized white calli originating near the zone of shoot emergence) onto fresh NB medium. Plates were sealed with Parafilm and placed in the dark at 28°C for 10-14 d.

Overnight culture of *Agrobacterium* carrying the gene(s) of interest were initiated 4 d prior to transformation in 10 ml LB medium containing rifampicin (50 µg ml-1) and kanamycin (50 µg ml-1) with shaking (200 rpm) at 28°C. The following morning 200 µl of the culture was spread onto plates of AB medium (Appendix III) containing rifampicin (50 µg ml^{-1}) and kanamycin (50 µg ml^{-1}). Plates were sealed with Parafilm and incubated inverted at 28°C for 3 d.

On the day of transformation, ¼ to ½ of the *Agrobacterium* was scraped off the AB medium plate using a sterile spatula into 30 ml of R2-CL liquid medium (Appendix III) in a sterile 50 ml tube. The culture was vortexed until completely homogenised and the cultures were adjusted to an OD_{600} of 0.7-1.0 (using R2-CL medium as a blank).

Up to 100 calli were placed into a sterile Petri dish and 25 ml of the *Agrobacterium* culture was poured into the dish. The dishes were gently agitated every 5 min. After 15 min the *Agrobacterium* culture was removed from the dish using a 25 ml sterile pipette and discarded. The calli were transferred with sterile forceps to autoclaved Whatman Chromatography filter paper and rolled across the surface until dry. Dry calli were transferred to dishes of R2-CS (Appendix III) medium (10 per dish), allowed to dry for 15 min, sealed with Parafilm and placed into the dark at 25°C for 3 d.

Selection for transformed calli began by moving calli from R2-CS medium to plates of R2-S medium (Appendix III) containing geneticin (200 mg l^{-1}) or hygromycin (50 mg l^{-1}), 10 calli per plate. Calli appearing wet and shiny were avoided because this indicated contamination by overgrowth of *Agrobacterium*. Dishes were dried under the flow hood, sealed with Parafilm and incubated in the dark at 28°C for 14 d. The calli began turning brown after 14 d, indicating death of untransformed cells, but the surface had small, white growths indicating dividing transformed cells.

Transformed calli were transferred to plates of NBS medium (Appendix III), 7 calli per plate, to allow the calli to proliferate. Plates were dried completely, sealed

with Parafilm and placed in the dark at 28°C for 14-21 d. After 7 d the dishes were opened and transformed calli were separated from the dying parent callus and spread over the entire surface of the plate. The calli originating from each parent callus were kept separate by drawing lines on the bottom of the dishes in order to keep potential clones together. Dishes were sealed with Parafilm and placed into the dark at 28°C for 7-14 d (depending on speed of callus growth).

Medium-large, healthy, yellow-white calli were transferred to plates of PR-AG medium (Appendix III) to induce shoot primordia. Each dish was divided into sections (by drawing lines on the bottom of dishes) and 10 calli from each parent callus was transferred to a section. Dishes were sealed with Parafilm and placed in the dark at 28°C for 7-8 d.

To regenerate shoots, calli were transferred to plates of RN medium (Appendix III), 7 per dish, ensuring that calli from the same parent callus were kept together. The dishes were sealed with Parafilm and incubated in the dark at 28°C for 2 d, then placed under lights (12 h light/dark cycle) at 28°C for 28-42 d.

To regenerate plantlets, a single, vigorously growing shoot was excised from each callus. The upper 2/3rd portion of the shoot and any root growth was removed with a sterile scalpel and placed into sterile 1 l plastic jars containing P medium (Appendix III). Jars were sealed with lids and placed into the 28°C growth chamber in the light for 21-28 d.

Regenerated plantlets were removed from jars and the shoots and roots were trimmed (leaving 2 cm of shoot and 1 cm of root). Regenerants were placed into Jiffy peat pots, which had been soaked, placed in trays in water and covered with a plastic dome. Trays were kept in a glasshouse at South Australian Research and Development Initiative (SARDI) in Adelaide with average temperatures of 30°C days and 20°C nights, full sun, and an average humidity of 60%. After 15 d regenerants were planted into soil (UC Davis mix) in 6" pots and grown to maturity in the glasshouse.

4.2.6 GAL4-GFP enhancer trap lines

The GAL4-GFP enhancer trap line used in the 1st transformation was AOS A05 (Figure 4.3), which had bright root and shoot GFP fluorescence and was used to ensure

that the constructed vectors would drive ethanol-inducible expression of either *RFP* or *GUS*.

Two GAL4-GFP enhancer trap lines were used in the 2nd transformation. The first line, AOH B03, has root epidermal/cortex specific GFP fluorescence and is referred to as the 'outer background' line (Figure 4.3). The second line, ASG F03, has root xylem parenchyma specific GFP fluorescence and is referred to as the 'inner background' line (Figure 4.3). Details descriptions of the GAL4-GFP enhancer trap patterns can be found in an online database (http://129.127.183.5/fmi/iwp/res/iwp_home.html) and their development is described in Johnson *et al.* 2005.

Figure 4.3: GAL4-GFP enhancer trap lines described in this chapter. Stereomicroscope images of root GFP fluorescence in AOS A05 line used in 1st rice transformation (a, b, and c). Confocal images of root epidermis/cortex-specific GFP fluorescence in AOH B03 line (Outer Background) used in 2nd rice transformation (d and e) and stereomicroscope image of transactivation of GUS in the same lines (f). Confocal images of root xylem parenchyma-specific GFP fluorescence in ASG F03 line (Inner Background) used in 2nd rice transformation (g and h) and stereomicroscope image of transactivation of GUS in the same line. Images courtesy of Dr. Alex Johnson.

4.2.7 Ethanol switch induction in callus and plants

Transformed callus was screened to provide an early indication of function of the ethanol switch. A small Petri dish of 100% ethanol was placed for 5 min in callus culture plates to induce the reporter gene expression. Calli were arranged around the edge of the plate and images were taken at several time points after induction.

T_0 plants were grown in Jiffy peat pots in plastic trays containing growth solution (RO water, Osmocote, and 5 mM NH_4NO_3). To induce the ethanol switch, growth solution was replaced with growth solution supplemented with 1% ethanol for 24 h (Caddick *et al.* 1998) and plants were covered with plastic domes in order to allow ethanol vapours to accumulate and aid in induction (Sweetman *et al.* 2002). Following the induction period, growth solution was replaced with ethanol-free growth solution and plants were cultured normally. Photographs were taken were taken immediately prior to ethanol application and several time points following ethanol application. Plants in Jiffy peat pots were removed from trays and intact roots were examined for GFP and RFP fluorescence.

4.2.8 Microscopy

Fluorescence was detected using a Leica MZ FLIII fluorescence stereomicroscope (Leica Microscopie Systemes SA, Heerbrugg, Switzerland) and a *GFP* Plus fluorescence filter set [*GFP*2, 480 nm excitation filter (bandwidth of 40 nm) and 510 nm barrier filter] for GFP fluorescence or a dsRED filter set (556 nm excitation filter and 586 nm barrier filter) for RFP fluorescence. Images were collected using a Leica DC 300F digital camera.

4.2.9 Production of transgenic *Arabidopsis*

Constructs were developed to constitutively and ethanol-inducibly silence expression of *AtHKT1;1* and ethanol-inducibly overexpress *AtHKT1;1* in *Arabidopsis* (Table 4.3).

Table 4.3: Summary of Gateway® entry vectors and the Gateway® Destination vectors transformed into *Arabidopsis*. Information includes the vector source, species the vector is used to transform, the antibiotic resistance gene for plant transformation, the antibiotic resistance gene for bacteria transformation, the intended purpose of the vector and whether the vector is compatible with the Gateway® cloning system.

Vector	Source	Species	Plant	Bact.	Intended Purpose	Gateway
pRS300	Detlef Weigel - Germany	*E. coli*	n/a	amp	Construction of amiRNA	No
pCR8/GW/TOPO TA + pRS300precursor (HKT)	Darren Plett - ACPFG	*E. coli*	n/a	spec	Gateway entry vector for pRS300precursor (HKT)	Yes
pCR8/GW/TOPO TA + pRS300precursor (miRNA)	Darren Plett - ACPFG	*E. coli*	n/a	spec	Gateway entry vector for pRS300precursor (miRNA)	Yes
pTOOL2	Andrew Jacobs - ACPFG	Plants	basta	amp	35Sx2 OEX	Yes
pTOOL2 + pRS300precursor (HKT)	Darren Plett - ACPFG	Plants	basta	amp	Constitutive amiRNA silencing of *AtHKT1;1*	Yes
pTOOL2 + pRS300precursor (miRNA)	Darren Plett - ACPFG	Plants	basta	amp	Constitutive amiRNA silencing of *AtHKT1;1*	Yes
pMDC100 + 35Sx2 + EtOH + nos + pRS300precursor (HKT)	Darren Plett - ACPFG	Plants	*nptII*	kan	Inducible amiRNA silencing of *AtHKT1;1*	Yes
pMDC100 + 35Sx2 + EtOH + nos + pRS300precursor (miRNA)	Darren Plett - ACPFG	Plants	*nptII*	kan	Inducible amiRNA silencing of *AtHKT1;1*	Yes
pMDC100 + 35Sx2 + EtOH + nos + *AtHKT1;1*	Darren Plett - ACPFG	Plants	*nptII*	kan	Inducible OEX of *AtHKT1;1*	Yes
pMDC100 + 35Sx2 + EtOH + nos + *RFP*	Darren Plett - ACPFG	Plants	*nptII*	kan	Inducible OEX of *RFP*	Yes

4.2.9.1 Cloning of artificial microRNA constructs

Cloning of artificial microRNAs (amiRNAs) was carried out according to a protocol available at (http://wmd.weigelworld.org/cgi-bin/mirnatools.pl, and Schwab *et al.* 2006). The artificial microRNA designer WMD (http://wmd.weigelworld.org/cgi-bin/mirnatools.pl) provided four oligonucleotide sequences (I to IV), which were used to engineer the artificial microRNA into the endogenous miR319a precursor by site-directed mutagenesis. The amiRNA was designed to specifically silence *AtHKT1;1* and the WMD program reported there to be no potential off-targets for this particular

amiRNA. It is recommended to engineer two separate amiRNAs designed to target different regions of the intended target gene in case one does not function, thus two separate amiRNAs were developed to silence *AtHKT1;1* (called precursor miRNA and precursor HKT). The plasmid pRS300 (courtesy of Detlef Weigel, MPI, Germany), which contains the miR319a precursor in the vector pBSK (cloned via *SmaI* site), was used as a template for the following PCRs (Figure 4.4).

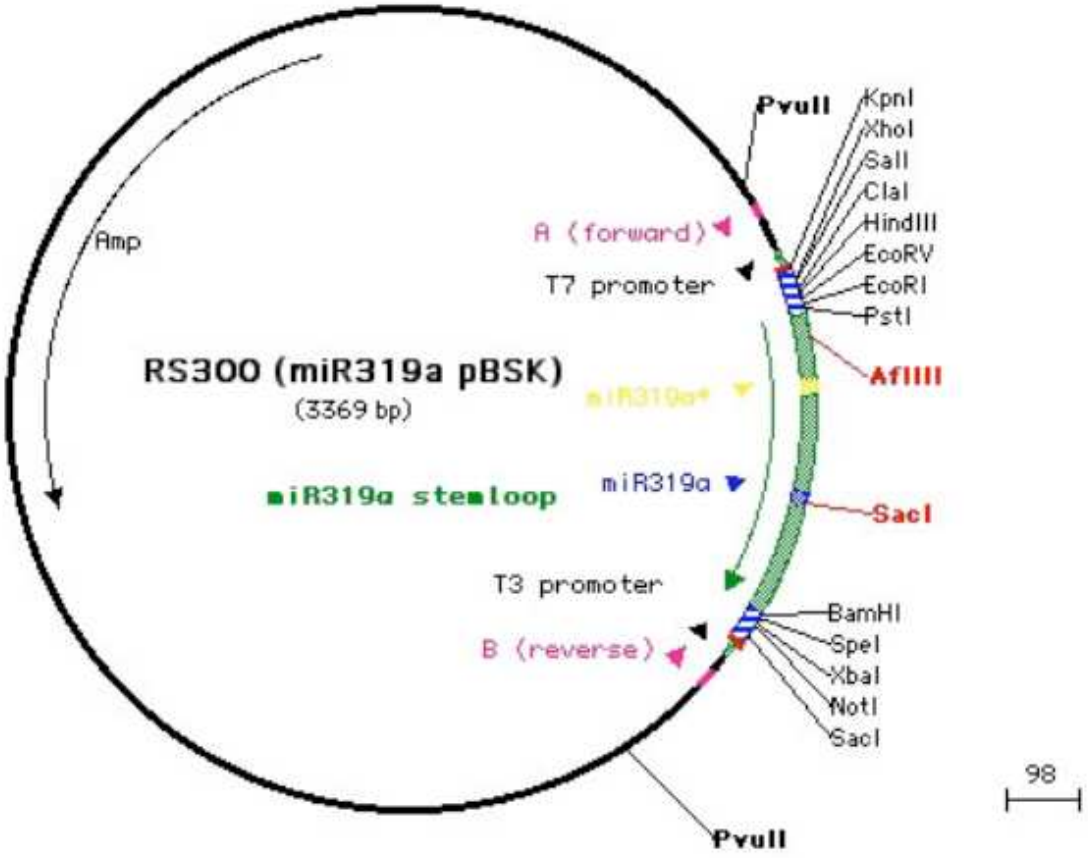

Figure 4.4: pRS300 vector for amiRNA construction. The pBSK cloning vector contains the endogenous *Arabidopsis* microRNA, miR319a.

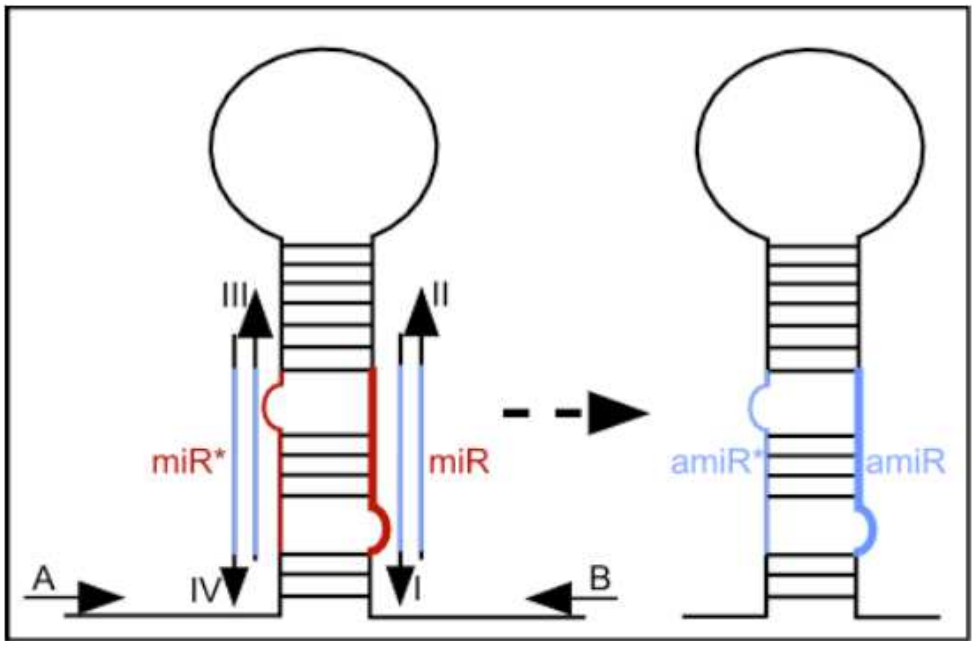

Figure 4.5: PCR strategy for site-directed mutagenesis of pRS300 to develop gene-specific amiRNA.

Two sets of four primers were used to mutate the endogenous microRNA in order to develop two amiRNAs specific to *AtHKT1;1* (Figure 4.5). In general these primers are known as I: microRNA forward, II: microRNA reverse, III: microRNA* forward (see Appendix I). Oligonucleotides A and B are based on the template plasmid sequence. They are located outside of the multiple cloning site of pBSK to generate bigger PCR products. Four separate PCRs were used to generate the amiRNA (Table 4.4). The first round of PCRs amplifies fragments (a), (b) and (c). Overlapping PCR is then used to fuse the three fragments together forming fragment (d).

Four PCR reactions were used in the construction of amiRNAs: (a), (b), (c) and (d). The 50 µl mix for PCR reactions (a), (b) and (c) contained 5 µl of 10X PCR buffer (with Mg^{2+}), 5 µl dNTPs at a concentration of 2 mM, 2 µl of each oligo (Appendix I) at a concentration of 10 µM, 2 µl of pRS300 plasmid DNA (1:100), 0.5 µl Elongase (Invitrogen), and 33.5 µl of water. The three PCR reactions were run with the following program: and initial step of 95°C for 2 min, then 24 cycles of 95°C for 30 sec, 55°C for 30 sec [50°C for (b)], and 72°C for 40 sec. The products were run on a 2 % agarose gel, extracted from the gel (see 4.2.1.5). The three products were used as

template for PCR reaction (d). The 50 µl mix for this PCR contained 5 µl of 10X PCR buffer (with Mg^{2+}), 5 µl of dNTPs at a concentration of 2 mM, 2 µl of oligo A at a concentration of 10 µM, 2 µl of oligo B at a concentration of 10 µM (Appendix I), 0.5 µl of PCR (a), 0.5 µl of PCR (b), 0.5 µl of PCR (c), 0.5µl of Elongase (Invitrogen) and 34.5 µl of water. PCR (d) was cycled as follows: an initial step of 95°C for 2 min, then 24 cycles of 95°C for 30 sec, 55°C for 30 sec and 72°C for 1 min and 30 sec. This product was run on a 1 % agarose gel and was gel extracted (see 4.2.1.5).

Table 4.4: List of PCRs to clone amiRNAs.

PCR	Forward Oligo	Reverse Oligo	Template	Product Length (bp)
(a)	A	IV	pRS300	269
(b)	III	II	pRS300	169
(c)	I	B	pRS300	296
(d)	A	B	(a) + (b) + (c)	694

PCR product (d) was then cloned into the Gateway® Entry vector pCR8/GW/TOPO TA and sequenced. This allowed the transfer of the amiRNA to a variety of Gateway® Destination vectors for silencing of *AtHKT1;1* using different expression systems. As mentioned above, two separate amiRNAs were constructed (named miRNA and HKT). These amiRNAs were recombined into the Destination vectors pTOOL2 (Figure 4.6) for constitutive silencing of *AtHKT1;1* and pMDC100 + 35Sx2 + EtOH + nos (Figure 4.12) for inducible silencing of *AtHKT1;1* (Table 4.3). The four constructs were transformed into WT Col-0 *Arabidopsis* as described in section 4.2.9.3.

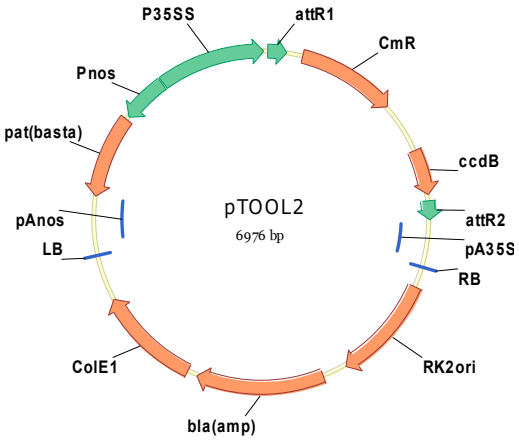

Figure 4.6: The vector pTOOL2 used to constitutively overexpress genes via the CaMV35S promoter. Vector backbone contains: ColE1 replication origin (ColE1); RK2 origin of replication (RK2 ori); and ampicillin resistance gene [bla (amp)]. From the right border sequence (RB) the T-DNA cassette contains: CaMV 35S 3'UTR poly A signal (pA35S); Gateway® recombination cassette [comprised of Gateway® recombination sequences (*attR1* and *attR2*), chloramphenicol resistance gene (Chloramphenicol resistance) and *ccdB* gene (ccdB)]; CaMV35S promoter (P35S); bacterial nopaline synthase promoter (Pnos); basta resistance gene [pat (basta)]; bacterial nopaline synthase terminator (pAnos) and left border sequence (LB). Further details are found in Table 4.6.

4.2.9.2 Inducible expression of *AtHKT1;1* and *RFP* in Arabidopsis

AtHKT1;1 and *RFP* genes, previously cloned into pCR8/GW/TOPO TA (section 4.2.2), were recombined into pMDC100 + 35Sx2 + EtOH + nos via LR Clonase recombination reactions. Constructs were transformed into Col-0 and C-24 *Arabidopsis* ecotypes as described in section 4.2.9.3.

4.2.9.3 *Arabidopsis* transformation

Vector constructs described in sections 4.2.9.1 and 4.2.9.2 were transformed into *Arabidopsis* plants by Deepa Jha and Mel Pickering (ACPFG) via the *Agrobacterium*-mediated floral dip method (Clough and Bent 1998). T_1 seed from plants transformed with the pMDC100 + 35Sx2 + EtOH + nos vector were selected on kanamycin (50 mg l^{-1}) plates and putative transformants were planted in soil. T_1 seed from plants transformed with the pTOOL2 vector (section 4.2.9.1) were sown in soil and selected by spraying with the herbicide Basta and putative transformants were transplanted to soil trays and self-pollinated to produce T_3 seed.

4.3 Results and Discussion

4.3.1 Vector construction

A large number of vectors were constructed (Plett *et al.* 2006) for the purpose of developing a better understanding of Na^+ transporter function and the effect(s) they have in plants when expressed (or silenced) in a spatial and temporal manner (Table 4.5). The following vectors were constructed using the standard cloning techniques described in section 4.2.1. All vectors were constructed using pMDC99, pMDC100 or pMDC123 (Table 4.2), thus have a common vector backbone containing: pVS1 stability function (pVS1 sta); pVS1 replication function (pVS1 rep); pBR322 basis of mobility (pBR322 bom); pBR322 origin of replication (pBR322 ori) and the kanamycin resistance gene (kanamycin (R)) (Figures 4.7 to 4.24). See Appendix I for sequences of all oligonucleuotide primers. Additionally, vectors were constructed (pMDC100 + alcA + nos + *bar* and pMDC100 + alcA +RNAi + *bar*, Figures 4.21 and 4.22) for crossing into GAL4-GFP lines (see full discussion in chapter 5).

Table 4.5: Summary of Gateway® Destination vectors constructed. Information includes the vector source, species the vector is used to transform, the antibiotic resistance gene for plant transformation, the antibiotic resistance gene for bacteria transformation, the intended purpose of the vector and whether the vector is compatible with the Gateway® cloning system. Overexpression (OEX).

Vector	Source	Species	Plant	Bact	Intended Purpose	Gateway
pMDC100 + 35Sx2 + nos (kan)	Vanessa Conn/Darren Plett - ACPFG	Plants	*nptII*	kan	OEX	Yes
pMDC100 + 35Sx2 + RNAi	Darren Plett - ACPFG	Plants	*nptII*	kan	RNAi	Yes
pMDC100 + 35Sx2 + RNAi (hyg)	Darren Plett - ACPFG	Plants	hyg	kan	RNAi	Yes
pMDC100 + 35Sx2 + EtOH + nos	Darren Plett - ACPFG	Plants	*nptII*	kan	Inducible OEX	Yes
pMDC100 + 35Sx2 + EtOH + RNAi	Darren Plett - ACPFG	Plants	*nptII*	kan	Inducible RNAi	Yes
pMDC123 + 35Sx2 + EtOH + nos	Darren Plett - ACPFG	Plants	basta	kan	Inducible OEX	Yes
pMDC99 + 35Sx2 + EtOH + nos	Darren Plett - ACPFG	Plants	hyg	kan	Inducible OEX	Yes
pMDC99 + 35Sx2 + EtOH + RNAi	Darren Plett - ACPFG	Plants	hyg	kan	Inducible RNAi	Yes
pMDC123 + UAS + nos	Darren Plett - ACPFG	*Arabidopsis*	basta	kan	Cell-specific OEX	Yes
pMDC123 + UAS + RNAi	Darren Plett - ACPFG	*Arabidopsis*	basta	kan	Cell-specific RNAi	Yes
pMDC123 + UAS + EtOH + nos	Darren Plett - ACPFG	*Arabidopsis*	basta	kan	Cell-specific, inducible OEX	Yes
pMDC123 + UAS + EtOH + RNAi	Darren Plett - ACPFG	*Arabidopsis*	basta	kan	Cell-specific, inducible RNAi	Yes
pMDC100 + UAS + nos	Darren Plett - ACPFG	Rice	*nptII*	kan	Cell-specific OEX	Yes
pMDC100 + UAS + EtOH + nos	Darren Plett - ACPFG	Rice	*nptII*	kan	Cell-specific, inducible OEX	Yes
pMDC100 + UAS + EtOH + RNAi	Darren Plett - ACPFG	Rice	*nptII*	kan	Cell-specific, inducible, RNAi	Yes
pMDC100 + UAS + RNAi	Darren Plett - ACPFG	Rice	*nptII*	kan	Cell-specific, RNAi	Yes
pMDC100 + alcA + nos + bar	Darren Plett - ACPFG	Plants	*nptII*	kan	Crossing vector for inducible OEX	Yes
pMDC100 + alcA + RNAi + bar	Darren Plett - ACPFG	Plants	*nptII*	kan	Crossing vector for inducible RNAi	Yes

4.3.1.1 pMDC100 + 35Sx2 + nos (kan)

The tandem CaMV35S promoters from the pMDC32 (Table 4.2) plasmid were amplified with the primers 35S*PmeI*F and 35S*PmeI*R. The purified PCR product was digested with *PmeI* along with the pMDC100 (Table 4.2) vector. The CaMV35S promoters were ligated into the linear vector creating pMDC100 + 35Sx2. The nos terminator was PCR amplified from pMDC32 with the primers nosTF*AleI* and nosTR*PacI* and the resulting product was digested with *AleI* and *PacI*. pMDC100 + 35Sx2 was digested with the same enzymes and the nos fragment was ligated into the vector creating pMDC100 + 35Sx2 + nos (kan) (Figure 4.7).

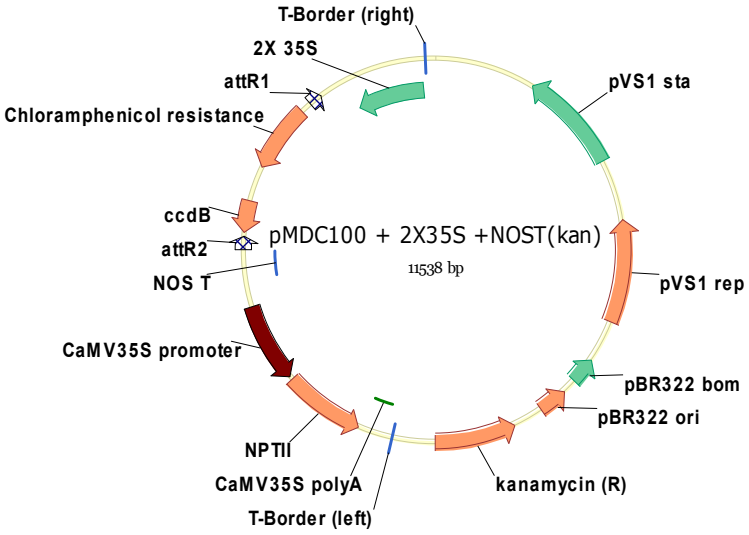

Figure 4.7: Vector diagram of pMDC100 + 35Sx2 + nos (kan) used for constitutive expression of transgenes in plants. From the right border sequence [T-Border (right)] the T-DNA cassette contains: dually-enhanced CaMV35S promoter (2 X 35S); Gateway® recombination cassette [comprised of Gateway® recombination sequences (*attR1* and *attR2*), chloramphenicol resistance gene (Chloramphenicol resistance) and *ccdB* gene (ccdB)]; bacterial nopaline synthase terminator (nosT); CaMV35S promoter (CaMV 35S promoter); neomycin phosphotransferase gene (nptII); CaMV 35S 3'UTR poly A signal (CaMV35S polyA); and left border sequence [T-Border (left)].

4.3.1.2 pMDC100 + 35Sx2 + RNAi

The PDK intron to OCS region (PDK-OCS) of the vector pHELLSGATE8 (Table 4.2) was PCR amplified using the primers PDK-OCSFAl and PDK-OCSRAl. The resulting product and the pMDC100 + 35Sx2 vector (section 4.3.1.1) were digested with *AleI* and the PDK-OCS fragment was ligated into pMDC100 + 35Sx2 to create pMDC100 + 35Sx2 + RNAi (Figure 4.8).

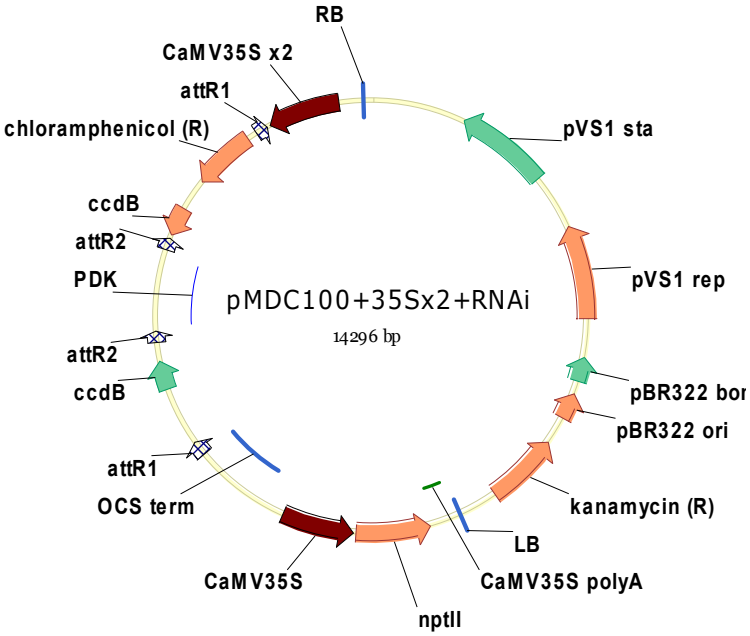

Figure 4.8: Vector diagram of pMDC100 + 35Sx2 + RNAi used for constitutive dsRNAi gene silencing in plants. From the right border sequence (RB) the T-DNA cassette contains: dually-enhanced CaMV35S promoter (CaMV35Sx2); Gateway® recombination cassette [comprised of Gateway® recombination sequences (*attR1* and *attR2*), chloramphenicol resistance gene (Chloramphenicol (R)) and *ccdB* gene (ccdB)]; PDK intron (PDK); inverse Gateway® recombination cassette [comprised of Gateway® recombination sequences (*attR1* and *attR2*) and *ccdB* gene (ccdB)] OCS terminator sequence (OCS term); CaMV35S promoter (CaMV 35S); neomycin phosphotransferase gene (nptII); CaMV 35S 3'UTR poly A signal (CaMV35S polyA); and left border sequence (LB).

4.3.1.3 pMDC100 + 35Sx2 + RNAi (hyg)

pMDC99 + 35Sx2 + EtOH + RNAi (Figure 4.18) was digested with *BlpI* to remove a fragment comprising the 35S promoter, hygromycin resistance gene, left border, and a portion of the kanamycin resistance gene. The vector pMDC100 + 35Sx2 + RNAi (Figure 4.8) was also digested with *BlpI* and the 35S-kanamycin fragment was ligated in to create the vector pMDC100 + 35Sx2 + RNAi (hyg) (Figure 4.9).

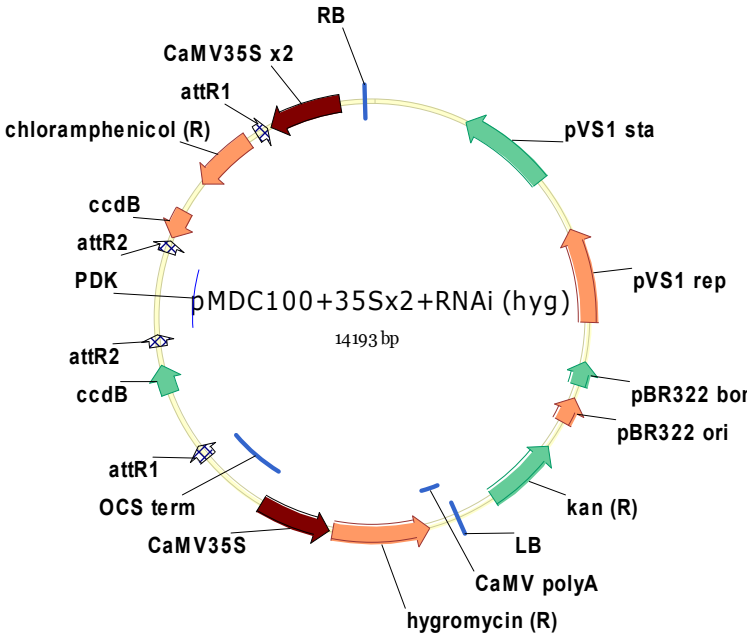

Figure 4.9: Vector diagram of pMDC100 + 35Sx2 + RNAi (hyg) used for constitutive gene silencing in plants. From the right border sequence (RB) the T-DNA cassette contains: dually-enhanced CaMV35S promoter (CaMV35Sx2); Gateway® recombination cassette [comprised of Gateway® recombination sequences (*attR1* and *attR2*), chloramphenicol resistance gene (Chloramphenicol (R)) and *ccdB* gene (ccdB)]; PDK intron (PDK); inverse Gateway® recombination cassette [comprised of Gateway® recombination sequences (*attR1* and *attR2*) and *ccdB* gene (ccdB)] OCS terminator sequence (OCS term); CaMV35S promoter (CaMV 35S); hygromycin phosphotransferase gene (hygromycin (R)); CaMV 35S 3'UTR poly A signal (CaMV35S polyA); and left border sequence (LB).

4.3.1.4 pMDC100 + UAS + EtOH + nos

The Syngenta pJH0022 plasmid (Table 4.2) was used a template in PCR with the oligonucleotides Eth*AscI*R and Eth*PmeI*R to amplify the alcR-nos-alcA region. Primer Eth*PmeI*R included a *PmeI* restriction enzyme site at the 5' terminus and primer Eth*AscI*R included an *AscI* restriction enzyme site at the 5' terminus for subsequent cloning steps. Resultant PCR products were digested with *Sbf*I/*AscI* restriction enzymes. The restriction fragment containing the nos-AlcA regions were cloned into the corresponding sites of a cut pMDC100 vector (Table 4.2) and the resultant plasmid was propagated in *E. coli*. Plasmid DNA was extracted and digested with *PmeI*/*Sbf*I. The AlcR fragment was purified and cut further with *PmeI*. The pMDC100 vector containing the nos-AlcA fragment was digested with *PmeI*/*Sbf*I and the compatible AlcR fragment was ligated in. The pGreen-UAS-nos plasmid (Table 4.2) was used as a template in PCR with the oligonucleotides UAS*PmeI*F and UAS*PmeI*R to amplify the UAS region. Primer UAS*PmeI*F included a *PmeI* restriction enzyme site at the 5' terminus as did primer UAS*PmeI*R for subsequent cloning steps. PCR was performed as described above and the purified PCR product was digested with *PmeI*. The pMDC100+AlcA-nos+alcR plasmid was cut with *PmeI* and the UAS *PmeI* fragment was ligated into the vector and propagated in *E. coli*. pMDC32 (Table 4.2) was used as a template in PCR using NosTF*AleI* and NosTR*PacI* to amplify the nopaline synthase (Nos) terminator. The PCR product was digested using *AleI* and *PacI* restriction enzymes. pMDC100+UAS+AlcA-nos+alcR was digested with *AleI* and *PacI* and the Nos terminator was ligated into the compatible sites. The resultant vector, designated pMDC100+UAS+EtOH+nos is shown in Figure 4.10.

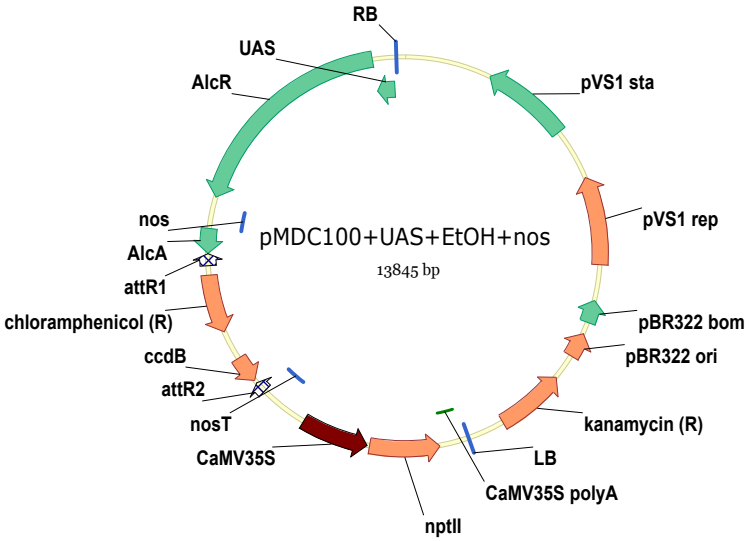

Figure 4.10: Vector diagram of pMDC100 + UAS + EtOH + nos used for cell-type specific, ethanol-inducible overexpression of transgenes in GAL4-GFP enhancer trap rice lines. From the right border sequence (RB) the T-DNA cassette contains: five tandem repeats of the upstream activation sequence element GAL4 binding site (UAS); AlcR transcription factor (AlcR); bacterial nopaline synthase terminator (nosT); alcA promoter (AlcA); Gateway® recombination cassette [comprised of Gateway® recombination sequences (*attR1* and *attR2*), chloramphenicol resistance gene (Chloramphenicol (R)) and *ccdB* gene (ccdB)]; bacterial nopaline synthase terminator (nosT); CaMV35S promoter (CaMV 35S); neomycin phosphotransferase gene (nptII); CaMV 35S 3'UTR poly A signal (CaMV35S polyA); and left border sequence (LB).

4.3.1.5 pMDC100 + UAS + EtOH + RNAi

The PCR product PDK-OCS (section 4.3.1.3) was digested with *AleI*. The vector pMDC100+UAS+alcA-nos-AlcR (section 4.3.1.4) was digested with *AleI* and the purified PCR product was ligated into the linear pMDC100+UAS+alcA-nos-AlcR vector. The resultant vector, designated pMDC100+UAS+EtOH+RNAi is shown in Figure 4.11.

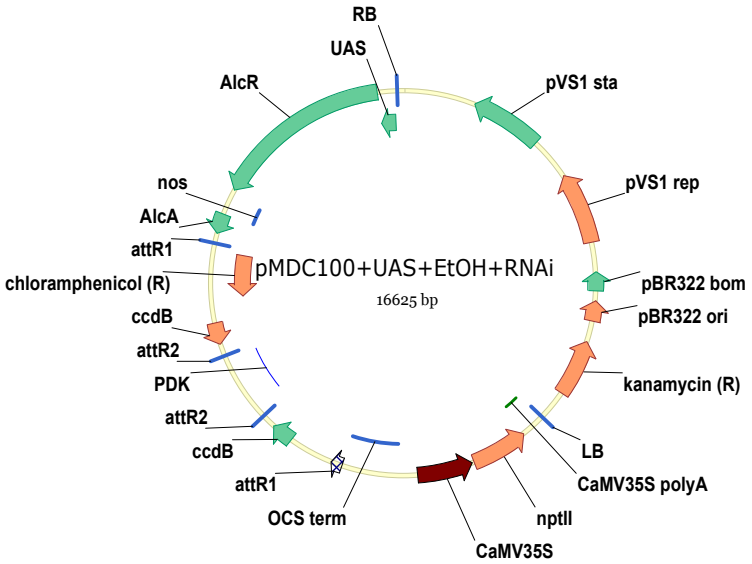

Figure 4.11: Vector diagram of pMDC100 + UAS + EtOH + RNAi used for cell-type specific, ethanol-inducible dsRNAi gene silencing in GAL4-GFP enhancer trap rice lines. From the right border sequence (RB) the T-DNA cassette contains: five tandem repeats of the upstream activation sequence element GAL4 binding site (UAS); AlcR transcription factor (AlcR); bacterial nopaline synthase terminator (nosT); alcA promoter (AlcA); Gateway® recombination cassette [comprised of Gateway® recombination sequences (*attR1* and *attR2*), chloramphenicol resistance gene (Chloramphenicol (R)) and *ccdB* gene (ccdB)]; PDK intron (PDK); inverse Gateway® recombination cassette [comprised of Gateway® recombination sequences (*attR1* and *attR2*) and *ccdB* gene (ccdB)] OCS terminator sequence (OCS term); CaMV35S promoter (CaMV 35S); neomycin phosphotransferase gene (nptII); CaMV 35S 3'UTR poly A signal (CaMV35S polyA); and left border sequence (LB).

4.3.1.6 pMDC100 + 35Sx2 + EtOH + nos

The tandem CaMV35S promoters of the pMDC32 plasmid (Table 4.2) were amplified with the primers 35S*PmeI*F and 35S*PmeI*R and the purified PCR product was digested with *PmeI* (section 4.3.1.1). pMDC100+AlcA-nos+alcR (section 4.3.1.4) was also digested with *PmeI* and the tandem CaMV35S promoters of the pMDC32 vector were ligated into the linear vector creating pMDC100+35Sx2+EtOH+nos (Figure 4.12).

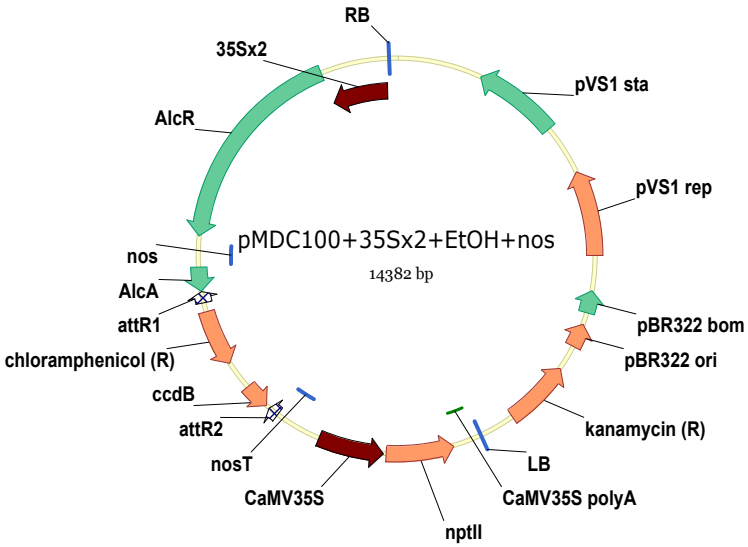

Figure 4.12: Vector diagram of pMDC100 + 35Sx2 + EtOH + nos used for inducible gene overexpression in plants. From the right border sequence (RB) the T-DNA cassette contains: dually-enhanced CaMV35S promoter (35Sx2); AlcR transcription factor (AlcR); bacterial nopaline synthase terminator (nosT); alcA promoter (AlcA); Gateway® recombination cassette [comprised of Gateway® recombination sequences (*attR1* and *attR2*), chloramphenicol resistance gene (Chloramphenicol (R)) and *ccdB* gene (ccdB)]; bacterial nopaline synthase terminator (nosT); CaMV35S promoter (CaMV 35S); neomycin phosphotransferase gene (nptII); CaMV 35S 3'UTR poly A signal (CaMV35S polyA); and left border sequence (LB).

4.3.1.7 pMDC100 + 35Sx2 + EtOH + RNAi

pMDC100+35Sx2+alcA-nos-AlcR (section 4.3.1.4) was digested with *AleI* and the digested *AleI* intron-OCS terminator fragment from pHellsgate8 (Table 4.2) described above was ligated into the linear vector. The resultant vector, designated pMDC100+35Sx2+EtOH+RNAi is shown in Figure 4.13.

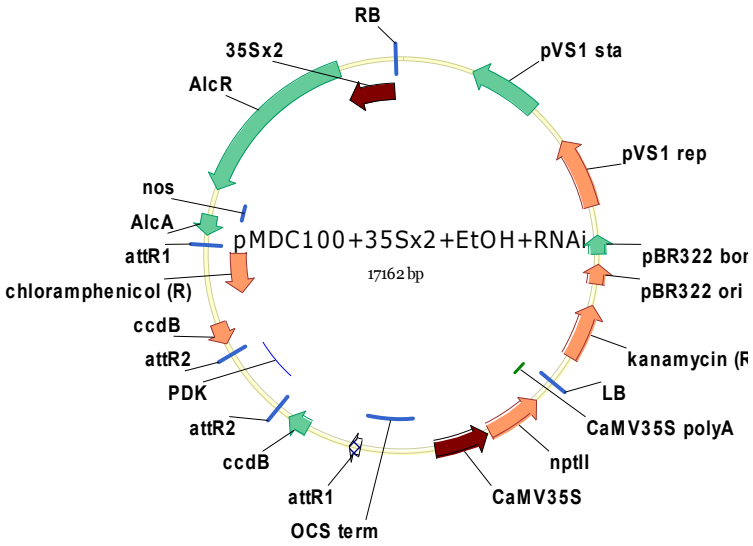

Figure 4.13: Vector diagram of pMDC100 + 35Sx2 + EtOH + RNAi used for ethanol-inducible dsRNAi gene silencing in plants. From the right border sequence (RB) the T-DNA cassette contains: five tandem repeats of the upstream activation sequence element GAL4 binding site (UAS); AlcR transcription factor (AlcR); bacterial nopaline synthase terminator (nosT); alcA promoter (AlcA); Gateway® recombination cassette [comprised of Gateway® recombination sequences (*attR1* and *attR2*), chloramphenicol resistance gene (Chloramphenicol (R)) and *ccdB* gene (ccdB)]; PDK intron (PDK); inverse Gateway® recombination cassette [comprised of Gateway® recombination sequences (*attR1* and *attR2*) and *ccdB* gene (ccdB)] OCS terminator sequence (OCS term); CaMV35S promoter (CaMV 35S); neomycin phosphotransferase gene (nptII); CaMV 35S 3'UTR poly A signal (CaMV35S polyA); and left border sequence (LB).

4.3.1.8 pMDC123 + 35Sx2 +EtOH + nos

The vectors pMDC100 + 35Sx2 + EtOH + nos (Figure 4.12) and pMDC123 (Table 4.2) were digested with *AleI* and *BlpI*. A fragment including the 35S promoter, *nptII* gene, CaMV35S polyA terminator, left border, and part of the kanamycin resistance gene was removed from pMDC100 + 35Sx2 + EtOH + nos and a similar fragment from pMDC123 including the 35S promoter, *bar* gene, CaMV35S polyA terminator, left border, and part of the kanamycin resistance gene was ligated in to create the pMDC123 + 35Sx2 + EtOH + nos vector (Figure 4.14).

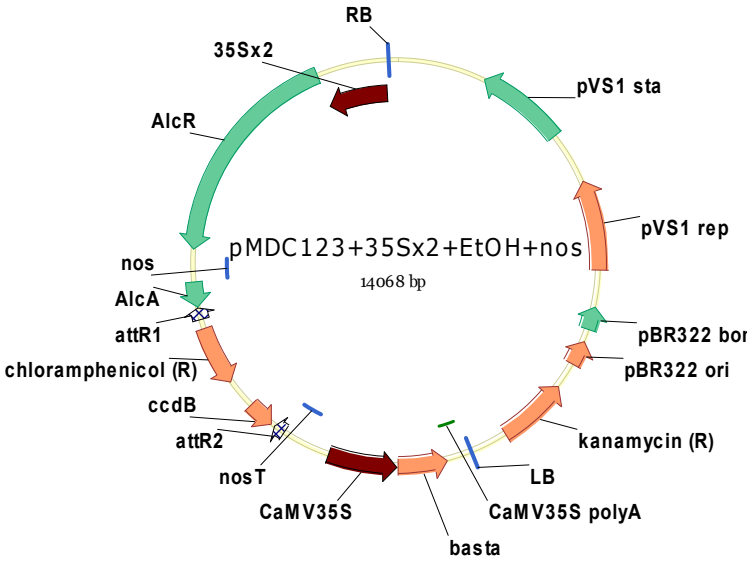

Figure 4.14: Vector diagram of pMDC123 + 35Sx2 +EtOH + nos used for ethanol-inducible gene overexpression in plants. From the right border sequence (RB) the T-DNA cassette contains: dually-enhanced CaMV35S promoter (35Sx2); AlcR transcription factor (AlcR); bacterial nopaline synthase terminator (nosT); alcA promoter (AlcA); Gateway® recombination cassette [comprised of Gateway® recombination sequences (*attR1* and *attR2*), chloramphenicol resistance gene (Chloramphenicol (R)) and *ccdB* gene (ccdB)]; bacterial nopaline synthase terminator (nosT); CaMV35S promoter (CaMV 35S); *bar* gene (basta (R)); CaMV 35S 3'UTR poly A signal (CaMV35S polyA); and left border sequence (LB).

4.3.1.9 pMDC123 + UAS + EtOH + nos

The pMDC100 + UAS + EtOH + nos vector (Figure 4.10) was restricted with *AleI*/*BlpI* to remove the *nptII* gene. The pMDC123 *AleI*/*BlpI* fragment (section 4.3.1.8), containing the *bar* gene, was then ligated into the linear pMDC100 + UAS + EtOH + nos vector. The resultant vector, designated pMDC123+UAS+EtOH+nos is shown in Figure 4.15.

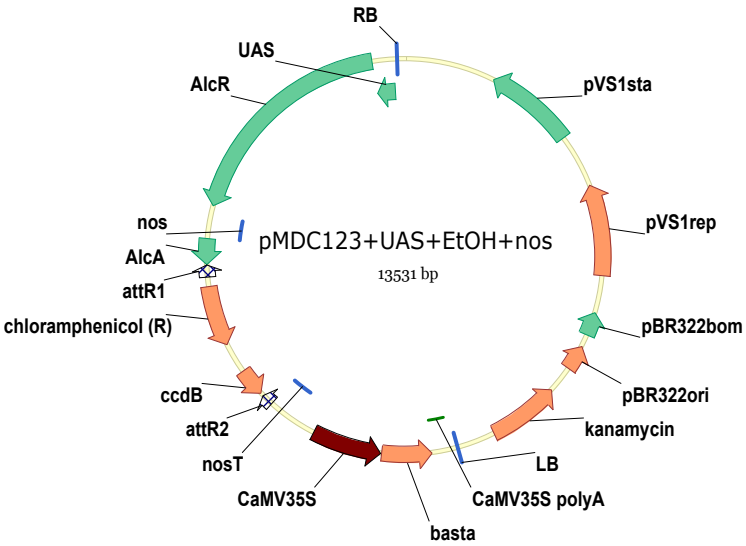

Figure 4.15: Vector diagram of pMDC123 + UAS + EtOH + nos used for cell-type specific, ethanol-inducible gene overexpression in GAL4-GFP enhancer trap *Arabidopsis* lines. From the right border sequence (RB) the T-DNA cassette contains: five tandem repeats of the upstream activation sequence element GAL4 binding site (UAS); AlcR transcription factor (AlcR); bacterial nopaline synthase terminator (nosT); alcA promoter (AlcA); Gateway® recombination cassette [comprised of Gateway® recombination sequences (*attR1* and *attR2*), chloramphenicol resistance gene (Chloramphenicol (R)) and *ccdB* gene (ccdB)]; bacterial nopaline synthase terminator (nosT); CaMV35S promoter (CaMV 35S); *bar* gene (basta (R)); CaMV 35S 3'UTR poly A signal (CaMV35S polyA); and left border sequence (LB).

4.3.1.10 pMDC123 + UAS + EtOH + RNAi

pMDC100+UAS+alcA-nos-AlcR was digested with *AleI* and *BlpI* to remove a fragment containing the *nptII* gene (section 4.3.1.4) and pMDC123 (Table 4.2) was digested with the same enzymes to remove a similar fragment containing the *bar* gene. The fragment containing the *bar* gene was then ligated into pMDC100 + UAS + alcA-nos-AlcR to create pMDC123 + UAS + alcA-nos-AlcR. This vector was digested with *AleI* and the *AleI* intron-OCS terminator fragment from pHellsgate8 (Table 4.2) was ligated into the linear vector. The resultant vector, designated pMDC123+UAS+EtOH+RNAi is shown in Figure 4.16.

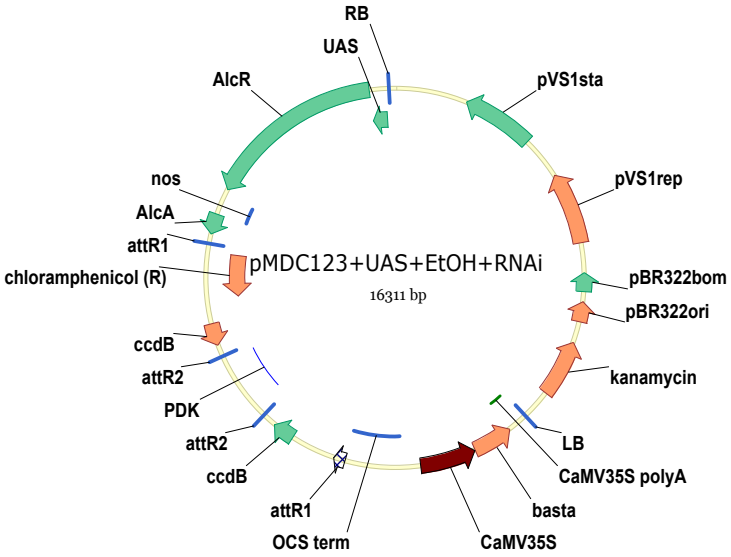

Figure 4.16: Vector diagram of pMDC123 + UAS + EtOH + RNAi used for cell-type specific, ethanol-inducible dsRNAi gene silencing in GAL4-GFP enhancer trap *Arabidopsis* lines. From the right border sequence (RB) the T-DNA cassette contains: five tandem repeats of the upstream activation sequence element GAL4 binding site (UAS); AlcR transcription factor (AlcR); bacterial nopaline synthase terminator (nosT); alcA promoter (AlcA); Gateway® recombination cassette [comprised of Gateway® recombination sequences (*attR1* and *attR2*), chloramphenicol resistance gene (Chloramphenicol (R)) and *ccdB* gene (ccdB)]; PDK intron (PDK); inverse Gateway® recombination cassette [comprised of Gateway® recombination sequences (*attR1* and *attR2*) and *ccdB* gene (ccdB)] OCS terminator sequence (OCS term); CaMV35S promoter (CaMV 35S); *bar* gene (basta (R)); CaMV 35S 3'UTR poly A signal (CaMV35S polyA); and left border sequence (LB).

4.3.1.11 pMDC99 + 35Sx2 + EtOH + nos

pMDC99 (Table 4.2) was cut with *AleI*/*BlpI* to remove the hygromycin resistance gene. Similiarly, pMDC100+35Sx2+EtOH+nos (Figure 4.12) was cut with *AleI*/*BlpI* to remove the *nptII* gene and the *AleI*/*BlpI* fragment containing the hygromycin resistance gene from pMDC99 was ligated in. The resultant vector, designated pMDC99+35Sx2+EtOH+nos is shown in Figure 4.17.

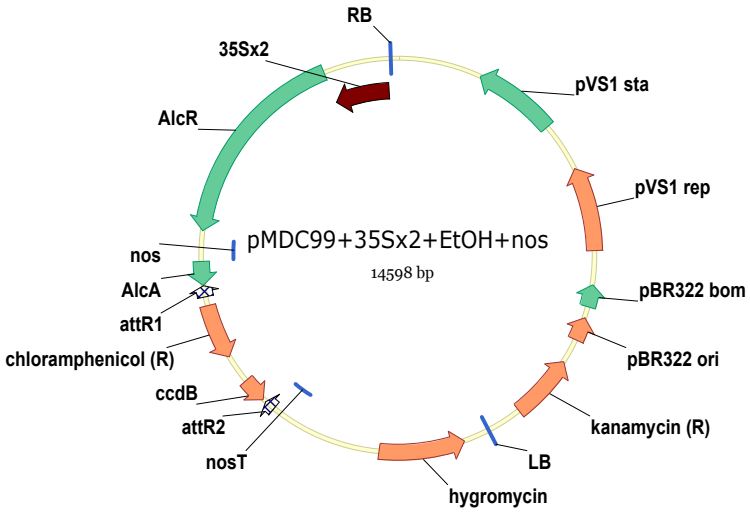

Figure 4.17: Vector diagram of pMDC99 + 35Sx2 + EtOH + nos used for ethanol-inducible gene overexpression in plants. From the right border sequence (RB) the T-DNA cassette contains: dually-enhanced CaMV35S promoter (35Sx2); AlcR transcription factor (AlcR); bacterial nopaline synthase terminator (nosT); alcA promoter (AlcA); Gateway® recombination cassette [comprised of Gateway® recombination sequences (*attR1* and *attR2*), chloramphenicol resistance gene (Chloramphenicol (R)) and *ccdB* gene (ccdB)]; bacterial nopaline synthase terminator (nosT); CaMV35S promoter (CaMV 35S) (not shown); hygromycin phosphotransferase gene (hygromycin (R)); CaMV 35S 3'UTR poly A signal (CaMV35S polyA) (not shown); and left border sequence (LB).

4.3.1.12 pMDC99 + 35Sx2 + EtOH + RNAi

pMDC100+35Sx2+alcA-nos-AlcR was digested with *AleI* and *BlpI* to remove a fragment containing the *nptII* gene (section 4.3.1.4) and pMDC99 (Table 4.2) was digested with the same enzymes to remove a similar fragment containing the hygromycin resistance gene. The fragment containing the hygromycin resistance gene was then ligated into pMDC100 + UAS + alcA-nos-AlcR to create pMDC99 + 35Sx2 + alcA-nos-AlcR. This vector was digested with *AleI* and the *AleI* intron-OCS terminator fragment from pHellsgate8 (Table 4.2) was ligated into the linear vector. The resultant vector, designated pMDC99 +35Sx2 + EtOH + RNAi is shown in Figure 4.18.

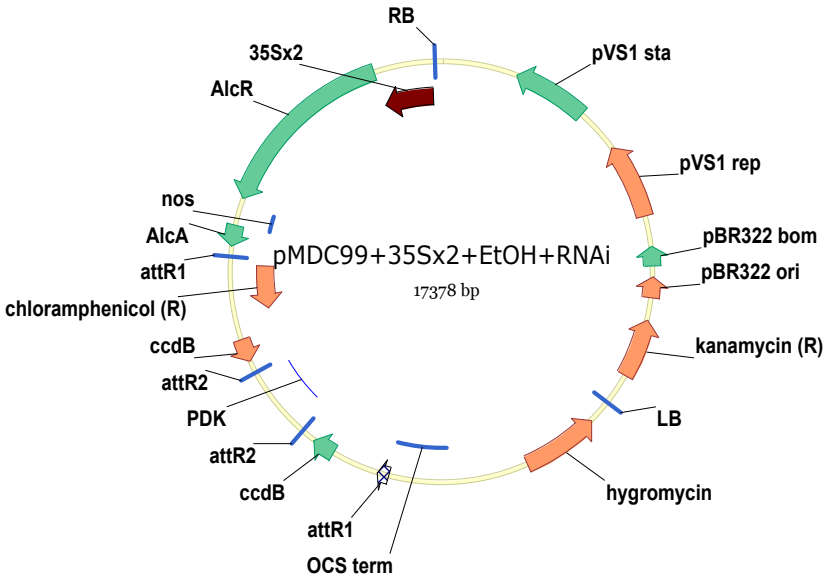

Figure 4.18: Vector diagram of pMDC99 + 35Sx2 + EtOH + RNAi used for ethanol-inducible dsRNAi gene silencing in plants. From the right border sequence (RB) the T-DNA cassette contains: dually-enhanced CaMV35S promoter (35Sx2); AlcR transcription factor (AlcR); bacterial nopaline synthase terminator (nosT); alcA promoter (AlcA); Gateway® recombination cassette [comprised of Gateway® recombination sequences (*attR1* and *attR2*), chloramphenicol resistance gene (Chloramphenicol (R)) and *ccdB* gene (ccdB)]; PDK intron (PDK); inverse Gateway® recombination cassette [comprised of Gateway® recombination sequences (*attR1* and *attR2*) and *ccdB* gene (ccdB)] OCS terminator sequence (OCS term); CaMV35S promoter (CaMV 35S) (not shown); hygromycin phosphotransferase gene (hygromycin (R)); CaMV 35S 3'UTR poly A signal (CaMV35S polyA) (not shown); and left border sequence (LB).

4.3.1.13 pMDC100 + UAS + nos

The pGreen-UAS-nos plasmid (Table 4.2) was used as a template in PCR with the oligonucleotides UAS*KpnI*F and UAS*AscI*R to amplify the UAS region. Primer UAS*KpnI*F included a *KpnI* restriction enzyme site at the 5' terminus and the primer UAS*AscI*R included an *AscI* restriction enzyme site for subsequent cloning steps. PCR was performed and the purified PCR product was cut with *KpnI* and *AscI*. The pMDC100 (Table 4.2) plasmid was cut with *KpnI* and *AscI* the compatible UAS fragment was ligated into the vector. The Nos terminator PCR fragment described above was then ligated into the pMDC100+UAS vector to generate pMDC100+UAS+nos (Figure 4.19).

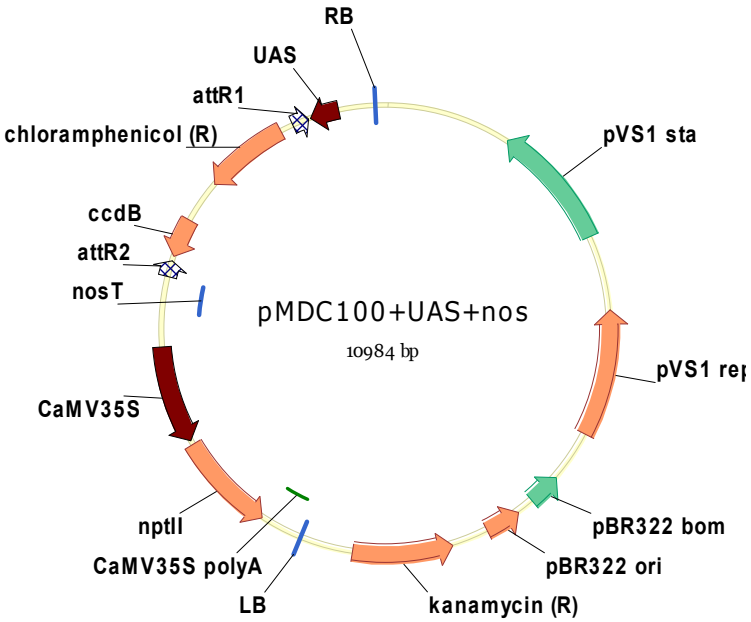

Figure 4.19: Vector diagram of pMDC100 + UAS + nos used for cell-type specific gene overexpression in GAL4-GFP enhancer trap rice lines. From the right border sequence (RB) the T-DNA cassette contains: five tandem repeats of the upstream activation sequence element GAL4 binding site (UAS); Gateway® recombination cassette [comprised of Gateway® recombination sequences (*attR1* and *attR2*), chloramphenicol resistance gene (Chloramphenicol (R)) and *ccdB* gene (ccdB)]; bacterial nopaline synthase terminator (nosT); CaMV35S promoter (CaMV 35S); neomycin phosphotransferase gene (nptII); CaMV 35S 3'UTR poly A signal (CaMV35S polyA); and left border sequence (LB).

4.3.1.14 pMDC100 + UAS + RNAi

pMDC100+UAS (section 4.3.1.13) was cut with *AleI* and the *AleI* intron-OCS terminator fragment from pHellsgate8 (Table 4.2) was ligated into the linear vector. The resultant vector, designated pMDC100+UAS+RNAi is shown in Figure 4.20.

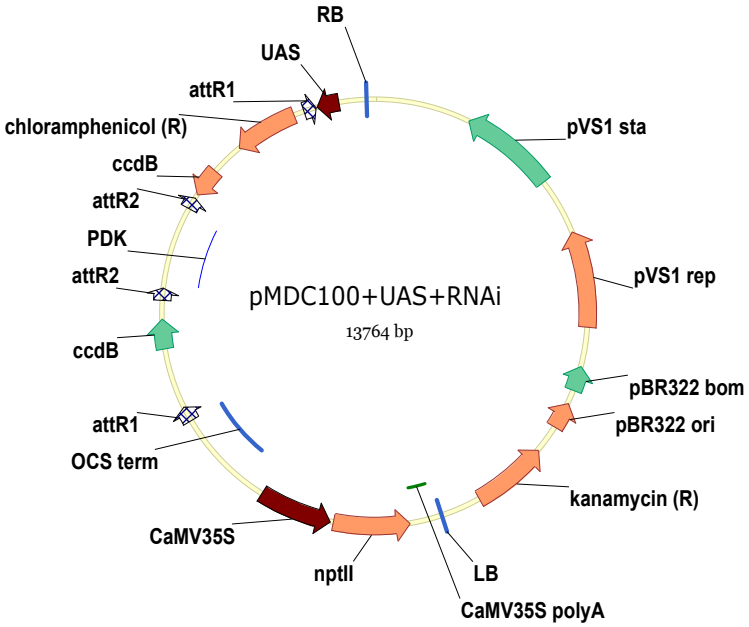

Figure 4.20: Vector diagram of pMDC100 + UAS + RNAi used for cell-type specific dsRNAi gene silencing in GAL4-GFP enhancer trap rice lines. From the right border sequence (RB) the T-DNA cassette contains: five tandem repeats of the upstream activation sequence element GAL4 binding site (UAS); Gateway® recombination cassette [comprised of Gateway® recombination sequences (*attR1* and *attR2*), chloramphenicol resistance gene (Chloramphenicol (R)) and *ccdB* gene (ccdB)]; PDK intron (PDK); inverse Gateway® recombination cassette [comprised of Gateway® recombination sequences (*attR1* and *attR2*) and *ccdB* gene (ccdB)] OCS terminator sequence (OCS term); CaMV35S promoter (CaMV 35S); neomycin phosphotransferase gene (nptII); CaMV 35S 3'UTR poly A signal (CaMV35S polyA); and left border sequence (LB).

4.3.1.15 pMDC123 + UAS + nos

pMDC123 (Table 4.2) was cut with *AleI* and *BlpI* to remove the *bar* gene. In a similar fashion the pMDC100 + UAS + nos plasmid (Figure 4.19) was cut with *AleI* and *BlpI* to remove the *nptII* gene. The *AleI*/*BlpI* Basta fragment was then ligated into the corresponding sites of the linear pMDC100 + UAS + nos vector (Figure 4.21).

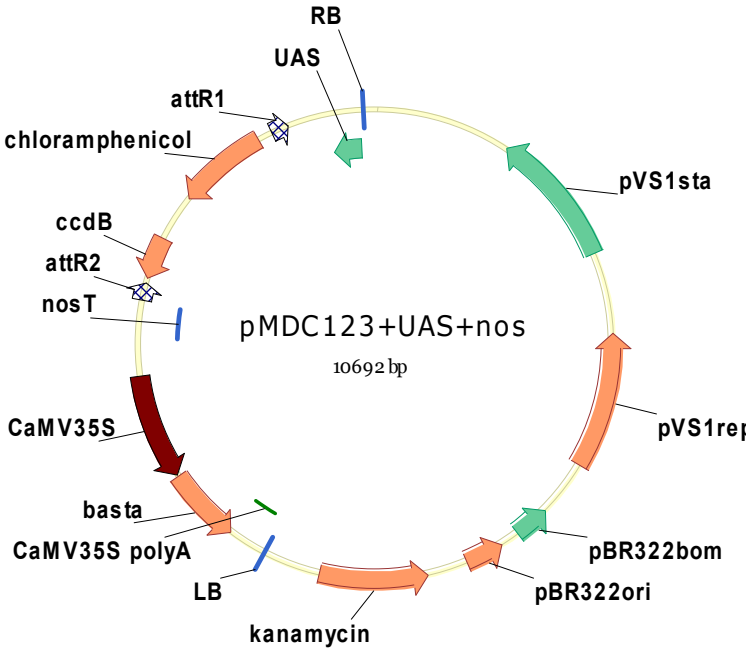

Figure 4.21: Vector diagram of pMDC123 + UAS + nos used for cell-type specific gene overexpression in GAL4-GFP enhancer trap *Arabidopsis* lines. From the right border sequence (RB) the T-DNA cassette contains: five tandem repeats of the upstream activation sequence element GAL4 binding site (UAS); Gateway® recombination cassette [comprised of Gateway® recombination sequences (*attR1* and *attR2*), chloramphenicol resistance gene (Chloramphenicol (R)) and *ccdB* gene (ccdB)]; bacterial nopaline synthase terminator (nosT); CaMV35S promoter (CaMV 35S); *bar* gene (basta (R)); CaMV 35S 3'UTR poly A signal (CaMV35S polyA); and left border sequence (LB).

4.3.1.16 pMDC123 + UAS + RNAi

pMDC100 + UAS (section 4.3.1.13) and pMDC123 (Table 4.2) were cut with *AleI* and *BlpI* to remove fragments containing *nptII* and *bar* genes, respectively. The fragment containing *bar* was ligated into the linear pMDC100 + UAS to create pMDC123 + UAS. pMDC123+UAS was then cut with *AleI* and the *AleI* intron-OCS terminator fragment from pHellsgate8 (Table 4.2) was ligated into the linear vector. The resultant vector, designated pMDC123+UAS+RNAi is shown in Figure 4.22.

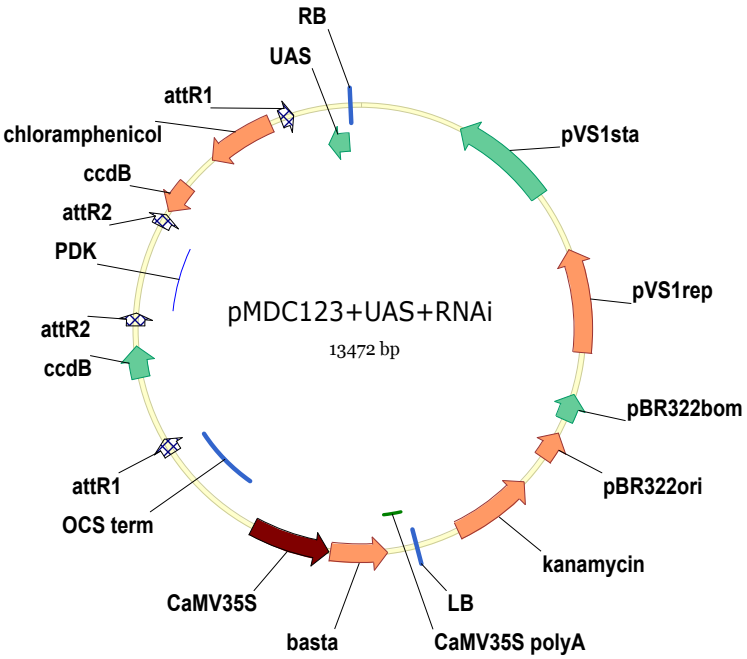

Figure 4.22: Vector diagram of pMDC123 + UAS + RNAi used for cell-type specific dsRNAi gene silencing in GAL4-GFP enhancer trap *Arabidopsis* lines. From the right border sequence (RB) the T-DNA cassette contains: five tandem repeats of the upstream activation sequence element GAL4 binding site (UAS); Gateway® recombination cassette [comprised of Gateway® recombination sequences (*attR1* and *attR2*), chloramphenicol resistance gene (Chloramphenicol (R)) and *ccdB* gene (ccdB)]; PDK intron (PDK); inverse Gateway® recombination cassette [comprised of Gateway® recombination sequences (*attR1* and *attR2*) and *ccdB* gene (ccdB)] OCS terminator sequence (OCS term); CaMV35S promoter (CaMV 35S); *bar* gene (basta (R)); CaMV 35S 3'UTR poly A signal (CaMV35S polyA); and left border sequence (LB).

4.3.1.17 pMDC100 + alcA + nos + *bar*

The alcA promoter was PCR amplified from the pJH0022 plasmid (Table 4.2) with the primers AlcA*PmeI*F and Eth*AscI*R. The purified PCR product was digested with *AscI* and *PmeI*. pMDC100 + UAS + nos (Figure 4.19) was digested with *AscI* and *PmeI* to remove the UAS fragment. The digested alcA promoter was ligated into the linear pMDC100 + UAS +nos to create pMCD100 + alcA + nos. A fragment containing the 35S promoter, *bar* gene and CaMV35S polyA was PCR amplified from pMDC123 (Table 4.2) with the primers polyA*SacI*F and 35S*SacI*R. The purified product was digested with *SacI*. The pMDC100 + alcA + nos vector was digested with *SacI* and the 35S-*bar*-polyA fragment was ligated in to create pMDC100 + alcA + nos + *bar* (Figure 4.23).

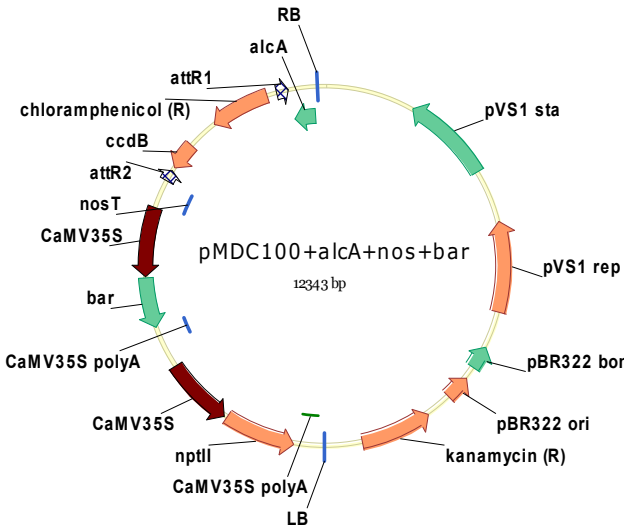

Figure 4.23: Vector diagram of pMDC100 + alcA + nos + *bar* used for crossing transgenes into lines expressing *RFP* inducibly via the ethanol switch in order to inducibly overexpress transgenes. From the right border sequence (RB) the T-DNA cassette contains: alcA promoter (AlcA); Gateway® recombination cassette [comprised of Gateway® recombination sequences (*attR1* and *attR2*), chloramphenicol resistance gene (Chloramphenicol (R)) and *ccdB* gene (ccdB)]; CaMV35S promoter (CaMV 35S); *bar* gene (basta (R)); CaMV35S promoter (CaMV 35S); neomycin phosphotransferase gene (nptII); CaMV 35S 3'UTR poly A signal (CaMV35S polyA); and left border sequence (LB).

4.3.1.18 pMDC100 + alcA + RNAi + *bar*

The *AscI*/*PmeI* digested alcA promoter fragment (section 4.3.1.17) was ligated into the pMDC100 + UAS vector (section 4.3.1.13), which had also been digested with *AscI*/*PmeI* to create pMDC100 + alcA. This vector was digested with *AleI* and the *AleI* digested INT-OCS fragment (section 4.3.1.2) was ligated in to create pMDC100 + alcA + RNAi. The *SacI* digested 35S-*bar*-polyA fragment (section 4.3.1.17) was ligated into the *SacI* digested pMDC100 + alcA + RNAi vector to create pMDC100 + alcA + RNAi + *bar* (Figure 4.24).

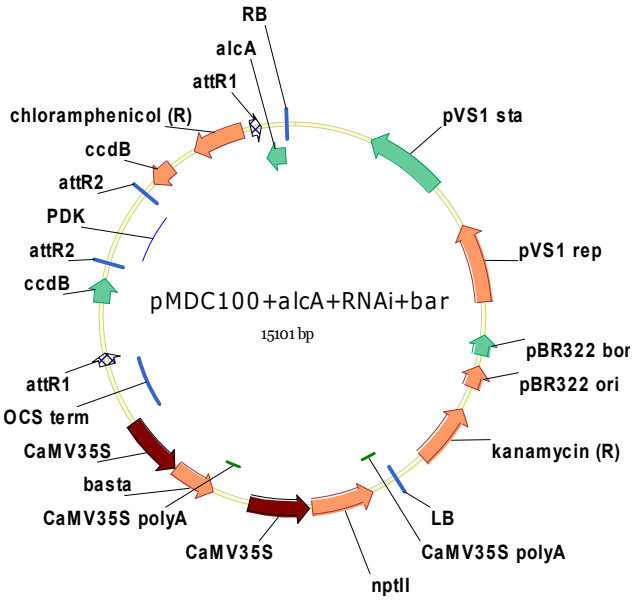

Figure 4.24: Vector diagram of pMDC100 + alcA + RNAi + *bar* used for crossing dsRNAi constructs into lines expressing *RFP* inducibly via the ethanol switch in order to inducibly silence genes. From the right border sequence (RB) the T-DNA cassette contains: alcA promoter (AlcA); Gateway® recombination cassette [comprised of Gateway® recombination sequences (*attR1* and *attR2*), chloramphenicol resistance gene (Chloramphenicol (R)) and *ccdB* gene (ccdB)]; PDK intron (PDK); inverse Gateway® recombination cassette [comprised of Gateway® recombination sequences (*attR1* and *attR2*) and *ccdB* gene (ccdB)] OCS terminator sequence (OCS term); CaMV35S promoter (CaMV 35S); *bar* gene (basta (R)); CaMV35S promoter (CaMV 35S); neomycin phosphotransferase gene (nptII); CaMV 35S 3'UTR poly A signal (CaMV35S polyA); and left border sequence (LB).

4.3.2 Rice transformation

4.3.2.1 1st transformation

The ability of the GAL4-GFP system to drive cell-type specific expression of transgenes was combined with the ethanol switch to enable cell-type specific and inducible expression of transgenes. The constructed vectors were trialled using *GFP*, *RFP* and *GUS* reporter genes in order to determine visually whether the vectors were functioning as intended. Several of the constructs described above were used to drive expression of the reporters in WT Nipponbare or the root-specific GAL4-GFP enhancer trap line (AOS A05). All three reporters were used in the WT transformations, while *RFP* and *GUS* were used in the enhancer trap transformations. Reporter genes were cloned into the Gateway®-enabled destination vectors via LR Clonase II (Invitrogen) cloning protocol (section 4.2.2) (Table 4.6).

Table 4.6: 1st round of rice transformation including the background line, vector construct reporter gene (GOI) and the number of independent T_0 plants produced.

Transformation Number	Background Line	Vector Construct	GOI	Number of Transformants
1	WT Nipponbare	pMDC100 + 35Sx2 + EtOH + nos	*RFP*	28
2	WT Nipponbare	pMDC100 + 35Sx2 + EtOH + nos	*GUS*	24
3	WT Nipponbare	pMDC100 + 35Sx2 + EtOH + nos	*GFP*	36
4	WT Nipponbare	pMDC32	*RFP*	16
5	WT Nipponbare	pMDC32	*GFP*	12
6	WT Nipponbare	pMDC32	*GUS*	14
7	GAL4-GFP Root-specific	pMDC100 + UAS + EtOH + nos	*RFP*	41
8	GAL4-GFP Root-specific	pMDC100 + UAS + EtOH + nos	*GUS*	36
9	GAL4-GFP Root-specific	pMDC100 + UAS + nos	*RFP*	26
10	GAL4-GFP Root-specific	pMDC100 + UAS + nos	*GUS*	10
TOTAL				**229**

4.3.2.1.1 Reporter gene expression in callus

Reporter gene fluorescence was analysed in transformed calli (spare calli not intended for plant regeneration) in response to an ethanol vapour treatment as an early indication of whether the ethanol-inducible component of the system was functioning correctly. The tissue culture system can become oxygen-limiting to the growth of cells on media, thus some background expression of reporter genes prior to ethanol treatment was observed in some of the calli examined (Figure 4.25). After a 5 min ethanol vapour treatment, GFP fluorescence intensity increased substantially in most of the examined calli. Noticeable fluorescence increases occurred as early as 1 h after treatment and climbed steadily to an apparent maximum 70 h after treatment at which point fluorescence decreased to a level similar to prior induction.

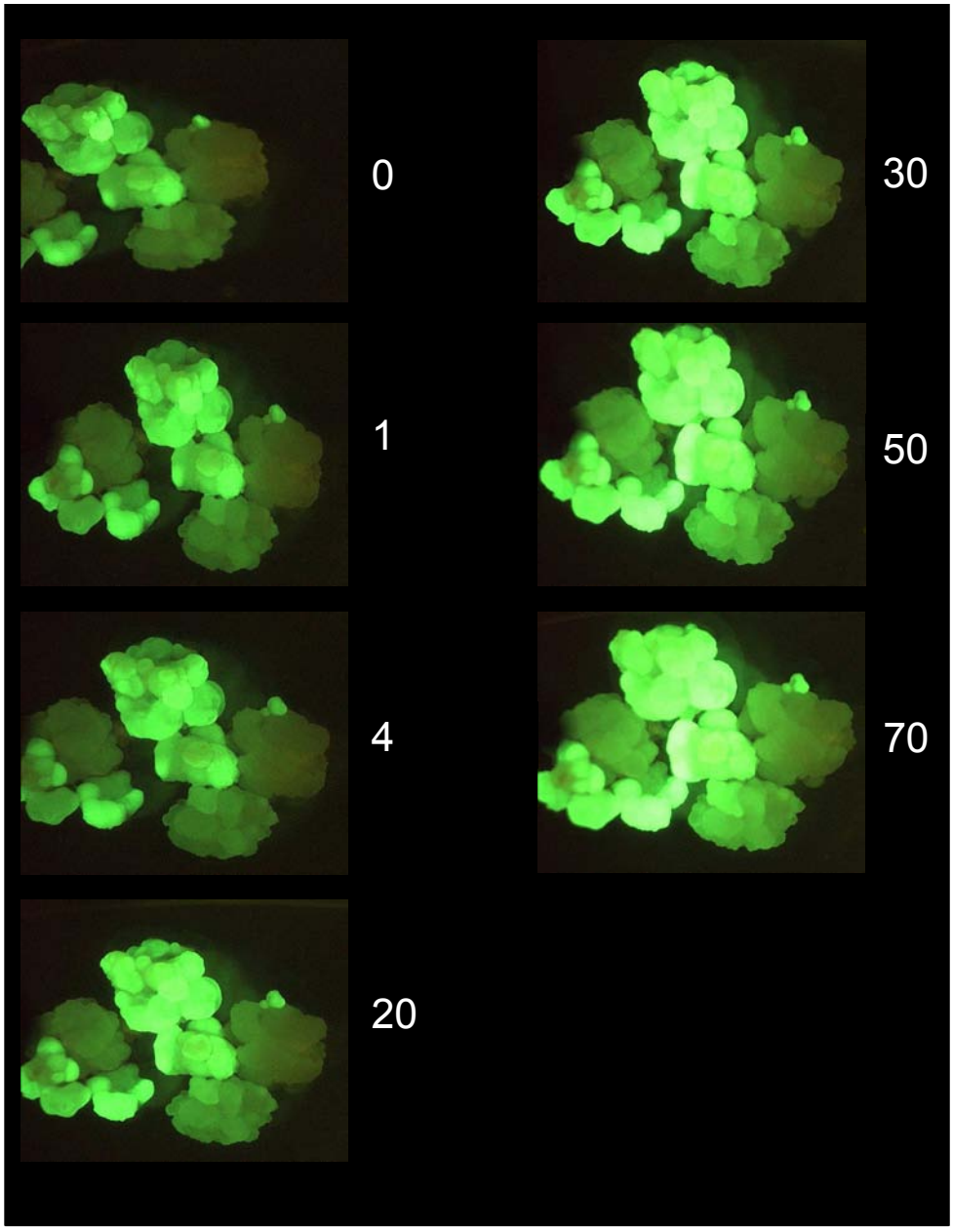

Figure 4.25: Ethanol switch test on AOS A05 calli transformed with pMDC100 + UAS + EtOH + nos construct to cell-type specifically express *GFP* in an ethanol-inducible manner. Calli were treated with 100 % ethanol vapour for 5 min and images (same microscope and camera settings in all images) were taken at successive time points following induction showing efficient induction of GFP fluorescence by ethanol indicating the successful function of the expression system. Time points are hours following induction and time point 0 is immediately prior to induction.

4.3.2.1.2 Reporter gene expression in plants

Based on the success of the calli experiment, the T_0 plants (GAL4-GFP line transformed with pMDC100 + UAS + EtOH + nos with *RFP*) were examined to determine if the system would be viable in plants as well. Prior to induction a few lines were observed to have RFP fluorescence in a root-specific pattern resembling the enhancer trap GFP pattern. Several of the lines did not express *RFP* following the ethanol treatment, despite expressing *GFP* in the original enhancer trap. However, approximately half of the lines did not have RFP fluorescence (or weak RFP fluorescence) prior to ethanol treatment and significantly increased RFP fluorescence over the course of 3 d, then fluorescence decreased to the level it was at prior to treatment (Figure 4.26). Based on these results, we decided that a second round of transformation was warranted because the system appeared to be functioning as expected. Thus, a full characterisation of this set of plants was not carried out in favour of more fully characterising the plants from the second round of transformation which had more specific and biologically interesting patterns of expression (Chapter 5).

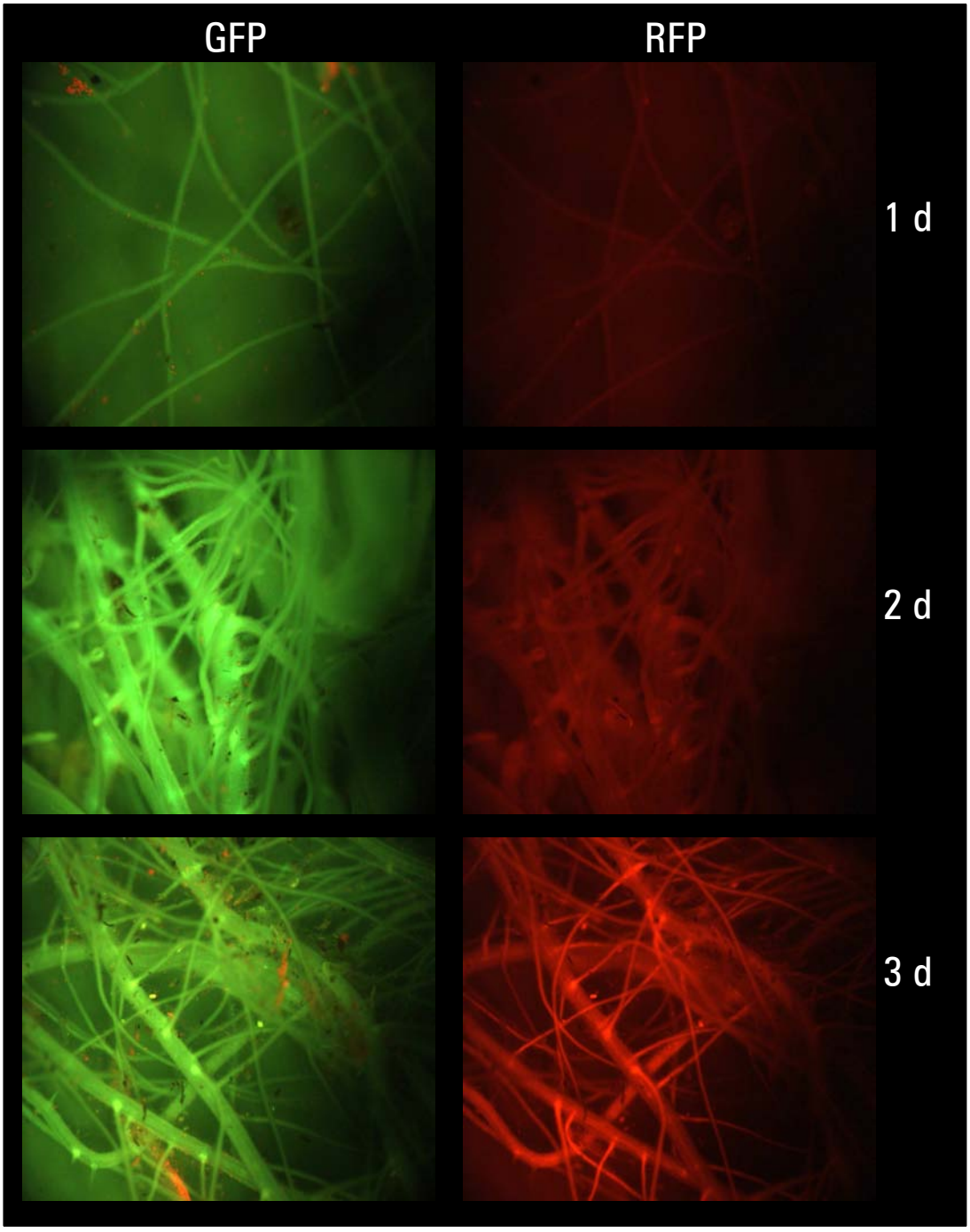

Figure 4.26: Ethanol switch test of T_0 plants from transformation number 7 in 1st round of rice transformation (pMDC100 + UAS + EtOH + nos used to express *RFP* in root specific GAL4-GFP enhancer trap line AOS A05). Ethanol (1 %) was applied for 24 h in the growth solution and images were taken for the 3 d following induction and show increase in RFP fluorescence with ethanol induction.

4.3.2.2 2nd rice transformation

The same Gateway®-enabled destination vectors (Table 4.5) trialled in the first transformation (section 4.3.2.1) were used to express *AtHKT1;1*, *PpENA1* and *RFP* (Table 4.7). The genes were cloned from Gateway® entry vectors into the Gateway®-enabled destination vectors via LR Clonase II (Invitrogen) mediated cloning protocol (section 4.2.2). Again 35S and 35S::Ethanol Switch constructs were transformed into WT Nipponbare. All UAS and UAS::Ethanol Switch constructs were transformed into the epidermis/cortex (Outer) and xylem parenchyma (Inner) GAL4-GFP enhancer trap lines, described in section 4.2.6. Transformed plants inducibly expressing *AtHKT1;1*, *PpENA1* and *RFP* are discussed in Chapter 5, while plants cell-specifically expressing *AtHKT1;1* and *PpENA1* are discussed in Chapter 6 and 7, respectively.

Table 4.7: 2nd round of rice transformations listing background line, vector construct, transgene (GOI) and the number of T_0 independent transgenic lines produced.

Transformation Number	Background Line	Vector Construct	GOI	Number of Transformants
1	GAL4-GFP Outer	pMDC100 + UAS + nos	*PpENA1*	15
2	GAL4-GFP Outer	pMDC100 + UAS + nos	*AtHKT1;1*	16
3	GAL4-GFP Outer	pMDC100 + UAS + nos	*RFP*	19
4	GAL4-GFP Inner	pMDC100 + UAS + nos	*PpENA1*	16
5	GAL4-GFP Inner	pMDC100 + UAS + nos	*AtHKT1;1*	19
6	GAL4-GFP Inner	pMDC100 + UAS + nos	*RFP*	14
7	GAL4-GFP Outer	pMDC100 + UAS + EtOH + nos	*PpENA1*	25
8	GAL4-GFP Outer	pMDC100 + UAS + EtOH + nos	*AtHKT1;1*	38
9	GAL4-GFP Outer	pMDC100 + UAS + EtOH + nos	*RFP*	38
10	GAL4-GFP Inner	pMDC100 + UAS + EtOH + nos	*PpENA1*	42
11	GAL4-GFP Inner	pMDC100 + UAS + EtOH + nos	*AtHKT1;1*	37
12	GAL4-GFP Inner	pMDC100 + UAS + EtOH + nos	*RFP*	38
13	WT Nipponbare	pMDC100 + 35Sx2 + nos	*PpENA1*	10
14	WT Nipponbare	pMDC100 + 35Sx2 + nos	*AtHKT1;1*	19
15	WT Nipponbare	pMDC100 + 35Sx2 + nos	*RFP*	19
16	WT Nipponbare	pMDC100 + 35Sx2 + EtOH + nos	*PpENA1*	30
17	WT Nipponbare	pMDC100 + 35Sx2 + EtOH + nos	*AtHKT1;1*	28
18	WT Nipponbare	pMDC100 + 35Sx2 + EtOH + nos	*RFP*	28
TOTAL				451

4.4 General Discussion

4.4.1 amiRNA-mediated silencing of *AtHKT1;1*

The precise role of AtHKT1;1 in *Arabidopsis* has been controversial with roles in Na^+ influx into roots and recirculation of Na^+ in phloem being early suggestions (Rus *et al.* 2001, Berthomieu *et al.* 2003). Detailed Na^+ flux analysis and mathematical modelling of *athkt1;1* knockout plants has shown that AtHKT1;1 apparently has a role in both root vacuolar loading and in retrieval of Na^+ from the xylem (Davenport *et al.* 2007). The question still remains whether AtHKT1;1 actually controls two separate Na^+ transport functions or whether one apparent role is related to the compensatory actions of the knockout plant to deal with the absence of a crucial Na^+ transporter. With this in mind, inducible gene silencing constructs were built and transformed into Col-0 *Arabidopsis* plants. Col-0 was chosen since, as mentioned above, there is evidence that other ecotypes have altered *AtHKT1;1* expression in their roots so would not provide an accurate starting point to disrupt *AtHKT1;1* expression. Gene silencing was undertaken using the artificial microRNA (amiRNA) technique. This method of gene silencing uses site-directed mutagenesis to alter an endogenous *Arabidopsis* pre-miRNA (miR319a) to create an amiRNA that will specifically silence the gene (or genes) of interest. A web-based amiRNA designer is used to determine the precise sequence of the amiRNA required to silence the gene of interest and whether there are any potential off-targets of the chosen amiRNA. Gene silencing via double-stranded RNA (dsRNAi) requires cloning of approximately 150 bp of the gene target, which is processed into 21 bp pieces by the RNA processing machinery of the plant, thus potential off-target silencing may be more probable with that technique. Thus, with ethanol induction *AtHKT1;1* is silenced, providing the opportunity to vary the degree of silencing based on the ethanol treatment. So, as is the case with inducible overexpression of *AtHKT1;1*, inducible gene silencing of *AtHKT1;1* provides the opportunity to silence the gene immediately prior to the physiological experiment being undertaken and thus may allow the function of the gene to be dissected from compensatory regulation by the plant. It also offers the opportunity to use microarrays to identify potential genes which are regulated differentially in response to the loss of *AtHKT1;1*.

4.4.2 Inducible overexpression of *RFP* and *AtHKT1;1* in *Arabidopsis*

The ethanol switch was used to inducibly overexpress and silence *AtHKT1;1* in *Arabidopsis*. Development of transgenic *Arabidopsis* plants overexpressing *AtHKT1;1* has been difficult since the gene appears to have negative effects on plant growth and development when expressed constitutively (D Jha and M Tester, unpublished data). Thus, it is difficult to determine the function of the gene when there is the confounding variable of weak plant growth affecting Na^+ transport. To separate these effects, *AtHKT1;1* was inducibly overexpressed in both the Col-0 and C-24 *Arabidopsis* ecotypes. It has been shown that C-24 plants accumulate up to 5 times the amount of Na^+ in their shoots as Col-0 plants (S Roy, D Jha and M Tester, unpublished results). Also, C-24 plants have little or no expression of *AtHKT1;1* in their roots (shoot expression appears very similar to Col-0). Similar Na^+ accumulation phenotypes have been found in two other ecotypes (Ts-1 and Tsu-1), and appears to be caused by a deletion in the *AtHKT1;1* promoter region, which eliminates their root *AtHKT1;1* expression without altering shoot *AtHKT1;1* expression (Rus *et al.* 2006). The two ecotypes are also more Na^+ tolerant than Col-0, which indicates Na^+ accumulation and Na^+ tolerance are unrelated in these ecotypes. When *AtHKT1;1* is overexpressed in Col-0 via the 35S promoter, shoot Na^+ accumulation is nearly double the level of the Col-0 WT. When *AtHKT1;1* is overexpressed in C-24 via the 35S promoter, shoot Na^+ is unchanged from the C-24 WT. Potentially, these results are obscured by the effect of *AtHKT1;1* overexpression on plant health, thus they may not reflect the true story. For instance, a moderate level of *AtHKT1;1* expression in the root xylem parenchyma (where the gene has been shown to function) in C-24 should, in theory, compensate for the lack of root *AtHKT1;1* expression in this line and restore the Col-0-like phenotype. However, strong overexpression (via the CaMV35S promoter) may be masking the positive effect of *AtHKT1;1* expression would have on shoot Na^+ accumulation in C-24. By expressing the gene inducibly, varying expression levels could be experimented with to deduce whether a mild overexpression of *AtHKT1;1* would rescue the phenotype. In a similar vein, overexpression of *AtHKT1;1* in Col-0 (which already has high root *AtHKT1;1* expression) may just result in negative growth effects, but a milder overexpression may improve the Na^+ transport phenotype.

CHAPTER 5: CELL TYPE-SPECIFIC, ETHANOL-INDUCIBLE EXPRESSION OF TRANSGENES

5.1 Introduction

More precise control over transgene expression in plants is a major goal in plant functional genomics. The inferred function of a particular transgene may change dramatically depending on the tissue type and/or growth stage the gene is expressed in. Thus, control over gene expression in both time and space is desirable.

The GAL4-GFP enhancer trap lines are useful not only for trapping enhancer elements involved in defining gene expression, but the GAL4 system can also be used to express transgenes ectopically in specific cell-types. This provides an excellent opportunity to express transgenes in cell-types which may not be otherwise possible with the current availability of cell type-specific promoters. The GAL4 system also provides the opportunity to screen for enhancer elements responsible for gene expression over time, such as elements expressed during specific growth stages of the plant or under particular growth or stress conditions. Again, the GAL4 system can be used to ectopically express transgenes in the temporal expression patterns of these enhancer elements. The difficulty of the screening required to identify temporally regulated enhancer elements has hindered their discovery, but chemical-inducible promoter systems can be used to provide similar control of gene expression in time.

Vectors were built to combine the spatial control provided by the GAL4 system with the temporal control of the ethanol switch, by fusing the GAL4 UAS to the ethanol switch (Chapter 4). These constructs were transformed into enhancer trap lines displaying GFP fluorescence in cell-type specific patterns of the root. The trapped enhancer will drive expression of the ethanol switch in the same pattern as the GFP fluorescence, thus the expression of a transgene fused to the ethanol switch will be both cell-type specific and ethanol inducible. The ethanol switch was chosen for the temporal component because it does not contain any GAL4 binding elements as do many other chemical-inducible gene switches that are commonly used in plants (e.g. dexamethasone-inducible system). The GAL4 binding element in an inducible switch could be affected by the GAL4 being driven by the trapped enhancer element, thus

driving expression even without the presence of the chemical inducer. Combination of the ethanol switch and the GAL4 system has recently been used in *Arabidopsis* by two groups to drive GUS activity in specific cell-types (Sakvarelidze *et al.* 2007, Jia *et al.* 2007), but this is the first time that this approach has been described in a cereal species.

The functional study of transporters is especially suited to this type of approach because their expression in different cell-types can result in different transport phenotypes. Also, constitutive overexpression has been shown to be detrimental at times to plant health and can result in up or down regulation of related and/or unrelated endogenous genes to compensate for the expressed gene. For these reasons, AtHKT1;1, the sodium transporter from *Arabidopsis*, and PpENA1, the Na^+-pumping ATPase from *Physcomitrella patens* were spatially and temporally expressed in rice using the GAL4-ethanol switch system to examine how Na^+ transport would be affected. The genes were chosen because of their importance to sodium transport in their respective species. Expressing them in rice may improve the sodium tolerance of rice and could give insight into the function of the two genes. The red fluorescent protein (*RFP*) was also expressed in this manner to provide initial proof-of-concept for the expression system.

5.2 Materials and Methods

5.2.1 Plant Material

Production of all rice lines in this chapter is described completely in Chapter 4 – Vector Construction and Transgenic Production (Table 4.3). The construct pMDC100 + UAS + EtOH + nos was used to cell-type specifically and inducibly overexpress *PpENA1* and *AtHKT1;1* in root xylem parenchyma (Transformation numbers 10 and 11). The same construct pMDC100 + UAS + EtOH + nos was used to cell-specifically and inducibly overexpress *RFP*. This construct was transformed into both epidermis/cortex (Transformation number 9 – Outer EtOH RFP) and xylem parenchyma (Transformation number 12 – Inner EtOH RFP) specific GAL4-GFP enhancer trap lines. The construct pMDC100 + 35S + EtOH + nos was also used to inducibly overexpress *RFP* (Transformation number 18 – 35S::EtOH::*RFP*).

5.2.2 Ethanol induction

T_0 plants were grown in Jiffy peat pots in plastic trays containing growth solution (RO water, Osmocote, and 5 mM NH_4NO_3). To induce gene expression, growth solution was replaced with growth solution supplemented with 1% ethanol for 24 h (Caddick *et al.* 1998) and plants were covered in plastic domes in order to allow ethanol vapors to accumulate and aid in induction (Sweetman *et al.* 2002). Following induction period, ethanol-free growth solution was returned and plants were cultured normally.

5.2.3 Tissue sampling and Q-PCR analysis of *PpENA1* and *AtHKT1;1* lines

Roughly 100 mg of total root tissue was harvested from primary transgenic plants and placed into 96-well plates. One root sample was taken immediately prior to the ethanol induction and a second was taken 2 d after ethanol induction (i.e. 3 d total between root sampling dates). Total RNA was extracted from all lines and cDNA (20 µL) was synthesised from 2 µL of RNA at AGRF (Adelaide). The original cDNA was diluted 1 in 20 and submitted to Neil Shirley (ACPFG) for Q-PCR analysis. However, it was found that transgene expression levels were extremely low (below a level that could be assumed to be more than 'background noise'), thus Q-PCR was repeated (only on samples from transformations 10 and 11) using a 1 in 2 dilution of the original cDNA. Analysis of cDNA from transgenic plants expressing *PpENA1* (see Chapter 4 – transformation numbers 7, 10 and 16) used *PpENA1* primers (Forward primer – AAGGCATTACCTGGGAGTGGA; Reverse primer – TCACATGTTGTAGGGAGTT; product size – 116 bp) and run in conditions as in Burton *et al.* 2004. Analysis of cDNA from transgenic plants expressing *AtHKT1;1* (see Chapter 4 – transformation numbers 8, 11 and 17) used *AtHKT1;1* primers (Forward primer – CCTCCATACACTTTATTTATGC; Reverse primer – CGGTGATTGAAATGAGAAAGAT; product size – 160 bp). Data was normalised against the control gene *OsGAPDH* (glyceraldehyde-3-phosphate-dehydrogenase) (Forward primer – GGGCTGCTAGCTTCAACATC; Reverse primer – TTGATTGCAGCCTTGATCTG; product size – 190 bp) copy numbers.

The Q-PCR data was normalised in two different ways. The first normalisation was carried out by averaging all the raw copy numbers of *OsGAPDH* in the cDNA

samples from one transformation (pre- and post-ethanol treatment). The *OsGAPDH* copy number in each individual cDNA sample was divided by the average *OsGAPDH* copy number to derive a normalisation factor for each sample. The transgene copy number was then divided by the individual normalisation factor to arrive at a normalised transgene copy number for each sample.

Since there was an extremely large difference in *OsGAPDH* copy numbers between the samples harvested pre- and post-ethanol treatment, the data was also normalised separately for pre- and post-ethanol samples. The raw copy numbers of *OsGAPDH* in the cDNA samples from one transformation were averaged separately for samples collected pre- or post-ethanol treatment. The *OsGAPDH* copy number in each individual cDNA sample was divided by its appropriate average *OsGAPDH* copy number to derive a normalisation factor for each sample. The transgene copy number was then divided by the individual normalisation factor to arrive at a normalised transgene copy number for each sample.

5.2.4 Screening of the RFP lines

Roots were analysed for RFP fluorescence immediately prior to ethanol induction and every 2 d post-ethanol induction. Roots were sampled by excising two root pieces approximately 2 cm in length (including the root tip) into individual wells containing growth solution in a 24-well plate. Plates were taken to the imaging lab and fluorescence was detected using a Leica MZ FLIII fluorescence stereomicroscope (Leica Microscopie Systemes SA, Heerbrugg, Switzerland) and a GFP Plus fluorescence filter set [GFP2, 480 nm excitation filter (bandwidth of 40 nm) and 510 nm barrier filter] for GFP fluorescence or a dsRED filter set (556 nm excitation filter and 586 nm barrier filter) for RFP fluorescence. Fluorescence was reported qualitatively as none, weak, medium or strong relative to all the samples examined each day. Microscope stage height and imaging settings remained the same to eliminate bias in fluorescence estimations. Images were collected using a Leica DC 300F digital camera.

5.3 Results and Discussion

5.3.1 Q-PCR analysis background

It was decided to check a subset of the samples of the lines described in Chapter 4 (Table 4.3) to ensure the expression system was functional before undertaking costly, labour intensive analysis of the entire set of lines. The lines expressing *PpENA1* and *AtHKT1;1* xylem parenchyma-specifically, inducibly were chosen as the subset (Transformations 10 and 11).

5.3.2 Q-PCR analysis of *PpENA1* lines from Transformation 10

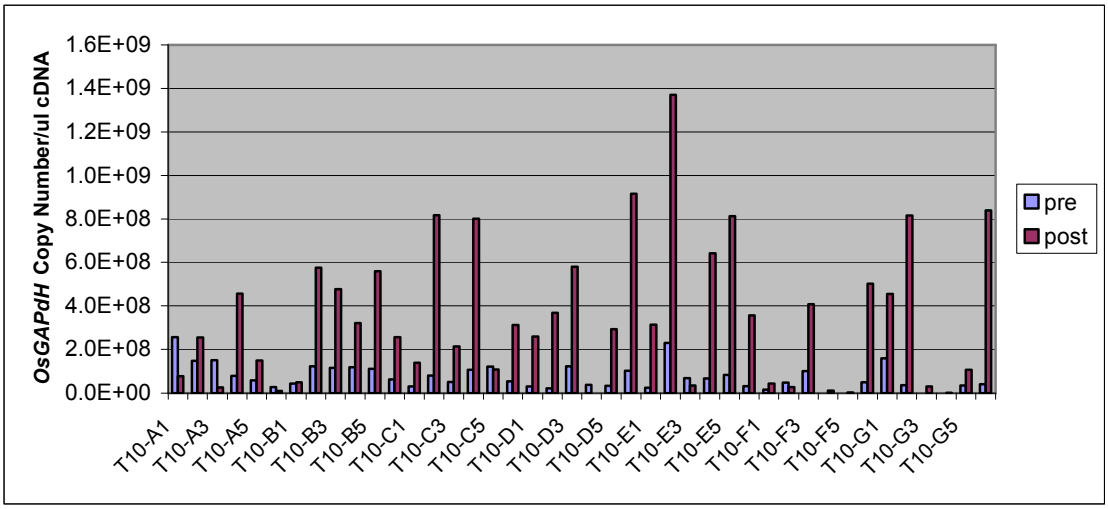

Figure 5.1: *OsGAPDH* expression (*OsGAPDH* copy number/µl cDNA) in independent T_0 lines (Transformation 10) expressing *PpENA1* in the xylem parenchyma root cells of rice under control of the ethanol switch. Values are pre- and post- a 24 h ethanol treatment (1%).

OsGAPDH was used as a control gene for the purpose of normalisation of transgene expression (only one control gene was run because of the sheer number of samples requiring analysis and it was to be a rough 'first glance' to choose lines to analyse more completely). Expression of *OsGAPDH* in the lines from Transformation 10 (xylem parenchyma-specific, inducible expression of *PpENA1*) was significantly higher (up to 10 fold higher) in the root samples harvested post-ethanol treatment than in those harvested pre- ethanol treatment (Figure 5.1). This is most likely related to variation in the quantity of RNA which was used to synthesise cDNA from pre- and post-ethanol treatment samples (the two sets of samples were on different plates in the

extraction and synthesis procedure). This cannot be verified because the RNA extraction and cDNA synthesis was outsourced, but it is known that the procedure involved using a standard volume of RNA for cDNA synthesis instead of a standard mass (synthesis occurred robotically, in 96-well plates), thus this explanation is entirely plausible. Analysis of a few RNA concentrations across the plates revealed large variation in quantity, thus this is likely the answer.

It cannot be ruled out that *OsGAPDH* expression is induced by ethanol treatment. It has been reported that the gene may not be an appropriate control gene as expression can be regulated by stress treatments (Kim *et al.* 2003), thus it is possible that it is upregulated by the ethanol treatment as well. Regardless of the cause, the large differences in *OsGAPDH* expression between samples from pre- and post-ethanol treatment are unsettling for purposes of normalising data.

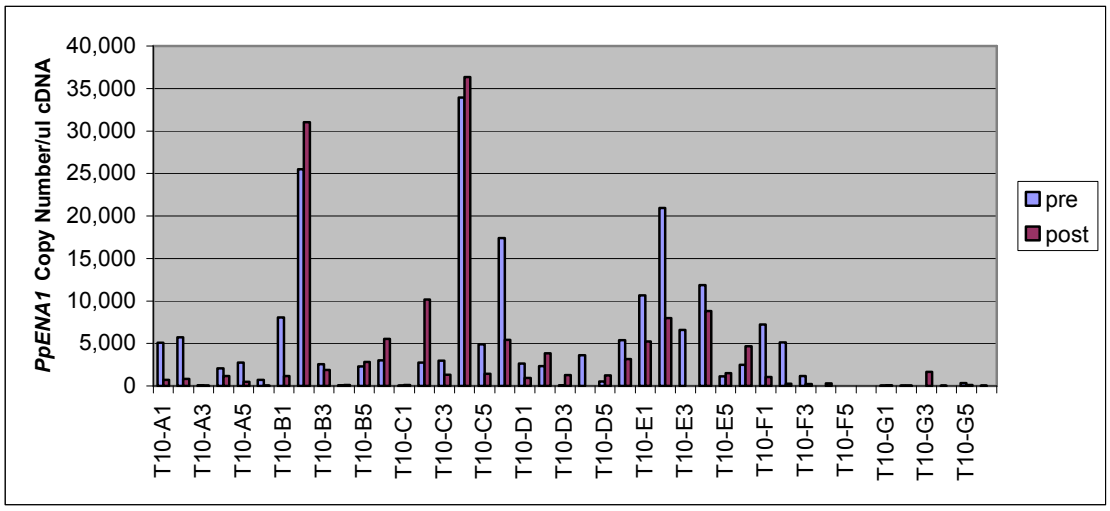

Figure 5.2: *PpENA1* expression (*PpENA1* copy number/µl cDNA) in independent T_0 lines (Transformation 10) expressing *PpENA1* in the xylem parenchyma root cells of rice under control of the ethanol switch. Values are pre- and post- a 24 h ethanol treatment (1%). Raw data is not normalised.

The *PpENA1* copy numbers measured in the lines from Transformation 10 were extremely wide ranging from no expression to 35,000 copies/µl cDNA (Figure 5.2). *PpENA1* copy numbers were similar between pre- and post-ethanol treatment samples for most of the individual lines, but data required normalisation in order to determine the true change in copy number with ethanol treatment. If the cDNA from the post-

ethanol treatment samples was synthesised with more RNA than in the pre- ethanol treatment samples and the proportion of *OsGAPDH* to *PpENA1* copies in each sample remains relatively constant, it would indicate that there is significantly less *PpENA1* in the post-ethanol treatment samples.

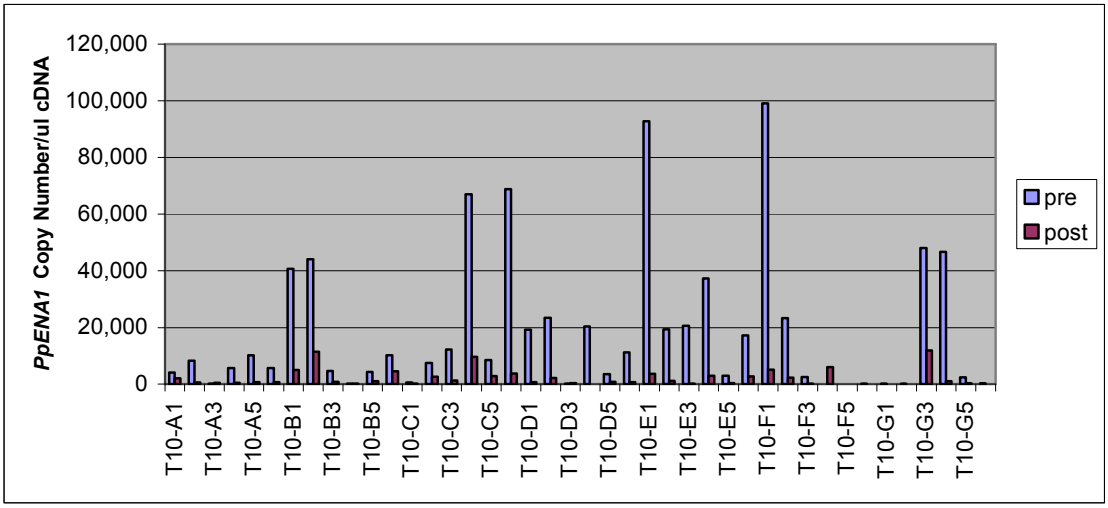

Figure 5.3: *PpENA1* expression (*PpENA1* copy number/µl cDNA) in independent T_0 lines (Transformation 10) expressing *PpENA1* in the xylem parenchyma root cells of rice under control of the ethanol switch. Values are pre- and post- a 24 h ethanol treatment (1%). Data is normalised with the 1st normalisation protocol.

The first normalisation protocol involved averaging the *OsGAPDH* copy numbers in all Transformation 10 samples and dividing the *OsGAPDH* copy number in each sample by this average to produce a normalisation factor. The *PpENA1* copy number measured for each sample was divided by it's normalisation factor to produce a normalised copy number for each sample (Figure 5.3). The data produced by this method indicated that there was significantly higher *PpENA1* expression in the pre-ethanol samples than in the post-ethanol samples, indicating the ethanol treatment had actually downregulated *PpENA1* expression up to 30 fold. As this result seems inconsistent with those typically obtained with the ethanol switch, a new method of normalisation was developed.

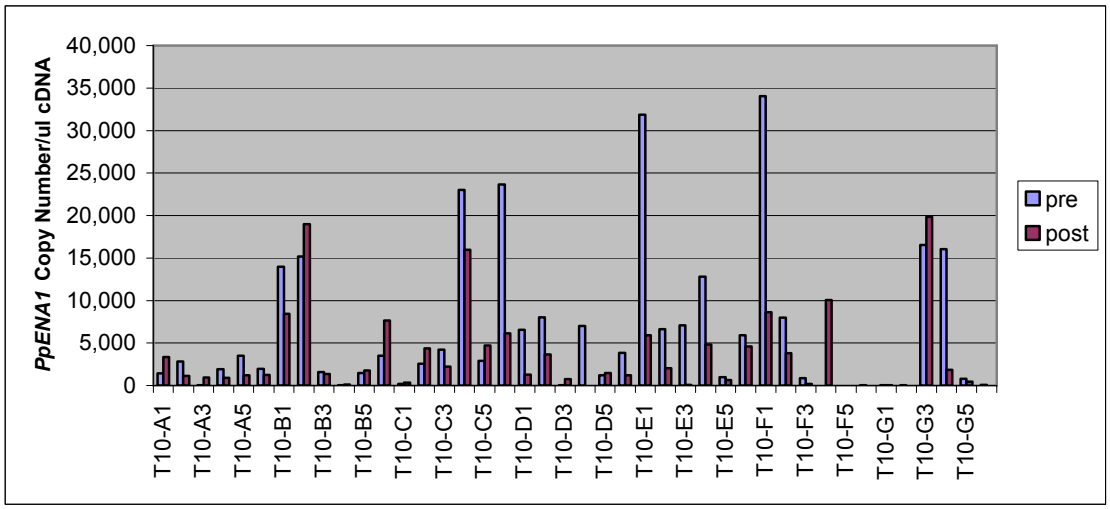

Figure 5.4: *PpENA1* expression (*PpENA1* copy number/µl cDNA) in independent T_0 lines (Transformation 10) expressing *PpENA1* in the xylem parenchyma root cells of rice under control of the ethanol switch. Values are pre- and post- a 24 h ethanol treatment (1%). Data is normalised with the 2nd normalisation protocol.

The second normalisation protocol accounted for the large difference in *OsGAPDH* expression level between the pre- and post-ethanol treatment samples, by developing separate normalisation factors for samples pre- and post-ethanol treatment. The *OsGAPDH* copy numbers measured in the pre-ethanol treatment samples were averaged and the *OsGAPDH* copy number in each sample were divided by this average to create the normalisation factor for the pre-ethanol treatment samples. The same process was used to develop a separate normalisation factor for the post-ethanol treatment sample. The *PpENA1* copy numbers in each sample were divided by the appropriate normalisation factor to determine the normalised *PpENA1* copy number in each sample. The results from this method indicated that *PpENA1* expression in the pre- and post-ethanol treatment for each line was much more similar than in the first normalisation (Figure 5.4). Overall, it still appears that *PpENA1* expression has been downregulated in most lines by the application of ethanol, but the largest downregulation is now approximately 5 fold. This still seemed an unlikely result, because there is no known reason that ethanol treatment of these lines should decrease *PpENA1* gene expression. Some possible reasons for these observations will be explored in the general discussion.

5.3.3 Q-PCR analysis of *AtHKT1;1* lines from Transformation 11

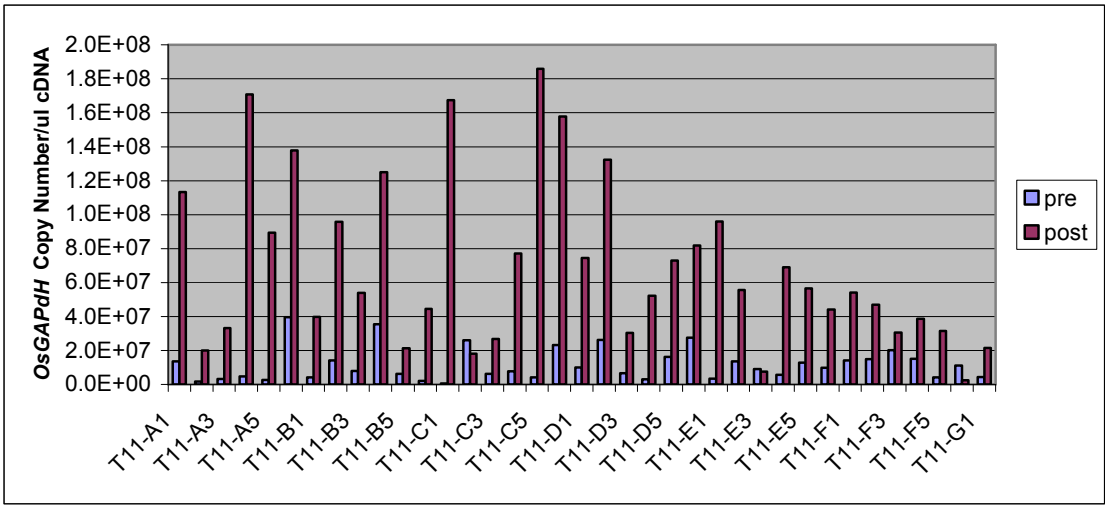

Figure 5.5: *OsGAPDH* expression (*OsGAPDH* copy number/µl cDNA) in independent T_0 lines (Transformation 11) expressing *AtHKT1;1* in the xylem parenchyma root cells of rice under control of the ethanol switch. Values are pre- and post- a 24 h ethanol treatment (1%).

A large increase in *OsGAPDH* expression between pre- and post-ethanol treatment samples was also observed in the lines expressing *AtHKT1;1* xylem parenchyma-specifically and ethanol inducibly. Some of the Transformation 11 lines had 50 fold higher *OsGAPDH* copy number in the post-ethanol treatment sample (Figure 5.5). The possible explanations are likely the same as for the *OsGAPDH* measurements in the Transformation 10 lines. It is quite likely that the difference is due to a large variation in the amount of RNA used to synthesise cDNA. However, as mentioned above it is difficult to rule out the option that *OsGAPDH* is upregulated by ethanol treatment.

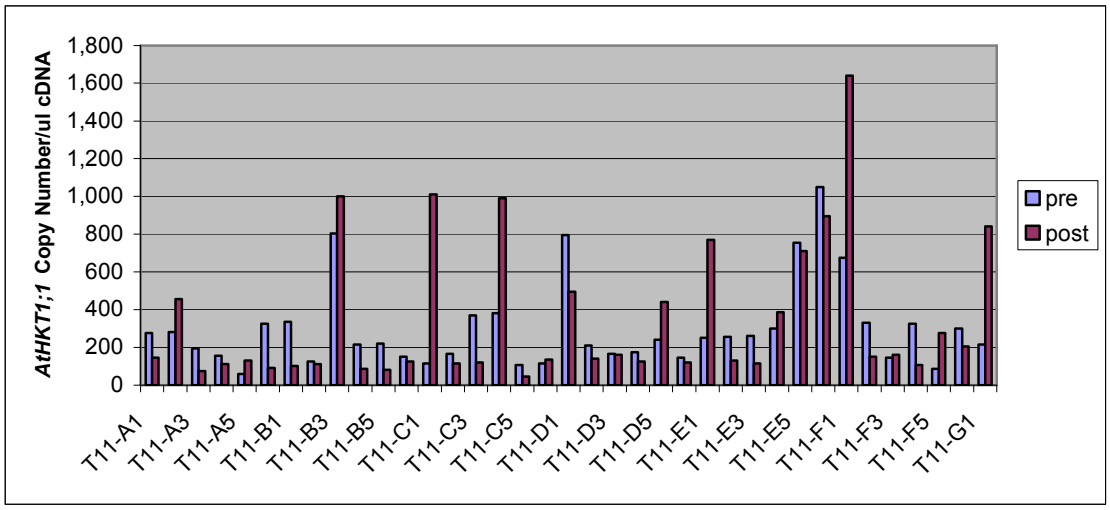

Figure 5.6: *AtHKT1;1* expression (*AtHKT1;1* copy number/µl cDNA) in independent T_0 lines (Transformation 11) expressing *AtHKT1;1* in the xylem parenchyma root cells of rice under control of the ethanol switch. Values are pre- and post- a 24 h ethanol treatment (1%). Raw data is not normalised.

The raw *AtHKT1;1* expression data for the Transformation 11 lines showed relatively similar copy numbers between the pre- and post-ethanol treatment samples for each line (Figure 5.6). Again, if the cDNA from the post-ethanol treatment samples was synthesised with more RNA than in the pre-ethanol treatment samples and the proportion of *OsGAPDH* to *AtHKT1;1* copies in each sample remains relatively constant, it would indicate that there is significantly less *AtHKT1;1* in the post-ethanol treatment samples. It is evident that *AtHKT1;1* was not expressed as highly as *PpENA1* in this system (Figure 5.2), perhaps indicating a problem with Q-PCR analysis of the *AtHKT1;1* lines. To determine whether binding of the *AtHKT1;1* primers was being affected by competitive binding of the primers to the endogenous *OsHKT* genes, a second set of primers was developed on a different region of the *AtHKT1;1* gene which was entirely unique in sequence to the *OsHKT* genes. The new primer set returned nearly identical data to the first primer set, thus it seems unlikely that the low *AtHKT1;1* expression values are a result of faulty Q-PCR analysis.

This same difference in expression level between lines expressing *PpENA1* and *AtHKT1;1* was also observed when the genes were expressed cell-type specifically or constitutively (Chapters 6 and 7). Potentially, this is related to the level of gene expression which becomes toxic to the plant or callus. It may be that high *PpENA1*

expression has less of an effect on plant transport processes (or other plant functions) than high *AtHKT1;1* expression does, thus plants expressing *AtHKT1;1* at similar levels to *PpENA1* are selected against as regenerating plants or earlier as transgenic callus.

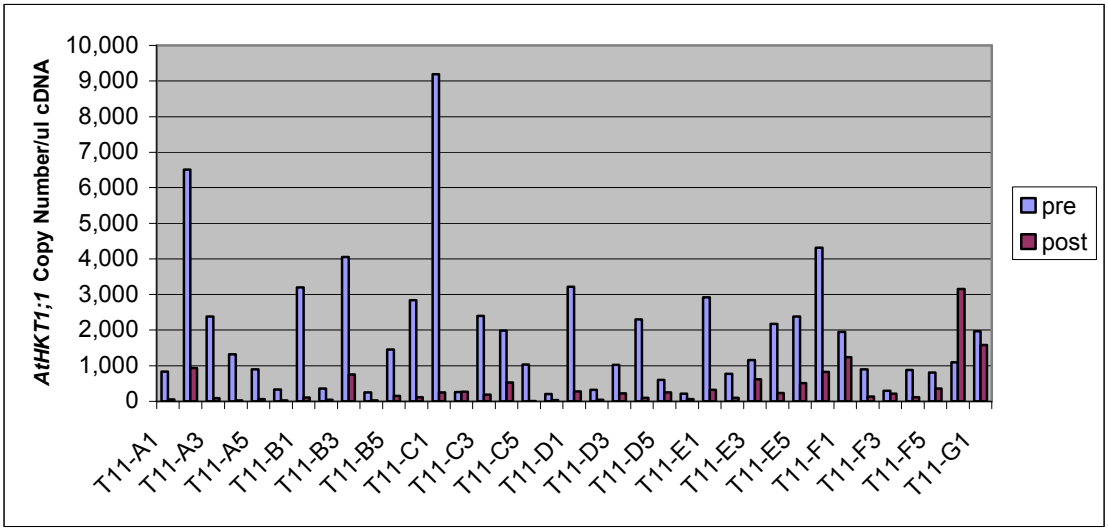

Figure 5.7: *AtHKT1;1* expression (*AtHKT1;1* copy number/µl cDNA) in independent T_0 lines (Transformation 11) expressing *AtHKT1;1* in the xylem parenchyma root cells of rice under control of the ethanol switch. Values are pre- and post- a 24 h ethanol treatment (1%). Data is normalised with the 1st normalisation protocol.

The data from the Transformation 11 lines was normalised using the first normalisation method described above (Figure 5.7). As was observed from the *PpENA1* data above, it appeared that there was a large downregulation of *AtHKT1;1* among most of the T11 lines (up to 40 fold). Again, this seemed unlikely, so the data was re-normalised.

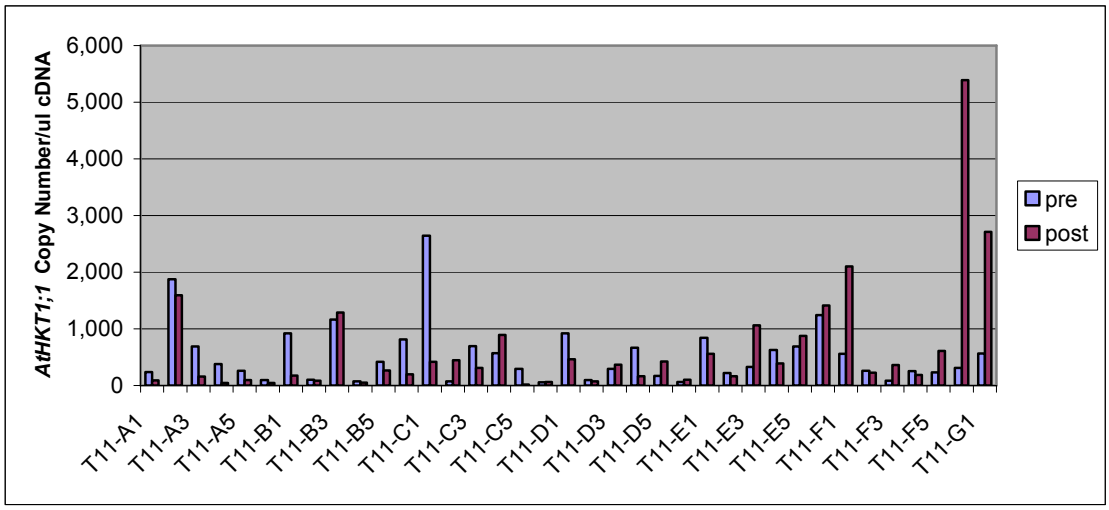

Figure 5.8: *AtHKT1;1* expression (*AtHKT1;1* copy number/µl cDNA) in independent T_0 lines (Transformation 11) expressing *AtHKT1;1* in the xylem parenchyma root cells of rice under control of the ethanol switch. Values are pre- and post- a 24 h ethanol treatment (1%). Data is normalised with the 2nd normalisation protocol.

The data was normalised with the 2nd normalisation protocol described above for *PpENA1* to avoid the problem with large *OsGAPDH* expression level differences between pre- and post-ethanol treatment samples. After this second normalisation the *AtHKT1;1* expression in most lines appeared similar between pre- and post-ethanol treatment samples (Figure 5.8). A few of the lines appeared to have an increase in *AtHKT1;1* expression following ethanol treatment, with T11-F6 having a 17 fold upregulation. However, the post-ethanol treatment sample from this line had exceptionally low *OsGAPDH* expression, which means the normalised *AtHKT1;1* was likely overrepresented.

5.3.4 Ethanol induction of cell-type specific *RFP* expression

Rice lines inducibly expressing *RFP* specifically within the root epidermis/cortex (Transformation 9) or xylem parenchyma (Transformation 12) or inducibly only (Transformation 18) were exposed to ethanol to induce *RFP* expression.

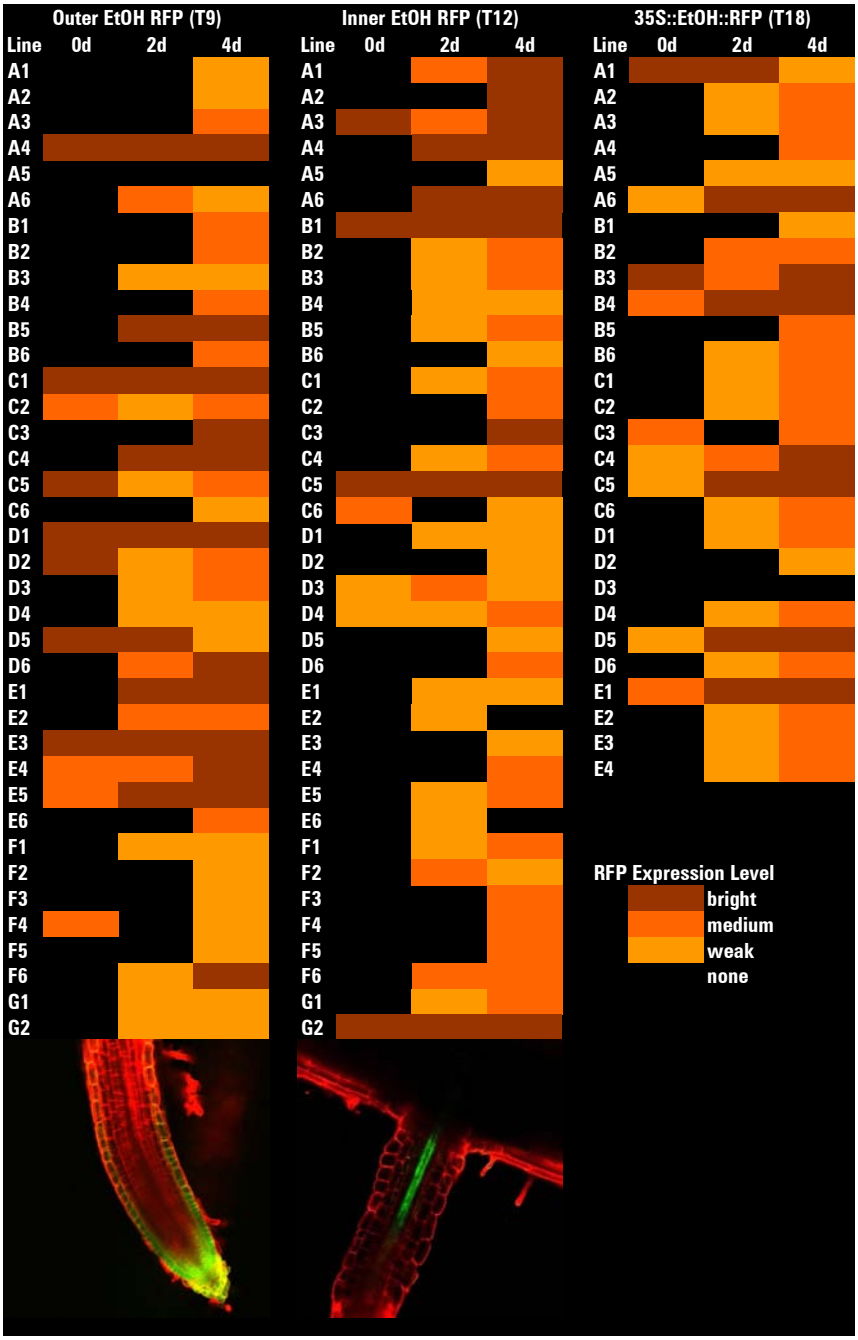

Figure 5.9: RFP fluorescence in Outer EtOH RFP (Transformation 9 - epidermis/cortex), Inner EtOH RFP (Transformation 12 - xylem parenchyma) and 35S::EtOH::*RFP* (Transformation 18) lines in response to 24 h ethanol treatment (1%). RFP fluorescence was examined using a stereomicroscope prior to ethanol treatment (0 d), 2 d post-ethanol induction (2 d) and 4 d post-ethanol induction (4 d). RFP fluorescence was classified as none, weak, medium or bright.

There was large variation in RFP fluorescence intensity among the lines both pre- and post-ethanol induction (Figure 5.9). Some lines displayed RFP fluorescence before ethanol induction, especially in the outer EtOH RFP lines. Several lines showed no increase in RFP fluorescence following ethanol induction. However, the majority of lines has little or no RFP fluorescence prior to ethanol induction and by 4 d post-induction showed medium or bright RFP fluorescence. The RFP fluorescence intensity was followed beyond 4 d and was observed to decrease to the fluorescence level of the line before ethanol induction in a further 3 d.

Each line from the three transformations (Outer EtOH RFP Inner EtOH RFP and 35S::EtOH::*RFP*) was classified as Responsive or Non-responsive based on the RFP fluorescence changes observed in the line (Table 5.1). Responsive lines had little or no fluorescence prior to ethanol induction and showed a large induction of RFP fluorescence following ethanol treatment. Lines were classified as Non-responsive if they showed significant RFP fluorescence prior to ethanol treatment (Bright 0 d), or if they did not show significant RFP fluorescence following ethanol treatment (Weak 4 d). The Outer EtOH RFP lines appeared the least responsive of the RFP lines with approximately a third of the lines being Responsive and two-thirds being Non-responsive. The Inner EtOH RFP and 35S::EtOH::*RFP* lines appeared much more responsive with 55 % and 68 %, respectively, of those lines being Responsive to ethanol treatment. This may be related to the larger number of cells displaying RFP fluorescence in the Outer EtOH RFP line making it appear that more lines were fluorescing brightly at 0 d when in reality the cells in the Inner EtOH RFP line were fluorescing to a similar level, but could not be observed as they make up a smaller proportion of the root. However, by this logic the 35S line should have had an even larger number of lines classed Non-responsive with RFP fluorescence prior to ethanol induction, so the reason for this discrepancy is still unclear. Whatever the case, there are a sufficient number of lines from each transformation that are responding suitably to ethanol treatment to warrant further investigation of this system.

Table 5.1: RFP fluorescence in Outer EtOH RFP, Inner EtOH RFP and 35S::EtOH::*RFP* independent T_0 lines. Responsive fluorescence is defined as no or weak fluorescence at 0 d and medium or bright fluorescence at 4 d. Non-responsive fluorescence was split into two categories based on whether the line failed because the fluorescence was medium or bright at 0 d (Bright 0 d) or there was no or weak fluorescence at 4 d (Weak 4 d).

Line	Total	Responsive	Non-responsive Bright 0 d	Non-responsive Weak 4 d
Outer EtOH RFP (T9)	38	13 (34 %)	11 (29 %)	14 (37 %)
Inner EtOH RFP (T12)	38	21 (55 %)	5 (13 %)	12 (32 %)
35S::EtOH::*RFP* (T18)	28	19 (68 %)	5 (18 %)	4 (14 %)

5.4 General Discussion

This study documents the first use of the ethanol switch in cereals. In fact very few chemical-inducible expression systems have been used in cereals other than the glucocorticoid switch (Ouwerkerk *et al.* 2001. There were preliminary concerns that the anoxic (or hypoxic) growth conditions of rice would produce too much endogenous ethanol for the ethanol switch to reliably function. These problems were avoided by using aerated solution culture and the significant development of aerenchyma likely provides sufficient O_2 to rice roots to avoid hypoxic growth conditions. The alternative systems, such as hormone-inducible systems, can cause growth defects (Amersadeghi *et al.* 2007) and are likely to affect physiological processes like transport more significantly than ethanol would. Also, most of the hormone switches contain a significant piece of the GAL4 gene in the first component of the switch, thus transcription could be significantly affected by GAL4 binding to this region.

The data from the RFP experiment indicates that the system reliably induced transgene expression in enhancer trap lines, but the data from the *PpENA1* and *AtHKT1;1* experiments is more difficult to determine. However, it unlikely that the Q-PCR data accurately reflects the true biological situation because it is difficult to explain why the ethanol treatment would result in decreasing transgene expression.

There appears to be the large differences in *OsGAPDH* expression, the normalisation gene, pre- and post-ethanol treatment. One possible explanation for the large increases in *OsGAPDH* post-treatment is that GAP is induced by the ethanol treatment, but there were large *OsGAPDH* differences between plates which indicates there was a large variation in the amount of RNA template going into each cDNA synthesis, thus a large difference in cDNA concentration in each Q-PCR reaction. In subsequent experiments in our laboratory it has become evident that *OsGAPDH* is not suitable for normalisation purposes since it seems to be quite variable in expression based on tissue-type, between samples and appears to be regulated by salinity stress (Ute Baumann, ACPFG, pers. comm.). It has also been shown to be less stably expressed across rice genotypes and stress treatments, than 18S rRNA (Kim *et al.* 2003). Thus, it is not stable enough to be reliable for evaluating changes in expression of genes. Comparison between expression levels before and after ethanol treatment in the same plant is not possible with this data set. It will be necessary to find a set of control genes that are stable across ethanol treatment, salt stress, transgene expression and time to be able to compare the transgene expression levels across cDNA samples. This may be best accomplished by running microarray analysis of cDNA from all the different treatments and looking for stably expressed genes. Wild-type Nipponbare rice lines could be subjected to an ethanol treatment, or salt-stress and gene expression in these treatments could be evaluated against control expression to identify highly expressed genes which remain stable across all treatments. These genes could then be used to normalise expression data in future Q-PCR experiments. It would be best to find a group of 4-5 genes to use as control genes to increase the confidence in the normalisation procedure. The Q-PCR experiments were hampered by the use of only one control gene, but the original hope was to use this data as a cursory 'first glance' to choose lines to analyse further.

Another issue may be that the actual number and size of the cells expressing transporters in the xylem parenchyma line is quite small in relation to the number of cells in an entire root sample. There may be a dilution effect on the actual induction of gene expression by the surrounding cells which are not expressing the transgene, thus

the actual expression of the transgene may appear smaller than it is within the target cell-type. Also, the increase in gene expression may diluted for the same reason.

Based on the RFP experiments, the choice to resample the *PpENA1* and *AtHKT1;1* lines 3 d after the first sample was appropriate because it appears that expression level was already strong in most lines 2 d after treatment and still rising until the 4 d point. At this point RFP fluorescence was observed to decline. Peak gene expression using the ethanol switch was observed at 4 d in *Arabidopsis* (Caddick *et al*. 1998) and 3 d in tomato (Garoosi *et al*. 2005).

There appears to be significant variation between independently transformed lines in terms of response of RFP fluorescence to ethanol treatment. Some lines show RFP fluorescence prior to ethanol application. This indicates either the presence of sufficient endogenous ethanol to activate the switch, or there are position effects caused by the random insertion of the ethanol switch construct into the rice genome. Gene or promoter elements located close to the switch could have some effect on proper functioning of AlcR binding to alcA or on the ability of alcA to drive gene expression without the proper binding of AlcR. The alcA promoter has a minimal -45 CaMV35S promoter fused to the 3' end and it is likely that this element is able to drive gene expression if integrated close to certain genomic elements. There were a large number of plants from each transformation that showed RFP fluorescence induction with ethanol application. This indicates it is unlikely endogenous ethanol production is sufficient to activate the ethanol switch. Also, previous studies have shown O_2 loss is low from rice roots even in stagnant growth conditions indicating it is unlikely rice roots are starved of O_2 to a level that would increase endogenous ethanol production (Colmer *et al.* 1998). Similar variability in reporter gene induction among ethanol switch transformed lines has been reported in *Arabidopsis* (Roslan *et al.* 2001) and tomato (Garoosi *et al.* 2005).

Identification of T_0 plants showing responsive induction of transgenes based soley on Q-PCR data appears it will be a difficult approach to selecting lines for further experimentation. With the variability observed between the lines this approach will require a large number of RNA extractions and Q-PCR runs which are expensive, labour-intensive and time consuming. Thus, a new approach has been developed which

involves crossing the transgene into a line which has shown to induce RFP fluorescence in a cell-type specific manner (Figure 5.10). The most responsive lines will be crossed with a second line transformed with a construct containing the alcA promoter fused to a gene of interest. This will significantly reduce the number of plants which require laborious analysis through RNA extractions and Q-PCR, because most of the screening will be done visually since the transgene will be expressed in the same pattern observed for the RFP fluorescence.

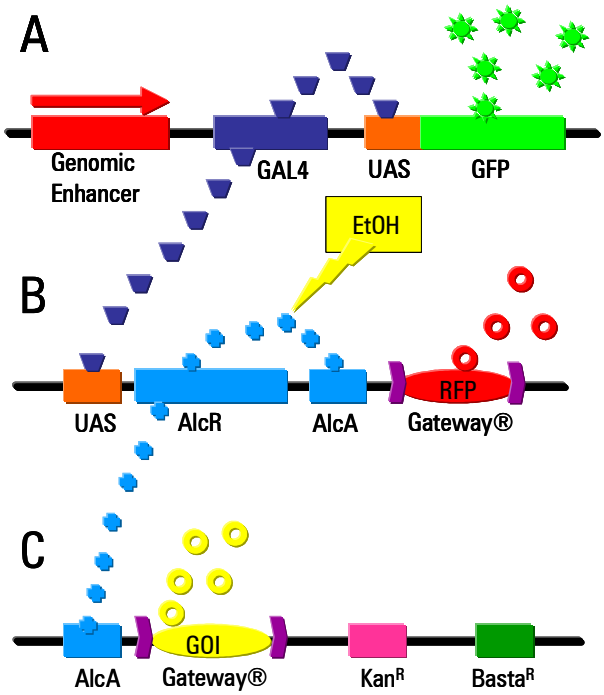

Figure 5.10: New strategy to produce rice lines expressing transgenes in a cell type-specific and ethanol-inducible manner. (A) The original enhancer trap in GAL4-GFP lines. (B) The pMDC100 + UAS + EtOH + nos construct which is transformed into the enhancer trap line to produce cell-type specific, ethanol-inducible expression of *RFP*. (C) The pMDC100 + alcA + nos + bar construct which is transformed into WT Nipponbare rice. This construct is crossed with a line containing constructs A and B to regulate the transgene (GOI) expression via GAL4 and the ethanol switch.

CHAPTER 6 - CELL-TYPE SPECIFIC EXPRESSION OF *AtHKT1;1*

6.1 Introduction

The *HKT* gene family of transporters has nine members in rice, several of which have been shown to be crucial to Na^+ transport (Horie *et al.* 2001, Gaciadeblas *et al.* 2003, Ren *et al.* 2005, Horie *et al.* 2007). *OsHKT1;5* is expressed in the stele of the root and shoot and appears to be responsible for retrieval of sodium from the xylem stream, thus limiting the sodium transported to the shoot where it does damage to the plant and reduces its productivity (Ren *et al.* 2005). *OsHKT1;4* is likely involved in retrieval of sodium from the xylem for storage in the sheath tissue, based on homology to the similar gene in wheat (Byrt *et al.* 2007). *OsHKT2;1* appears to be involved in uptake of Na^+ under K^+ starved conditions (Horie *et al*. 2007). Na^+ appears to partially rescue plants grown in K^+ starved conditions, thus the gene is upregulated by K^+ starvation (and downregulated by excess Na^+). *OsHKT1;1* also appears to be involved in low affinity Na^+ transport, and is expressed predominantly in the roots (Horie *et al.* 2001). *OsHKT2;2* appears to be absent in *japonica* varieties, but has been shown in indica varieties to be similar in function to *OsHKT2;1* (Horie *et al.* 2001). *OsHKT1;2* is a pseudogene in rice and is unlikely to have any functional transport properties (Platten *et al.* 2006). *OsHKT2;3* and *OsHKT2;4* are nearly identical in homology and together with *OsHKT1;3* are relatively unknown in terms of function in Na^+ or K^+ transport (Platten *et al.* 2006).

The *Arabidopsis* genome contains a single *HKT* gene which shares most significant homology to *OsHKT1;5* in the rice gene family. It also appears to have similar physiological function in Na^+ transport in *Arabidopsis* as *OsHKT1;5* does in rice. It is predominantly expressed in the stele of the root (possibly the xylem parenchyma) and appears to be responsible for retrieval of Na^+ from the xylem stream (Sunarpi *et al.* 2005). *AtHKT1;1* gene knockout plants exhibit elevated Na^+ accumulation in the shoot combined with lower root Na^+ accumulation than WT, which indicates the gene is responsible for controlling the amount of Na^+ reaching the shoot tissue by retrieving Na^+ from the xylem to xylem parenchyma cells (Davenport *et al.* 2007).

Allelic and promoter differences in *HKT* genes have been shown in both rice and *Arabidopsis* to be responsible for major differences in both Na^+ accumulation and tolerance (Ren *et al.* 2005, Rus *et al.* 2006). Thus, overexpression of a single *HKT* gene may improve the Na^+ tolerance of a plant. The rice genome does not contain a gene of exact homology to *AtHKT1;1* so expressing it in rice may improve Na^+ exclusion and Na^+ tolerance.

Constitutive overexpression of transporters can be a problem in plants. Overexpression of *AtHKT1;1* in *Arabidopsis* via the 35S promoter has been shown to increase Na^+ accumulation in the shoot tissue and to create plants which are more salt sensitive and often infertile (D Jha and M Tester, unpublished data). Another issue with conventional constitutive overexpression is that expressing a gene in all cell-types within a plant may be counter-productive to altering net accumulation in shoots. Overexpressing the transporter *AtHKT1;1* in all root cells would mean the gene is expressed in the xylem parenchyma and may increase the xylem retrieval of Na^+, thereby improving salinity tolerance. However, the gene would also be expressed in the epidermal cells of the root, which may increase influx of Na^+ into the root cells, which would result in more Na^+ being transported to the shoot and ultimately in decreased Na^+ tolerance. Thus, this hypothesis was tested by expressing *AtHKT1;1* in either the epidermal/cortex (outer) or xylem parenchyma (inner) cells of rice roots.

To achieve cell-specific expression, GAL4-GFP enhancer trap lines were identified which had trapped enhancer elements responsible for gene expression specifically in epidermal/cortex or xylem parenchyma cells of the root. These lines were transformed a second time with a construct containing a GAL4-UAS fused to *AtHKT1;1,* thereby *AtHKT1;1* was expressed in the same cell-types as *GFP* in the enhancer trap lines. These transactivation lines were then examined for changes in various Na^+ transport properties such as root, sheath and blade accumulation of Na^+, cell-type specific accumulation of several elements and Na^+ influx rate. Also, Na^+ transport properties of lines expressing *AtHKT1;1* cell-specifically were compared to those of the 35S::*AtHKT1;1* overexpression lines.

6.2 Materials and Methods

6.2.1 Plant materials

Generation of all transgenic plant material is described in Chapter 4 on transformation and vectors. The root epidermal/cortex enhancer trap line (AOH B03) is also referred to as the Outer Background line (see Chapter 4). The root xylem parenchyma enhancer trap line (ASG F03) is also referred to as the Inner Background line (see Chapter 4).

6.2.2 Quantitative-PCR (Q-PCR)

Total root tissue was harvested (at least 100 mg) from primary transgenic plants into 96-well plates. Total RNA was extracted from all lines and cDNA (20 µL) was synthesised from 2 µL of cDNA at the Australian Genome Research Facility (AGRF) in Adelaide. The original cDNA was diluted 1 in 20 and submitted to Neil Shirley (ACPFG) for Q-PCR analysis. However, it was found that transgene copy numbers were extremely low at this cDNA concentration, thus Q-PCR analysis was repeated with original cDNA diluted 1 in 2. *AtHKT1;1* primers were used (Forward primer – CCTCCATACACTTTATTTATGC; Reverse primer – CGGTGATTGAAATGAGAAAGAT; product size – 160 bp) and run in conditions as in Burton *et al.* 2004. Data was normalised against the control gene *OsGAPDH* (glyceraldehyde-3-phosphate-dehydrogenase) (Forward primer – GGGCTGCTAGCTTCAACATC; Reverse primer – TTGATTGCAGCCTTGATCTG; product size – 190 bp) copy numbers. Subsequently, it became evident that *OsGAPDH* was not an ideal control gene (see section 5.4), but analysis was completed by this time and could not be repeated. While the resulting analysis may not be ideal as a result, it was sufficient for this experiment.

6.2.3 T_0 Na^+ accumulation analysis

Following root tissue sampling for Q-PCR, transgenic plants with roots growing out of the bottom of Jiffy Peat Pots in trays were subjected to Na^+ treatment of 5 mM NaCl for 13 d. The plants also received 5 mM NH_4NO_3 and Osmocote (Scotts Company) in the growth solution. After 13 d the youngest fully emerged leaf blades (YEB) were excised into 50 mL Falcon tubes for Na^+ accumulation analysis. Fresh weights of samples were taken, the tissue was dried in a 70°C oven for 12 h and dry

weights were measured. Samples were digested in 10 mL of 1% nitric acid for 4 h at 70°C. Digested samples were then analysed using a flame photometer (Sherwood Scientific Ltd., Cambridge, U.K.) for Na^+ and K^+ content. Values from the flame photometer were converted into Na^+ and K^+ concentration values on a tissue water basis (millimolar).

6.2.4 T_1 Growth conditions

Seed was sterilised and grown in hydroponic culture as described in Chapter 2 (2.2.2).

6.2.5 T_1 Na^+ accumulation analysis – Experiment 1

Based on the Q-PCR and Na^+ accumulation results (and on the availability of T_1 seed) lines were chosen for further analysis. Lines were chosen to adequately represent the average Na^+ accumulation and transgene expression levels observed for the entire population of primary transgenic plants from a particular transformation. Two outer *AtHKT1;1* lines (2-A5 and 2-B5) and two inner *AtHKT1;1* lines (5-B4 and 5-C4) were analysed for Na^+ accumulation and Na^+ tolerance levels in the T_1 generation. Wild-type Nipponbare plants were included in the hydroponic growth experiment as controls. All transgenic plants were genotyped in all accumulation experiments. Genomic DNA was extracted from a small piece of leaf tissue via the 'rapid extraction' DNA extraction method (Wang *et al.* 1993) and used as template for PCR using the same primers as used for Q-PCR analysis of the primary transgenic cDNA. Null segregants were removed from the data analysis. There were insufficient numbers of null segregants to use as controls for transgenic plants, thus other controls were used, such as transgenic plants expressing *RFP* with the same expression system, wild-type plants and the background enhancer trap lines. Plants were grown in a glasshouse at South Australian Research and Development Initiative (SARDI) in Adelaide with average temperatures of 30°C days and 20°C nights, full sun, and an average humidity of 60%. In this experiment plants were grown without added NaCl for 10 d, then given 10 d of 10 mM NaCl (+ 0.2 mM $CaCl_2$) and 10 d of 50 mM NaCl (+ 0.75 mM $CaCl_2$). The solution was changed every 4-5 d to prevent depletion of nutrients. After the 10 d salt-stress at 10 mM, the YEB was harvested for analysis via flame photometry as mentioned above (called 10-yeb). The growth solution was then

changed to 50 mM NaCl and the plants were grown a further 10 d. After this salt-stress the new YEB was harvested for flame photometry (called 50-yeb). The leaf blade which emerged immediately following the YEB harvested after the initial 10 d 10 mM NaCl stress (was easily identifiable as original excised YEB was obvious) was harvested as well (called 50-old). The complete root system was also harvested by excising the roots immediately below the seed, washing them in RO water and patting them dry with paper towel before placing them in Falcon tubes. These samples were all treated exactly as previously mentioned for flame photometry analysis.

6.2.6 T_1 Na^+ accumulation/Na^+ stress tolerance analysis – Experiment 2

In Experiment 2 the seedlings were grown in a growth chamber at AGRF with tightly controlled growth conditions of 28°C days, 26°C nights, 16 h of full light (high-pressure sodium lamps), and 90% humidity during the days and 80% humidity at night. Plants were grown on ACPFG solution without added Na^+ for 8 d instead of the usual 10 d, then on 10 mM for 4 d instead of the usual 10 d, then on 20 mM for 4 d instead of the usual 10 d. Plants were harvested as in the previous experiment except a subsample of root tissue was weighed and immediately frozen in liquid nitrogen for future RNA extraction and Q-PCR analysis.

6.2.7 35S::*AtHKT1;1* experiments

Seeds of the 35S::*AtHKT1;1* line and WT were germinated on Petri dishes as in all previous experiments except one group of seeds was supplemented with 5 mM Na^+ and one dish with 5 mM K^+ (as well as one on RO water alone). After 5 d on Petri dishes seedlings from the 35S::*AtHKT1;1* were transferred to 1 L beakers (covered with plastic film) and 2 mM $Ca(NO_3)_2$ was added to the growth solution (30 mL). Seedlings were grown in a growth chamber in the same conditions mentioned previously in section 6.2.6. The seedlings were harvested after 7 d, separated into shoots and roots (roots were rinsed in RO water) and the Na^+ and K^+ accumulation was measured using the flame photometer. The large plants in each treatment were harvested individually, but the small plants in each treatment were too small to analyse individually and were pooled to make one small plant root and shoot sample for each treatment.

T_1 seed was analysed via Radial ARL Inductively Coupled Plasma Atomic Emission Spectrometry (ICPAES) for the elemental profile. The lines analysed were 35S::*RFP* (15-C5), Outer RFP (3-A5), Inner RFP (6-A5) (all representative of the Na^+ accumulation phenotype seen in the screening of the individual populations of primary transgenic lines), 35S::*AtHKT1;1* (14-A1), Outer *AtHKT1;1* (2-B5) and Inner *AtHKT1;1* (5-C4) lines. Four replicates of four seeds per replicate (approximately 0.08 g per replicate) were submitted to Waite Analytical Services (Adelaide) for acid digestion and elemental analysis via ICPAES.

6.2.8 $^{22}Na^+$ influx analysis

Refer to the flux experimental protocol chapter (Chapter 2) for the flux analysis methodology. The protocol used for analysis of the transgenic lines is the same as the one used for the flux analysis of the 11 *indica* rice cultivars (Experiment 8, section 2.3.6).

6.2.9 Cryoscanning electron microscopy and X-ray microanalysis

Seeds were prepared and grown in hydroponics as listed above in section 6.1.6. Roots from three plants of each line were examined. Three-week old seedlings were pre-treated for 5 d with 50 mM Na^+ + 0.75 mM $CaCl_2$. Roots were cut 5 mm from the root tip and inserted into a hole in a brass stub which supported the root sections to stand vertically for examination in the microscope. Four roots of each genotype (outer background, inner background, outer *AtHKT1;1* and inner *AtHKT1;1*) were placed in the same stub in each experiment with a drop of growth solution surrounding them and snap frozen in liquid N_2. The frozen specimen was transferred under vacuum to a cryo-microtome where it was cryoplaned using a liquid N_2 cooled microtome blade. Thus, the actual surface examined was 4 mm from the root tip to ensure a section without aerenchyma, but expressing the transgene, was examined. The samples were transferred to the specimen stage of the scanning electron microscope and were etched for 1.5 min at -92°C to sublimate some cellular water in order to more easily observe cellular structure. Samples were cooled to -120°C and sputter coated with platinum for 1.5 min to ensure proper electrical conductivity between the specimen and the stub. The coated specimens were then loaded onto the microscope stage (held at a temperature below -150°C) and analysed in a Philips XL 30 Scanning Electron

Microscope (Philips Electron Optics) fitted with a CT1500 HF cryotransfer stage (Oxford Instruments) and an EDAX energy-dispersive x-ray detector (EDAX International). XRMA spectra were recorded at a voltage of 10 kV, a working distance of 10 μm and a data collection time of 100 s. Spectra were analysed with eDXi software (EDAX) and results presented were measurements of peak over background. Data was compiled using XRMAplot (courtesy of Elena Kalashyan and Ute Baumann, ACPFG). Cell-types analysed were epidermis (EP), exodermis (EX), cortical fibers (CF), outer cortex (OC), inner cortex (IC), endodermis (EN), pericycle (PR), xylem parenchyma (XP) and metaxylem (MX). Elements measured were sodium, potassium, chloride, calcium and magnesium. Data is presented for sodium and potassium with chloride, calcium and magnesium data presented in Appendix IV. The actual mM amounts of the various ions could not be determined, but values are given as the semi-quantitative peak over background values (P/B). Running known Na^+ and K^+ solution standards through x-ray microanalysis was attempted, but did not work apparently because freezing the solutions in liquid nitrogen pushes the ions in the solution ahead of the freezing front and results in highly variable measurements of the ions in the solution.

6.3 Results and Discussion

6.3.1 T_0 Q-PCR vs. Na^+ accumulation

Expression levels of the *AtHKT1;1* transgene in the primary transgenic lines was analysed by Q-PCR. The *AtHKT1;1* expression level in the roots of 35S-driven overexpression lines was approximately the same as it was when *AtHKT1;1* was expressed in the outer root cells via GAL4 transactivation while expression levels were much lower in the inner *AtHKT1;1* lines (Figures 6.1, 6.3 and 6.5). The actual number of cells and the size of the cells in the xylem parenchyma line which were expressing the transgene was significantly smaller than in the outer line, thus if all cells express the transgene to a similar level this result would be expected. It may also indicate that the 35S overexpression line and the outer *AtHKT1;1* line are expressing the transgene in approximately the same cells and to approximately the same level. However, the

35S line also expresses *AtHKT1;1* highly in the shoots, thus expression over the entire plant is different between the lines.

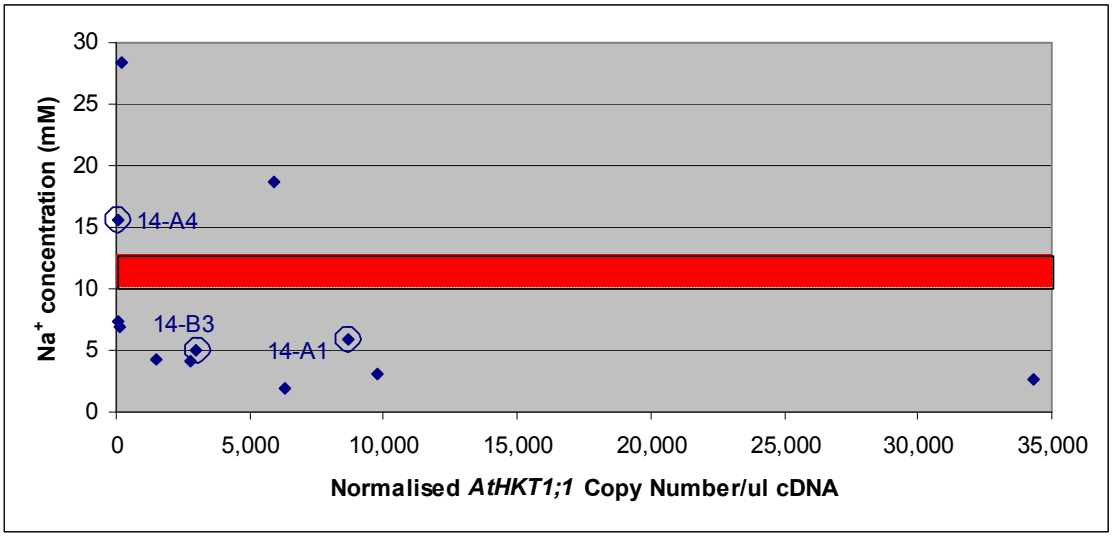

Figure 6.1: T_0 35S::*AtHKT1;1* lines – Na^+ concentration (mM) in the YEB (after a 13 d treatment of 5 mM Na^+) versus normalised *AtHKT1;1* copy number/µl cDNA in the root for each independent transformant. Red box indicates the average (plus and minus the standard error) Na^+ accumulation in 35S::*RFP* T_0 plant population (11.3 +/- 1.2 mM → 10.1 – 12.5 mM). T_0 35S::*AtHKT1;1* population had lower Na^+ accumulation than the 35S::*RFP* T_0 population. Independent lines analysed in the T_1 generation are highlighted.

The majority of the 35S::*AtHKT1;1* lines accumulated less Na^+ than did the RFP control lines (Figure 6.1). Only one line with relatively high expression level (~6000 copies/µl cDNA) had higher Na^+ accumulation than the control. It appears that plants having higher levels of transgene expression have decreased Na^+ accumulation. Only three lines produced any T_1 seed, probably due to a combination of the effects of *AtHKT1;1* overexpression and inadequate glasshouse conditions (low humidity and low night time temperatures). One of these lines (14-A4) had little to no transgene expression, but two other lines (14-A1 and 14-B3) had expression levels average for the population and represented the overall Na^+ accumulation phenotype of the population so were chosen for further experiments. Two lines were eliminated from the data set, one had no expression and extremely high Na^+ accumulation and the other had four times the expression level of the next most highly expressing line and also had

extremely high expression of *AtHKT1;1*. Both lines did not produce seed so could not be evaluated further, but it appears there may be an ideal mid-range of constitutive expression around 5-10,000 copies/µl cDNA to have the effects of gene expression along with maintenance of normal plant growth and fertility.

The K^+ accumulation was higher in the *AtHKT1;1* lines than the RFP control lines, but there was no apparent relationship between gene expression level and K^+ accumulation indicating *AtHKT1;1* expression has no effect on K^+ transport (Figure 6.2). It does appear that the K^+ accumulation across all *AtHKT1;1* lines in all expression systems is around 250 mM (Figures 6.2, 6.4 and 6.6), thus it would appear that 35S overexpression of *RFP* may have decreased the K^+ accumulation in those plants.

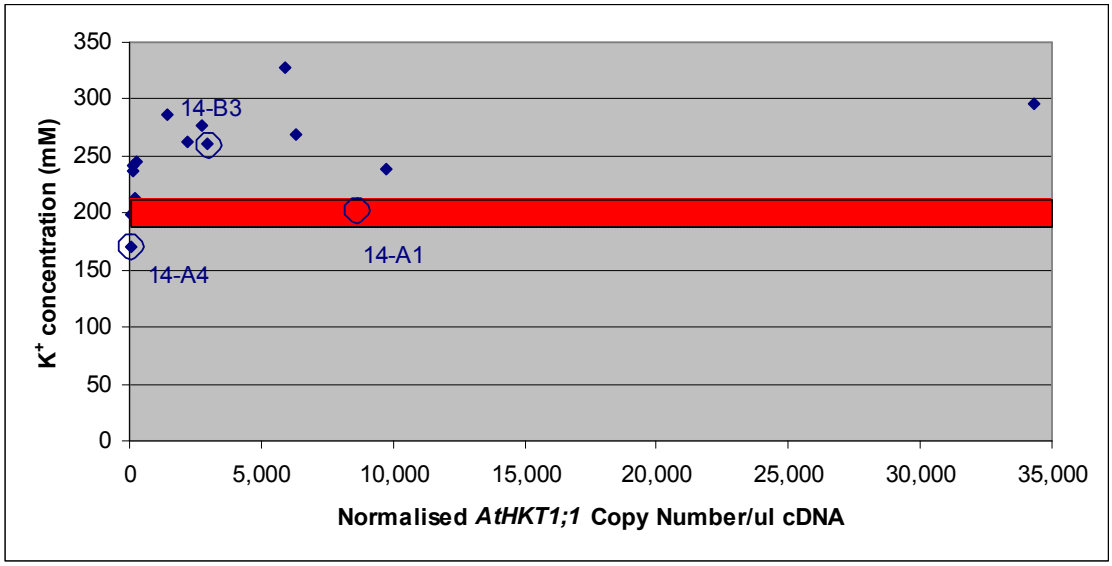

Figure 6.2: T_0 35S::*AtHKT1;1* lines – K^+ concentration (mM) in the YEB (after a 13 d treatment of 5 mM Na^+) versus normalised *AtHKT1;1* copy number/µl cDNA in the root for each independent transformant. Red box indicates the average (plus and minus the standard error) K^+ accumulation in 35S::*RFP* T_0 plant population (199 $^+$/- 8 mM → 191 - 207 mM). T_0 35S::*AtHKT1;1* population had higher K^+ accumulation than the 35S::*RFP* T_0 population. Independent lines analysed in the T_1 generation are highlighted.

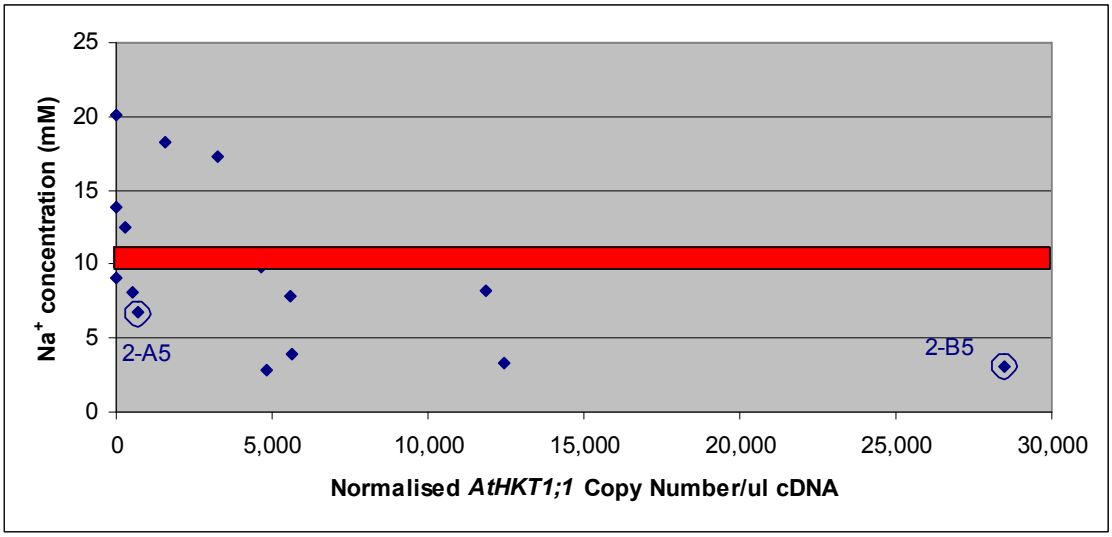

Figure 6.3: T_0 Outer *AtHKT1;1* lines – Na^+ concentration (mM) in the YEB (after a 13 d treatment of 5 mM Na^+) versus normalised *AtHKT1;1* copy number/µl cDNA in the root for each independent transformant. Red box indicates the average (plus and minus the standard error) Na^+ accumulation in Outer RFP T_0 plant population (10.3 +/- 0.8 mM → 9.6 – 11.1 mM). T_0 Outer *AtHKT1;1* population had lower Na^+ accumulation than the Outer RFP T_0 population. Independent lines analysed in the T_1 generation are highlighted.

The majority of the outer *AtHKT1;1* lines accumulated less Na^+ in the leaf blade than the control lines did (Figure 6.3). It appears that as *AtHKT1;1* expression levels increased, Na^+ accumulation in the blade decreased indicating the higher expressing lines would be better choices for maximising sodium exclusion in this expression system. Only two lines with expression levels above 1000 copies/µl cDNA accumulated more Na^+ than the controls while eight lines accumulated similar or smaller amounts than the controls. At copy numbers higher than 4000/µl cDNA all seven lines accumulated less Na^+ than the controls, thus this expression system appears to lower leaf blade accumulation of Na^+. Representative lines were again chosen based on the observed phenotype of the population as a whole, and again, based on availability of T_1 seed. A much higher proportion of the primary transgenic lines produced seed than in the 35S::*AtHKT1;1* lines indicating that perhaps the cell-type specific expression system was not as detrimental to plant fertility and seed production as is 35S::*AtHKT1;1* expression. Two lines were chosen to evaluate in the T_1 generation: 2-A5 which had low gene expression and low accumulation of Na^+ and 2-

B5 with high gene expression and low Na^+ accumulation. As mentioned previously, transgene copy numbers in the roots were similar between the 35S lines and the epidermal lines, but the number of fertile plants was vastly different indicating that perhaps the epidermal expression system is a better option for producing salt excluding lines that also function normally otherwise.

The outer *AtHKT1;1* lines accumulated less K^+ than the outer RFP control lines did, but as with the 35S lines there is no apparent relationship between gene expression level and K^+ accumulation indicating that the gene is not altering K^+ transport (Figure 6.4). As mentioned above, there is a significant difference in K^+ accumulation between the lines expressing *RFP* in different systems, yet there is little difference in the K^+ accumulation in the lines expressing *AtHKT1;1* in different systems. It has been observed that RFP is toxic to cells at high expression levels (callus tissue growth is inhibited by high expression levels, strongly expressing calli rarely regenerate into seedlings in tissue culture) and K^+ is often a measure of plant health, so it is possible that the 35S::*RFP* lines were not as healthy due to high levels of RFP production and this was apparent in the K^+ accumulation. However, why expressing *RFP* in the outer background line would result in an increased level of K^+ accumulation (or healthier plants) requires further investigation. Perhaps the expression of the *RFP* gene in the outer cells of the root confines RFP accumulation to the vacuoles of the cortical cells and this creates less toxicity for the plant.

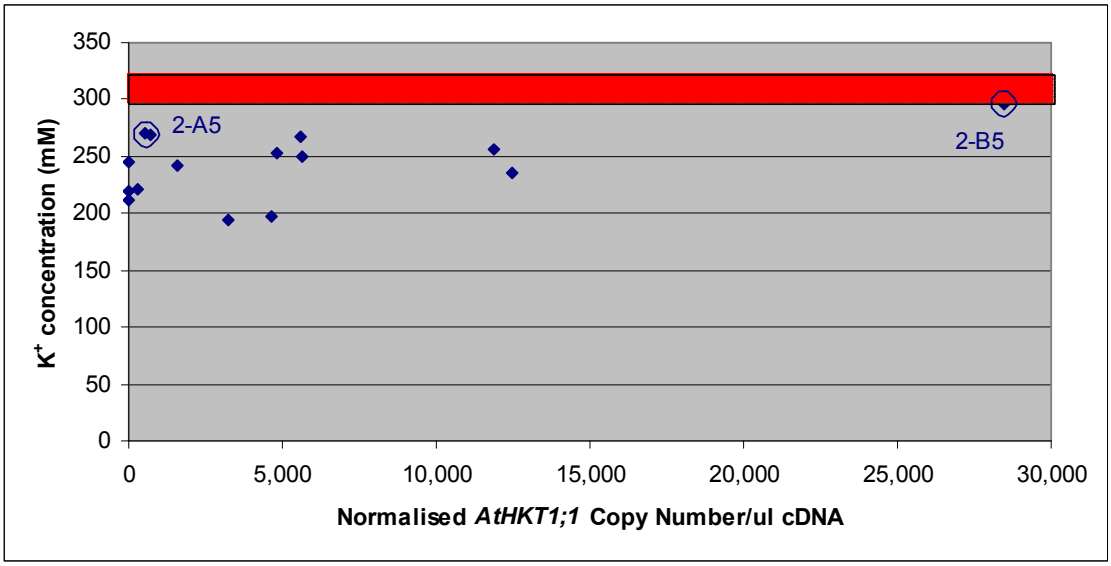

Figure 6.4: T_0 Outer *AtHKT1;1* lines – K^+ concentration (mM) in the YEB (after a 13 d treatment of 5 mM Na^+) versus normalised *AtHKT1;1* copy number/µl cDNA in the root for each independent transformant. Red box indicates the average (plus and minus the standard error) K^+ accumulation in Outer RFP T_0 plant population (306 +/- 9 mM → 297 - 315 mM). T_0 Outer *AtHKT1;1* population had lower K^+ accumulation than the Outer RFP T_0 population. Independent lines analysed in the T_1 generation are highlighted.

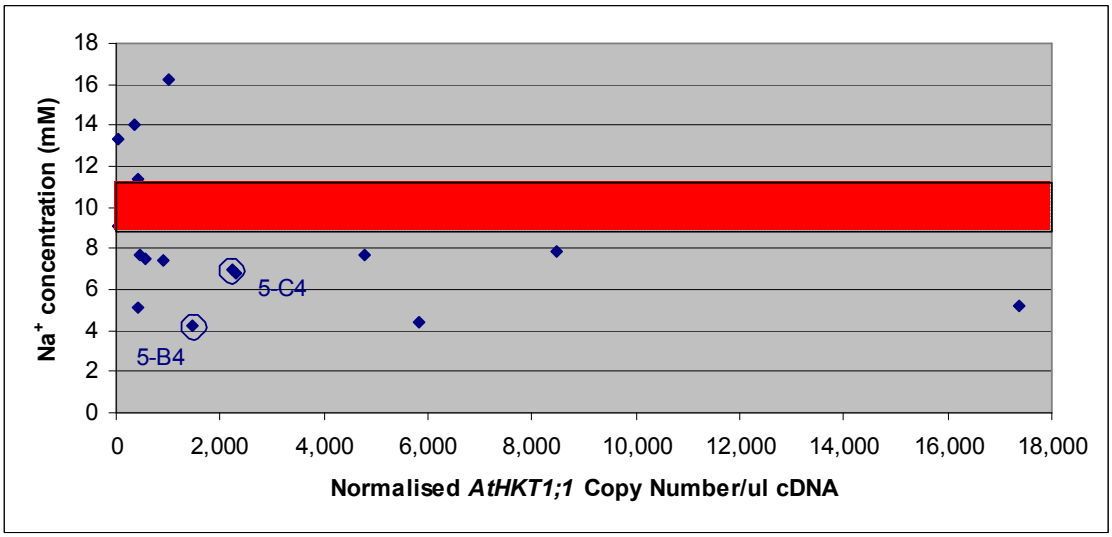

Figure 6.5: T_0 Inner *AtHKT1;1* lines – Na^+ concentration (mM) in the YEB (after a 13 d treatment of 5 mM Na^+) versus normalised *AtHKT1;1* copy number/µl cDNA in the root for each independent transformant. Red box indicates the average (plus and minus the standard error) Na^+ accumulation in Inner RFP T_0 plant population (10.0 +/- 1.3 mM → 8.7 – 11.3 mM). T_0 Inner *AtHKT1;1* population had lower Na^+ accumulation than the Inner RFP T_0 population. Independent lines analysed in the T_1 generation are highlighted.

Lines expressing *AtHKT1;1* in the inner root cells had lower whole root levels of expression than the 35S or outer *AtHKT1;1* lines (Figure 6.1, 6.3 and 6.5). This makes sense intuitively since the size and number of xylem parenchyma cells in a rice root is much smaller than the proportion made up by the cortical or epidermal cells. One primary transgenic line was documented as expressing *AtHKT1;1* at a level almost 15 times higher than the next highest transformant (and accumulated low Na^+) and so was removed from the analysis as it was likely an error in Q-PCR. The majority of the lines expressing *AtHKT1;1* accumulated less Na^+ than did the control RFP lines (Figure 6.5). Once again, as expression level of *AtHKT1;1* increased the resulting level of Na^+ accumulation in the leaf blade decreased. Of the lines expressing *AtHKT1;1* at 500 copies/µl cDNA and above only one had higher Na^+ accumulation than the control, while nine lines accumulated less Na^+ than the control. All seven lines expressing 1000 copies/µl cDNA or more accumulated less Na^+ in the leaf blade than the control lines. Based on the phenotype for the population as a whole, lines expressing *AtHKT1;1* at a level higher than 1000 copies/µl cDNA were chosen to represent the low Na^+ accumulation phenotype (5-B4 and 5-C4). Once again, a much higher proportion of the primary transgenic lines were fertile than for the 35S lines indicating that cell-type specific expression of *AtHKT1;1* is more likely to allow normal plant function and fertility than high levels produced by the 35S promoter (probably also useful to have the expression confined to the root, so shoot processes are not altered).

Accumulation of K^+ was not significantly different from that of the control lines (Figure 6.6). This may be an indication of the low toxicity of RFP in xylem parenchyma cells (since so small a proportion of total cells are actually expressing *RFP*). Again, there is no apparent effect of gene expression level on K^+ accumulation so it is unlikely K^+ transport is affected by expression of *AtHKT1;1*.

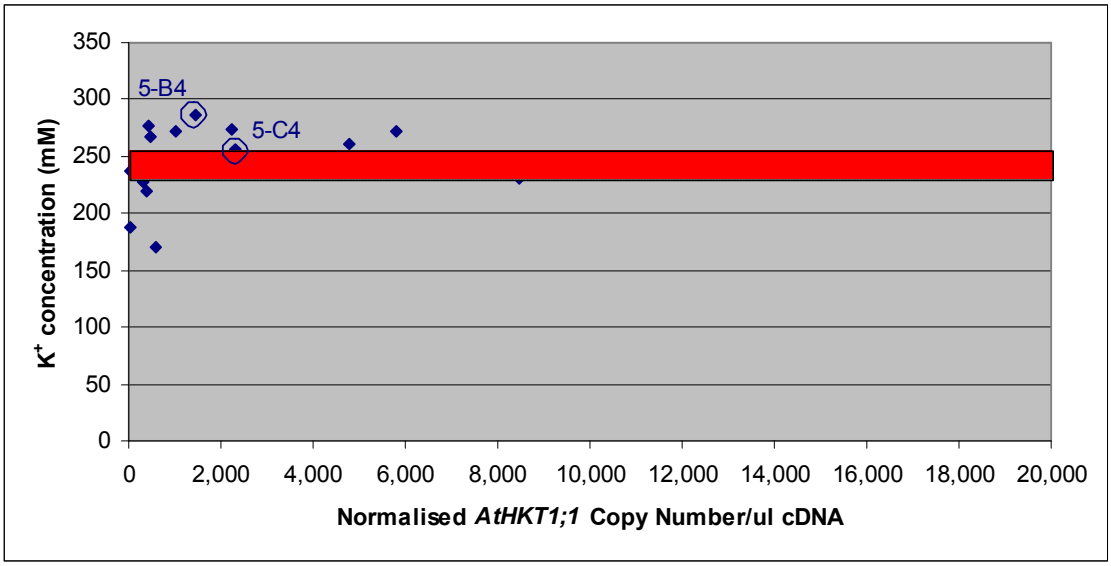

Figure 6.6: T_0 Inner *AtHKT1;1* lines – K^+ concentration (mM) in the YEB (after a 13 d treatment of 5 mM Na^+) versus normalised *AtHKT1;1* copy number/µl cDNA in the root for each independent transformant. Red box indicates the average (plus and minus the standard error) K^+ accumulation in Inner RFP T_0 plant population (245 $^+$/- 10 mM → 235 - 255 mM). T_0 Inner *AtHKT1;1* population had similar K^+ accumulation to the Inner RFP T_0 population. Independent lines analysed in the T_1 generation are highlighted.

6.3.2 T_1 Na^+ accumulation – Experiment 1

The primary transgenic lines chosen from the Q-PCR and Na^+ accumulation experiments were analysed in the T_1 generation to characterise Na^+ accumulation more completely and to discern whether the analysis of the T_0 lines was an accurate measure of the true phenotype of the line. All null segregants were removed from further analysis, while WT or background enhancer trap lines were used as experimental controls.

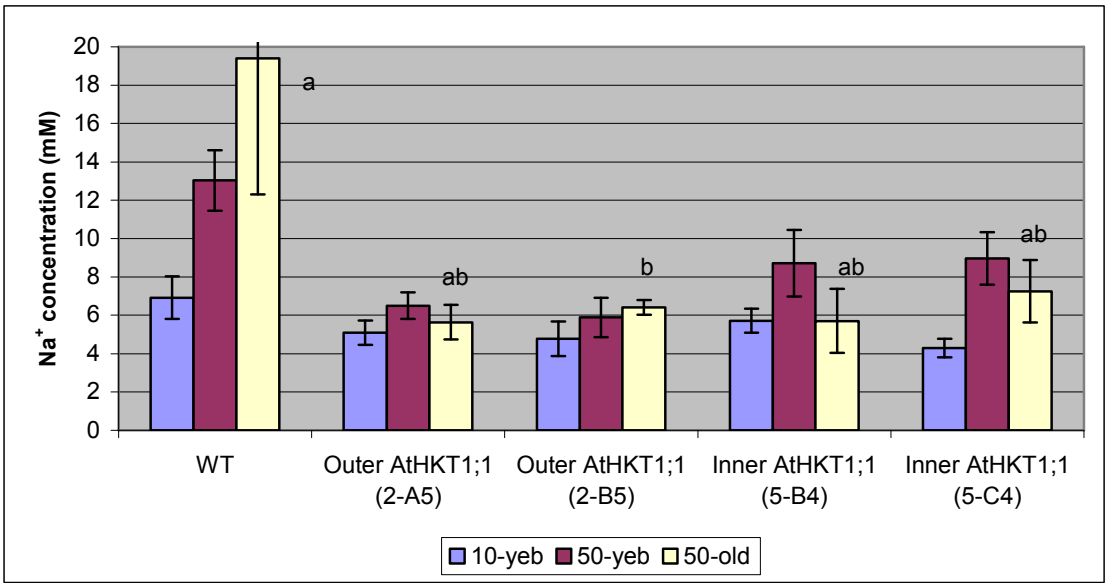

Figure 6.7: Na^+ accumulation in the leaf blades of two Outer *AtHKT1;1* and two Inner *AtHKT1;1* T_1 lines selected from T_0 analysis is lower than in WT leaf blades. The YEB was analysed after 10 d of 10 mM Na^+ stress (10-yeb), then a further 50 mM Na^+ stress was imposed for 10 d and the new YEB was analysed (50-yeb) as well as the blade immediately following the 10-yeb (50-old). Bars represent an average of 3-5 plants with standard error. No significant differences exist at $P<0.05$ between the means of 10-yeb and 50-yeb measurements, while the same letters above 50-old bars indicates the means are not significantly different at $P<0.05$ according to the Kruskal-Wallis and Dunn's Multiple Comparisons tests.

After 10 d of 10 mM Na^+-stress the YEB (10-yeb) was harvested from all plants and used to determine the Na^+ accumulation of the transgenic plants. All four *AtHKT1;1* lines contained less Na^+ in the YEB than the WT, but the differences were not large, thus the plants were grown for a further 10 d on 50 mM Na^+ (Figure 6.7). After the further 10 d the new YEB (50-yeb) was harvested as was the leaf blade immediately following the original YEB (10-yeb) which was easily distinguishable as the site of the original excised blade was simple to identify (50-old). Root tissue was also harvested at this time for Na^+ accumulation analysis. In the 50-yeb and 50-old the differences between transgenic and WT control plants was much larger than in the 10-yeb. The WT plants had much higher Na^+ accumulation in the 50-old than in the 50-yeb, but the outer *AtHKT1;1* lines and the inner *AtHKT1;1* lines had more similar levels of Na^+ accumulation between the two blades. Whether this was a factor of the gene expression or whether it was related to the much lower level of Na^+ accumulation

in the shoot as a whole is difficult to determine. The outer *AtHKT1;1* lines had even lower Na^+ in the 50-yeb than the inner *AtHKT1;1* lines in the 50-yeb, but both were lower than the WT. All four lines had similar levels in the 50-old and were all lower in Na^+ accumulation compared to the WT with an even larger differential existing in the 50-old than in the 50-yeb. This data confirmed that the analysis done on the T_0 plants was valid and was an accurate prediction of the Na^+ accumulation properties in later generations. It was also determined that the choice of blade to harvest for analysis of Na^+ accumulation phenotypes for comparison of the various lines made little difference (at least for the transgenic lines). Therefore, in future experiments all blades were harvested into one sample to simplify the harvest by getting both Na^+ accumulation and FW data for tolerance measurements from the same sample. Also, it appeared there was no significant difference between the selected pairs of outer and inner *AtHKT1;1* lines, thus individual lines with sufficient seed numbers could be used for further analysis.

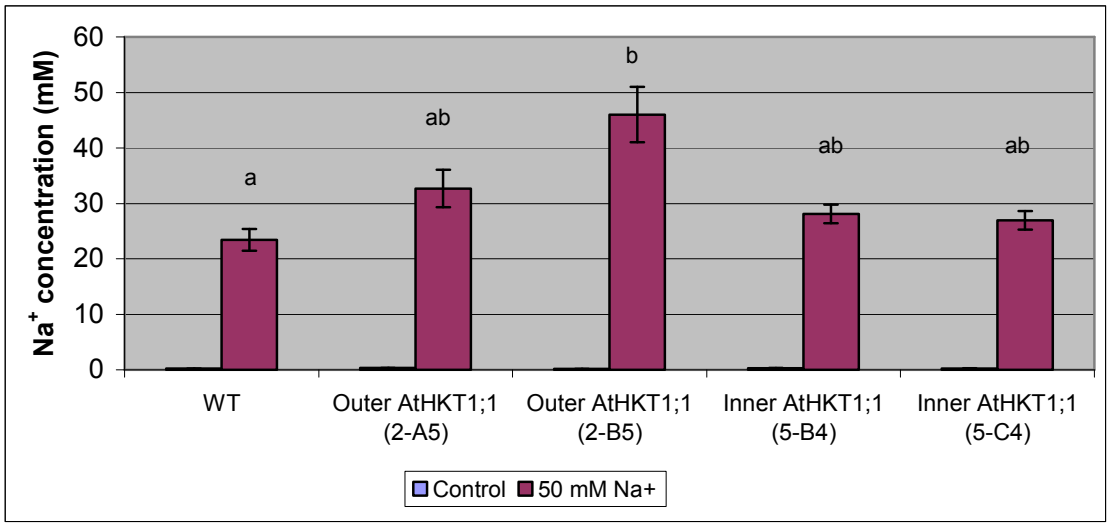

Figure 6.8: Na^+ accumulation in the roots of two Outer *AtHKT1;1* and two Inner *AtHKT1;1* T_1 lines selected from T_0 analysis. Accumulation of Na+ in roots of Outer *AtHKT1;1* lines is higher than WT and Inner *AtHKT1;1* lines. The roots were analysed after a 10 d 10 mM Na^+ stress and a further 10 d 50 mM Na^+ stress. Roots from plants grown in ACPFG solution without added Na^+ are presented as control. Bars represent an average of 3-5 plants with standard error. The same letters above bars indicates no significant difference exists between means at $P<0.05$ according to the Kruskal-Wallis and Dunn's Multiple Comparisons tests.

All four UAS::*AtHKT1;1* lines had increased levels of Na^+ accumulation in the roots, with the inner *AtHKT1;1* lines accumulating slightly more Na^+ than the WT and the outer *AtHKT1;1* lines accumulating more Na^+ than both the WT and the inner *AtHKT1;1* lines (Figure 6.8). Again the two independent lines of outer and inner *AtHKT1;1* resembled each other, thus it appeared either line of the pair could be used for further analysis, although the outer *AtHKT1;1* line 2-B5 did have a higher level of Na^+ accumulation in the root than the 2-A5 line. It appears as though the expression of *AtHKT1;1* in specific cells of the root results in the roots retaining the Na^+ that would otherwise be transported to the shoot, thereby lowering the shoot Na^+ accumulation. The outer *AtHKT1;1* line 2-B5 had higher transgene expression than the 2-A5 line in the analysis of the T_0 plants and retains more Na^+ in it's root.

The 5-C4 line had only slightly higher transgene expression than the 5-B4 line, and the Na^+ accumulation data from this experiment shows very little difference in accumulation between the two lines. Inner *AtHKT1;1* lines did not accumulate Na^+ in root cells much more significantly than the control lines (at least to the same extent as does the outer *AtHKT1;1* lines), but had lower shoot Na^+ accumulation. Regardless, both inner and outer root expression of *AtHKT1;1* seem effective at increasing Na^+ exclusion from the shoot, which is the aim of the experiment.

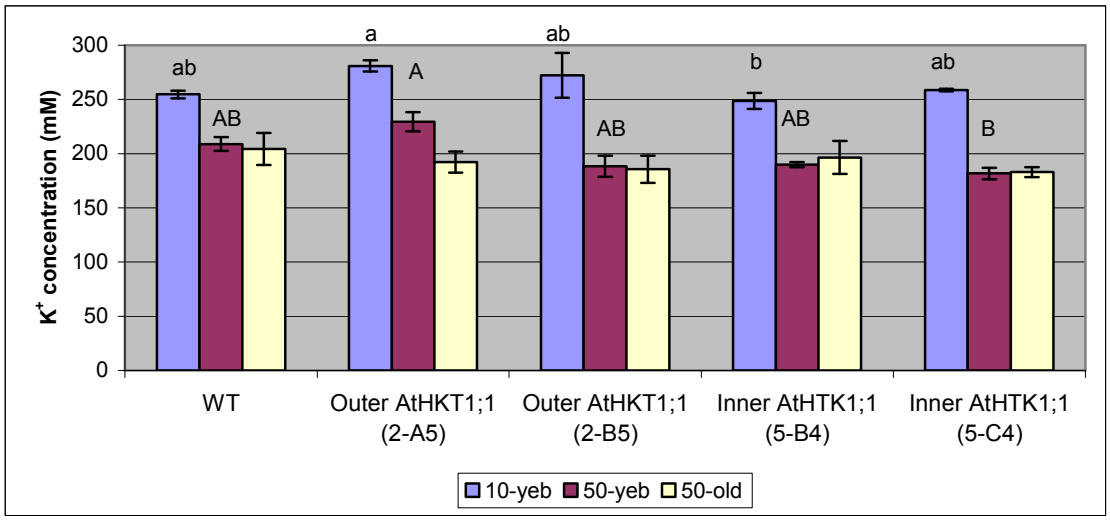

Figure 6.9: K^+ accumulation in leaf blades of two Outer *AtHKT1;1* and two Inner *AtHKT1;1* T_1 lines selected from T_0 analysis compared to WT. The YEB was analysed after 10 d of 10 mM Na^+ stress (10-yeb), then a further 50 mM Na^+ stress was imposed for 10 d and the new YEB was analysed (50-yeb) as well as the blade immediately following the 10-yeb (50-old). Bars represent an average of 3-5 plants with standard error. No significant differences exist between means of 50-old measurements at $P<0.05$, while the same letters above 10-yeb and 50-yeb bars indicates no significant difference exists between means at $P<0.05$ according to the Kruskal-Wallis and Dunn's Multiple Comparisons tests.

The K^+ accumulation in blades of all lines decreased after the second Na^+ stress, even though there was no accompanying increase in Na^+ accumulation in the blades (Figure 6.9). The outer *AtHKT1;1* lines appeared to have slightly higher K^+ accumulation in the 10-yeb than the WT or inner *AtHKT1;1* lines after the first 10 mM 10 d Na^+ stress. After the 50 mM 10 d Na^+ stress the outer *AtHKT1;1* line 2-A5 still had higher K^+ accumulation than the other lines in the in the 50-yeb. Perhaps this was a general sign of the health of this line. No significant differences existed between the lines in the 50-old.

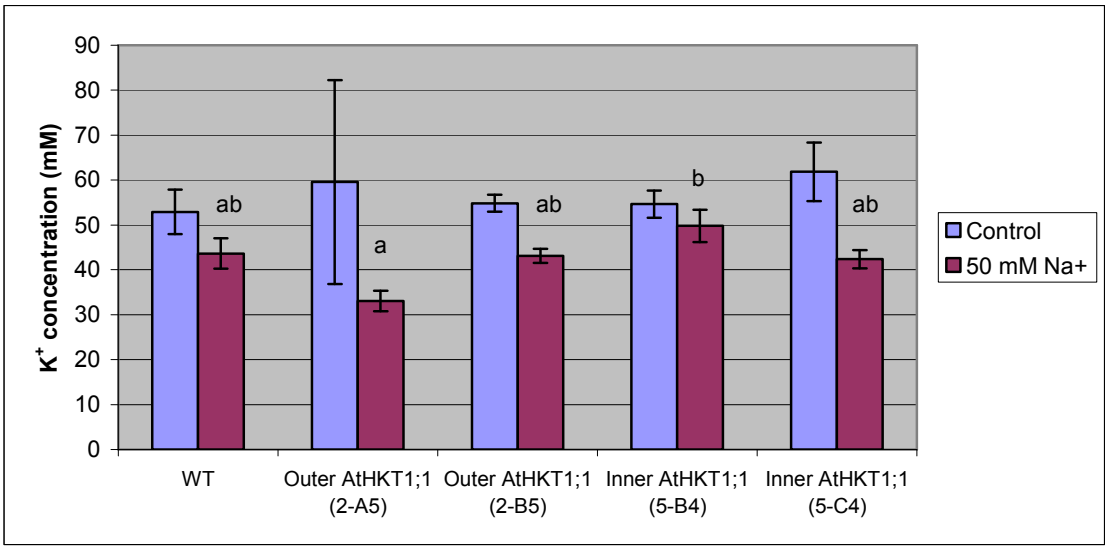

Figure 6.10: K^+ accumulation in the roots of two Outer *AtHKT1;1* and two Inner *AtHKT1;1* T_1 lines selected from T_0 analysis compared to WT. The roots were analysed after a 10 d 10 mM Na^+ stress and a further 10 d 50 mM Na^+ stress. Roots from plants grown in ACPFG solution without added Na^+ are presented as control. Bars represent an average of 3-5 plants with standard error. No significant differences exist between control means at $P<0.05$, while the same letters above 50 mM Na^+ bars indicates no significant differences exist between means at $P<0.05$ according to the Kruskal-Wallis and Dunn's Multiple Comparisons tests.

The roots show a similar decrease in K^+ accumulation after Na^+ stress in all lines (Figure 6.10). The decrease in the 2-A5 line is much more significant, which is odd considering that the 2-B5 line is the one with the larger accumulation of Na^+ in the roots and would be expected to show the larger K^+ decrease as a result (maintaining ionic balance).

6.3.3 T_1 Na^+ accumulation/Na^+ stress tolerance – Experiment 2

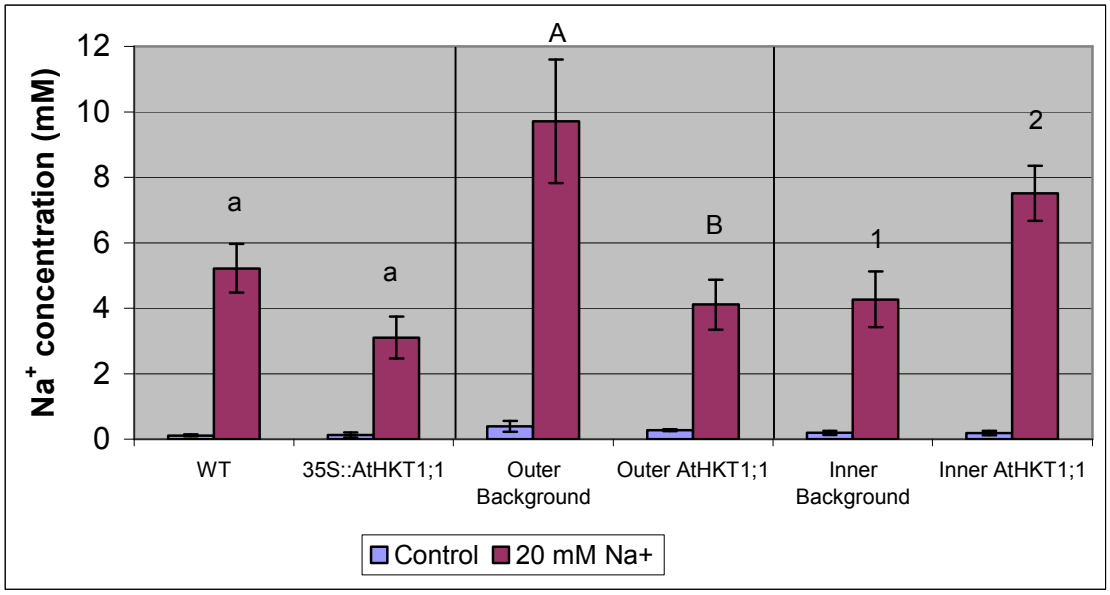

Figure 6.11: Na^+ accumulation in all leaf blades of WT Nipponbare, 35S::*AtHKT1;1* (14-A1), Outer Background, Outer *AtHKT1;1* (2-B5), Inner Background and Inner *AtHKT1;1* (5-C4) lines. 35S::*AtHKT1;1* and Outer *AtHKT1;1* lines showed lower Na^+ accumulation than their respective controls (left and middle panels, respectively), while the Inner *AtHKT1;1* line had higher Na^+ accumulation than it's control (right panel). Plants were harvested and analysed after a Na^+ treatment of 4 d at 10 mM, and 4 d at 20 mM. Bars represent an average of 8 plants with standard errors, except for 35S::*AtHKT1;1* control and 20 mM Na^+ are averages of 3 and 6, respectively (see text for details). The same letters or numbers above bars indicates the means are not significantly different at $P<0.05$ according to the Mann-Whitney test.

Analysis of the Na^+ accumulation in the leaf blades revealed a large difference between the 'control' lines (Figure 6.11). The outer background line had nearly double the Na^+ accumulation in the leaf blades compared to the WT, while the inner background line had slightly less Na^+ accumulation. This indicates that the original insertion of the GAL4-GFP enhancer trap in the genome of the outer background line has altered a genetic element that is relevant to Na^+ accumulation. However, the enhancer trap insertion site was not able to be identified via the standard protocol for locating Flanking Sequence Tags (FST), likely because the outer background line was found to have multiple copies of the T-DNA. The inner background line is not statistically different from WT in terms of blade Na^+ accumulation and this would

indicate the enhancer trap has not altered a genetic element affecting Na^+ transport in any significant manner. The FST for this line was identified and the T-DNA was inserted into a DHHC zinc-finger domain containing protein (TIGR Locus Identifier: LOC_Os12g16210), but this element does not appear to be related to Na^+ transport. Both background lines grow normally and are indistinguishable from each other and from WT, although they both are slightly larger plants than the WT (see FW figures). One potential reason for this is that the enhancer trap was transformed into Nipponbare seed stock in Montpellier, France, while the Nipponbare seed used in these experiments was obtained from a supplier in Victoria, Australia. This could mean that the seed stocks used in the experiment were slightly different in genetic makeup and could alter their growth slightly. Regardless, the large difference in the outer background and WT blade accumulation of Na^+ means that all the lines in this experiment cannot be compared in one analysis. Each *AtHKT1;1* line can only properly be compared to the line it was derived from. In other words the 35S::*AtHKT1;1* line can only be compared to the WT, the outer *AtHKT1;1* can only be compared to the outer background line and the inner *AtHKT1;1* line can only be compared to the inner background line.

The 35S overexpression of *AtHKT1;1* reduced the blade accumulation of Na^+, thus based purely on this observation it would seem that the overexpression strategy is suitable for increasing Na^+ exclusion with this gene in rice. Analysis of 35S-driven GUS activity in rice has revealed strong activity in the vascular tissue of the shoot and strong activity in the vascular and cortical tissues in the roots, with weak activity in the epidermis. If 35S provides strong expression of *AtHKT1;1* within the same tissues this may actually improve the recovery of Na^+ from the xylem in the root and sheath (or prevent Na^+ transport to the xylem) resulting in less Na^+ transported to the blades.

Expression of *AtHKT1;1* in the outer cells of the root significantly lowered Na^+ accumulation in the blade to less than half that of the outer background line. This agrees well with the previous experiment which showed this line had decreased Na^+ in the blades, thus it appears this is another good strategy for reducing blade Na^+ accumulation.

The inner *AtHKT1;1* line accumulated significantly more Na^+ in the leaf blade than the inner background line. This does not correspond well with the previous experiment in which this line showed similarly low Na^+ accumulation in leaf blades to the outer *AtHKT1;1* lines. The most obvious explanation is that the conditions between the previous experiment and this one were quite different. The humidity was much higher and more stable in this experiment, the daytime temperatures were more stable, the night time temperatures were more stable and higher and the light level was more consistent (but, maybe a lower level on average) in this experiment since it was grown in a controlled growth chamber. This would impact growth rate and transpiration rate of the plants and these factors can have a serious impact on water relations and transport properties in a plant and could have altered the results for the inner *AtHKT1;1* line between experiments. A second experiment under each set of conditions would be required to confirm this hypothesis. However, the outer *AtHKT1;1* phenotype is obviously more robust than the inner *AtHKT1;1* phenotype as it performed equally well under both sets of conditions having much improved Na^+ exclusion in both environments.

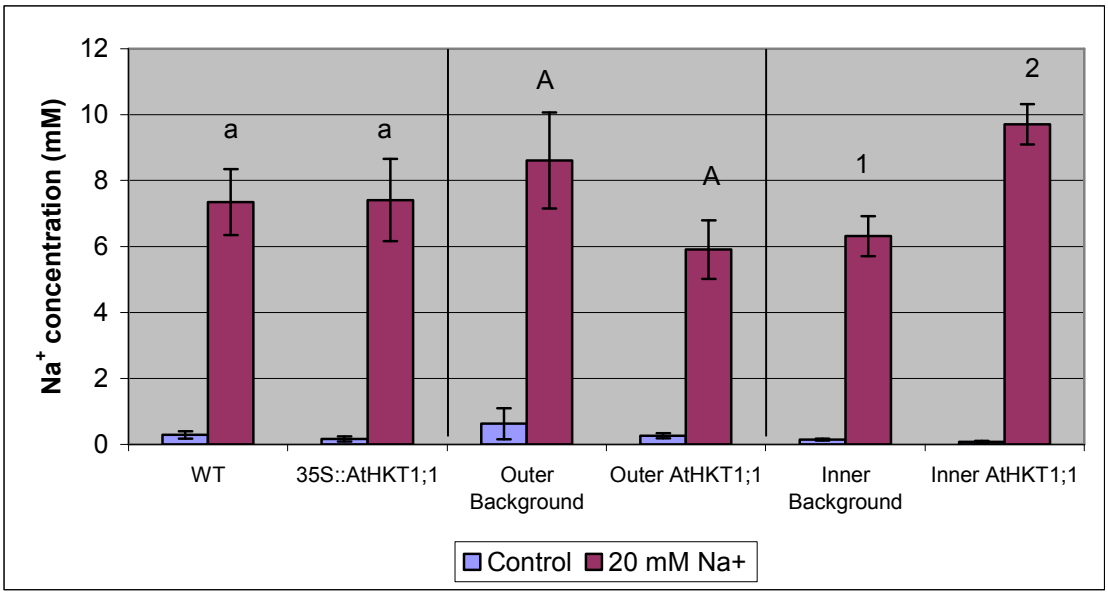

Figure 6.12: Na^+ accumulation in the sheath tissue of WT Nipponbare, 35S::*AtHKT1;1* (14-A1), Outer Background, Outer *AtHKT1;1* (2-B5), Inner Background and Inner *AtHKT1;1* (5-C4) lines. 35S::*AtHKT1;1* had similar Na^+ accumulation to WT (left panel). Outer *AtHKT1;1* had lower Na^+ accumulation than the Outer Background line (middle panel). Inner *AtHKT1;1* had higher Na^+ accumulation than Inner Background (right panel)Plants were harvested and analysed after a Na^+ treatment of 4 d at 10 mM, and 4 d at 20 mM. Bars represent an average of 8 plants with standard errors, except for 35S::*AtHKT1;1* control and 20 mM Na^+ are averages of 3 and 6, respectively (see text for details). The same letters or numbers above bars indicates there is no significant difference between the means at $P<0.05$ according to the Mann-Whitney test.

Interestingly, the large differences in Na^+ accumulation observed between the lines in the blades are smaller in the sheath (Figure 6.12). All lines have approximately 2 mM more Na^+ in their sheath tissue than in their blade tissue except 35S::*AtHKT1;1* is 4 mM higher in the sheath than in the blade and the outer background is 1 mM lower in its sheath than in its blade. This means that the 35S::*AtHKT1;1* line stores a more significant proportion of the Na^+ reaching its shoot in the sheath tissue as compared to the WT. This agrees well with previously mentioned notion that the 35S promoter expresses more strongly in the vascular tissue of the shoot and this may result in increased retrieval of Na^+ from the xylem to the sheath tissue, thereby limiting the Na^+ transported to the blade. Similarly, the outer background line appears unable to retain Na^+ within the sheath and allows a greater proportion to arrive in the blade. The outer *AtHKT1;1* line has a lower blade to sheath Na^+ accumulation ratio than the outer

background line indicating that it either has less Na^+ reaching the shoot to retrieve from the xylem in the sheath, or it has better xylem retrieval properties in the sheath. There is no difference in the blade to sheath ratio of Na^+ accumulation in the inner background and inner *AtHKT1;1* lines indicating there has been no alteration of sheath Na^+ retrieval by expressing *AtHKT1;1* in the inner root cells.

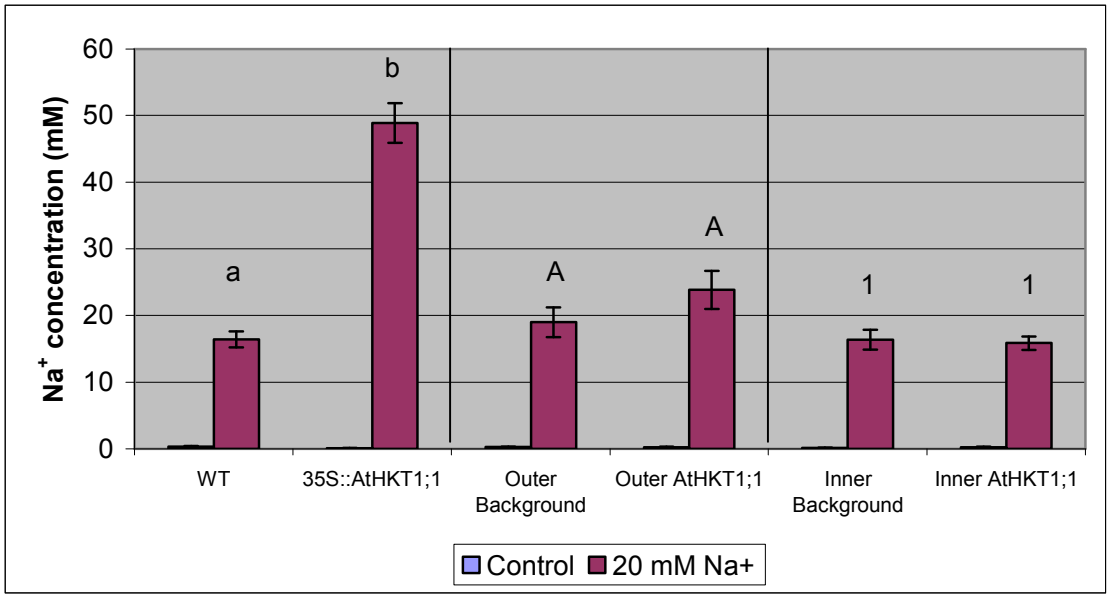

Figure 6.13: Na^+ accumulation in the roots of WT Nipponbare, 35S::*AtHKT1;1* (14-A1), Outer Background, Outer *AtHKT1;1* (2-B5), Inner Background and Inner *AtHKT1;1* (5-C4) lines. 35S::*AtHKT1;1* and Outer *AtHKT1;1* had higher Na^+ accumulation than their respective controls (left and middle panel, respectively), while Inner *AtHKT1;1* had lower Na^+ accumulation than it's control (right panel). Plants were harvested and analysed after a Na^+ treatment of 4 d at 10 mM, and 4 d at 20 mM. Bars represent an average of 8 plants with standard errors, except for 35S::*AtHKT1;1* control and 20 mM Na^+ are averages of 3 and 6, respectively (see text for details). The same letters or numbers above bars indicates no significant difference exists between the means at $P<0.05$ based on the Mann-Whitney test.

The Na^+ accumulation in the roots of the WT, outer background and inner background lines appear quite similar (Figure 6.13). There is more Na^+ reaching the shoot of the outer background line, but it appears that root xylem retrieval has not been affected or there would be a decreased level of root Na^+ accumulation. This would seem to indicate the insertion of the enhancer trap in the outer background line has affected root influx or efflux properties. .

The 35S::*AtHKT1;1* line retains three times more Na^+ in its root tissue than the WT does, thus it appears this line is more efficient at either retrieval of Na^+ from the xylem in the root, or limiting Na^+ transfer through the root tissue by accumulating it in the root cells. Either way less Na^+ is entering the xylem stream in the root, and a relatively large proportion of the Na^+ entering the xylem stream is being retrieved and sequestered into the sheath tissue, thus both factors result in low Na^+ accumulation in the blade.

The outer *AtHKT1;1* line accumulates more Na^+ in the root than does the outer background, which corresponds well with the previous T_1 data that showed increased Na^+ accumulation in the roots of both the outer *AtHKT1;1* lines. In this case it appears the outer *AtHKT1;1* line accumulates enough extra Na^+ in the roots to significantly limit the Na^+ arriving in the blade compared to the outer background line.

The inner *AtHKT1;1* line accumulates a similar amount of Na^+ in the root as the inner background line, but it has higher Na^+ accumulation in the shoot than the inner background line does. Thus, it appears that root influx in the inner *AtHKT1;1* line is higher than in the inner background line or root efflux has decreased in the inner *AtHKT1;1* line. This would seem odd considering the expression of the gene is in the stele of the root so should not affect flux properties with the soil. Another option may be that the xylem parenchyma expression of *AtHKT1;1* has increased the flux into the inner root and with the extra Na^+ being drawn across the endodermis there is an increase in Na^+ entering the xylem stream and reaching the shoot of the inner *AtHKT1;1* line.

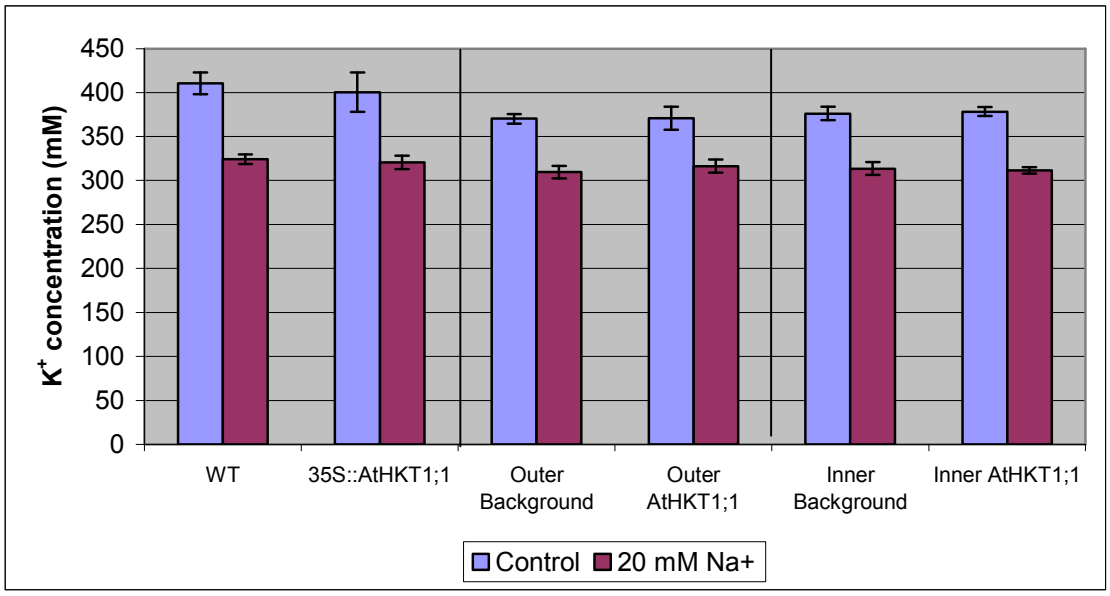

Figure 6.14: K^+ accumulation in all blades of WT Nipponbare, 35S::*AtHKT1;1* (14-A1), Outer Background, Outer *AtHKT1;1* (2-B5), Inner Background and Inner *AtHKT1;1* (5-C4) lines. Plants were harvested and analysed after a Na^+ treatment of 4 d at 10 mM, and 4 d at 20 mM. Bars represent an average of 8 plants with standard errors, except for 35S::*AtHKT1;1* control and 20 mM Na^+ are averages of 3 and 6, respectively (see text for details). No significant differences exist between the Control or 20 mM Na^+ means at $P<0.05$ according to the Mann-Whitney test.

Wild-type and 35S::*AtHKT1;1* lines accumulated slightly higher K^+ in the leaf blades than the outer and inner background and *AtHKT1;1* lines with no Na^+ stress, but this difference disappears when the plants are under salt stress (Figure 6.14). It appears the insertion of the enhancer trap in the outer background line has not affected K^+ transport as it has Na^+ transport, thus the mutation appears to be Na^+ specific. It is again apparent that the expression of *AtHKT1;1* has affected the Na^+ transport to the shoot and not the K^+ accumulation. It is interesting that there is almost no difference in K^+ accumulation between the lines under Na^+ stress, despite there being large differences in Na^+ accumulation. This may be a sign that the lines were not experiencing sufficient Na^+ stress.

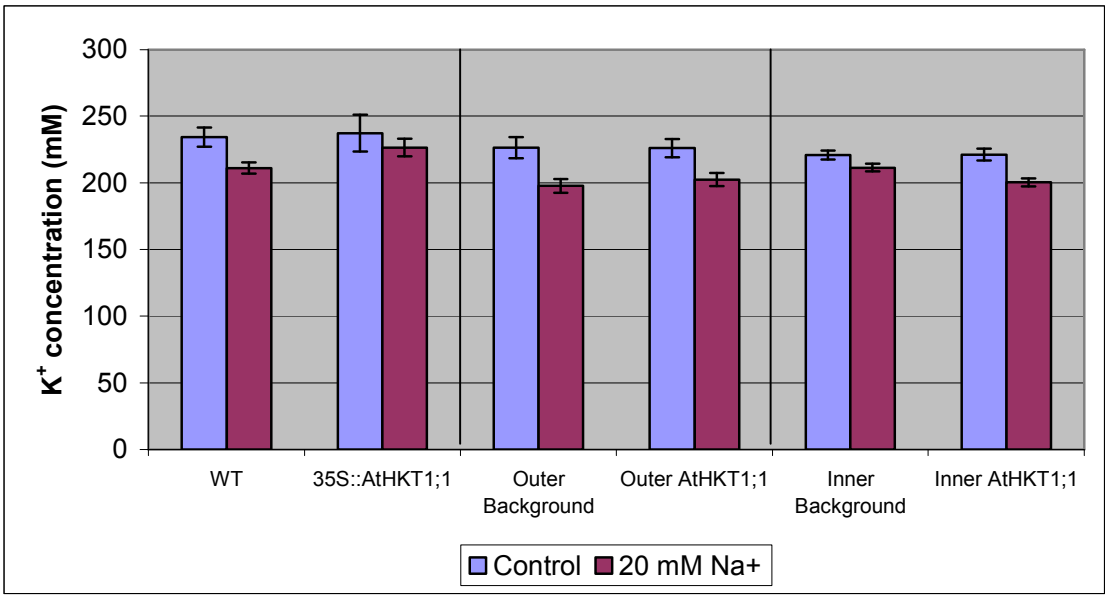

Figure 6.15: K^+ accumulation in the sheath tissue of WT Nipponbare, 35S::*AtHKT1;1* (14-A1), Outer Background, Outer *AtHKT1;1* (2-B5), Inner Background and Inner *AtHKT1;1* (5-C4) lines. Plants were harvested and analysed after a Na^+ treatment of 4 d at 10 mM, and 4 d at 20 mM. Bars represent an average of 8 plants with standard errors, except for 35S::*AtHKT1;1* control and 20 mM Na^+ are averages of 3 and 6, respectively (see text for details). No significant differences exist between the Control or 20 mM Na^+ means at $P<0.05$ according to the Mann-Whitney test.

There was very little difference between the lines in terms of sheath K^+ accumulation except that the 35S::*AtHKT1;1* line may have slightly higher K^+ under Na^+ stress than the WT line, which is strange considering the blade does not show this phenotype and the sheath shows very little difference in terms of Na^+ accumulation to the WT (Figure 6.15).

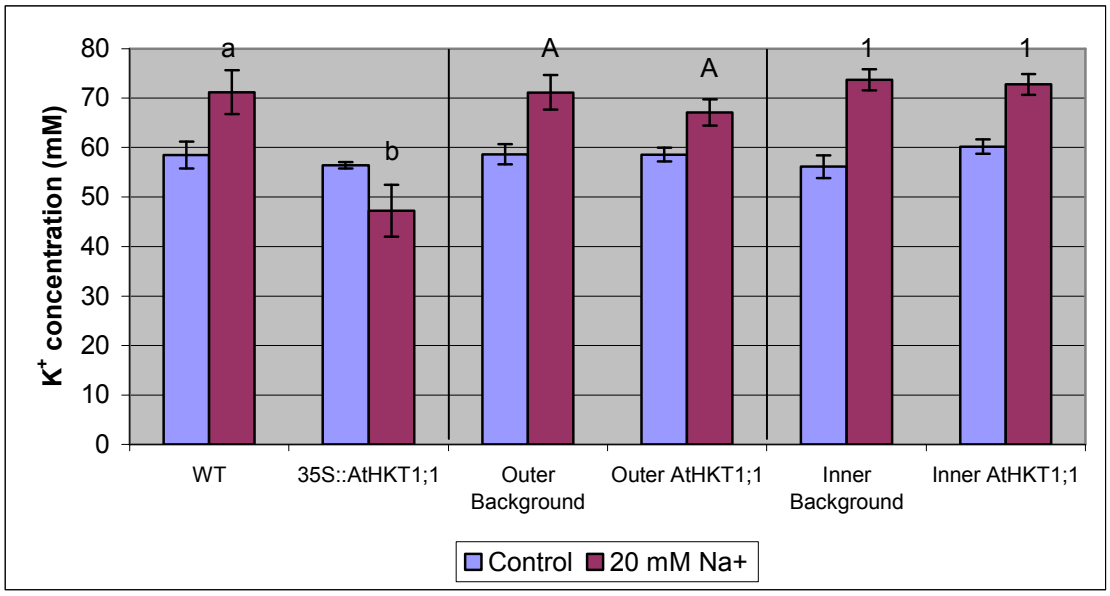

Figure 6.16: K^+ accumulation in the roots of WT Nipponbare, 35S::*AtHKT1;1* (14-A1), Outer Background, Outer *AtHKT1;1* (2-B5), Inner Background and Inner *AtHKT1;1* (5-C4) lines. 35S::*AtHKT1;1* plants had lower K^+ accumulation than WT (left panel), while the Outer *AtHKT1;1* and Inner *AtHKT1;1* lines did not differ from their respective control lines (middle and right panels, respectively). Plants were harvested and analysed after a Na^+ treatment of 4 d at 10 mM, and 4 d at 20 mM. Bars represent an average of 8 plants with standard errors, except for 35S::*AtHKT1;1* control and 20 mM Na^+ are averages of 3 and 6, respectively (see text for details). No significant difference existed between the Control means at $P<0.05$, while the same letters above 20 mM Na^+ bars indicates no significant difference exists between means at $P<0.05$ according to the Mann-Whitney test.

Generally Na^+ stressed plants will accumulate decreased amounts of K^+ (like in the blade and sheath measurements), but in this experiment there is a significant increase in K^+ accumulation in the roots of all lines except the 35S::*AtHKT1;1* line (Figure 6.16). This line had a significant decrease in K^+ accumulation which was most likely related to the overaccumulation of Na^+ in the root tissue of these lines. This was not seen in the first T_1 experiment, but has been seen in all the T_1 experiments following. It could be that the plants are not sufficiently stressed to show the typical depressed K^+ accumulation after Na^+ stress. Or perhaps the root K^+ influx transporters have been significantly upregulated by the Na^+ stress, but the sheath and blade data should show a similar trend if this were the case.

The outer *AtHKT1;1* line has slightly lower K^+ accumulation after Na^+ stress than the outer background line, which coincides with the overaccumulation of Na^+ in

the roots of this line. There was no difference between the inner *AtHKT1;1* and the inner background lines in terms of root K^+ accumulation.

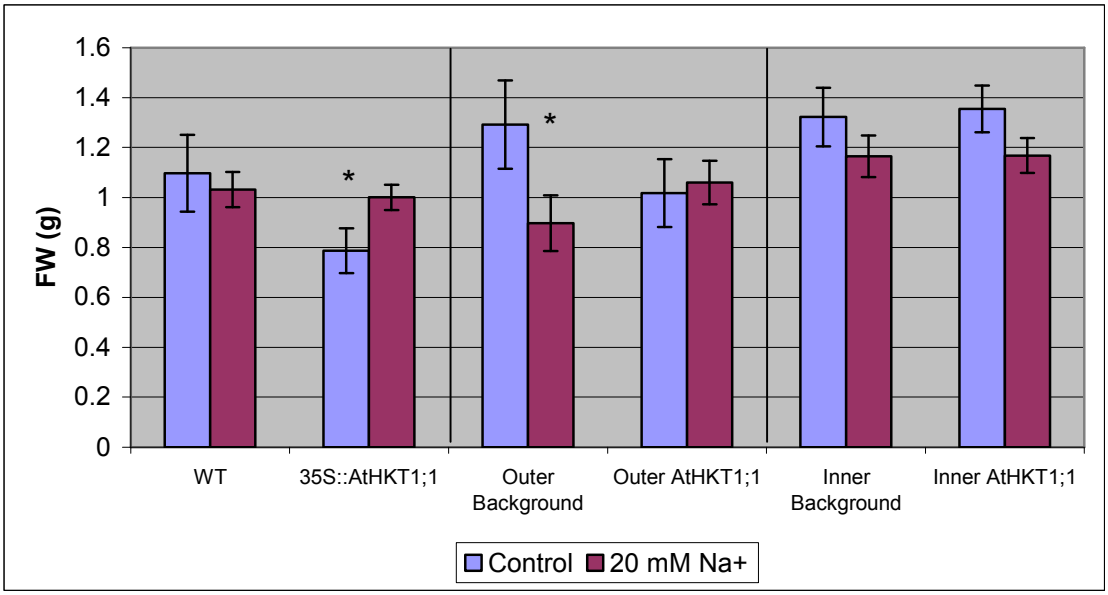

Figure 6.17: FW of all blades of WT Nipponbare, 35S::*AtHKT1;1* (14-A1), Outer Background, Outer *AtHKT1;1* (2-B5), Inner Background and Inner *AtHKT1;1* (5-C4) lines. 35S::*AtHKT1;1* and Outer *AtHKT1;1* lines were more Na^+-tolerant than their control lines (right and middle panels, respectively), while Inner *AtHKT1;1* was similarly Na^+-tolerant to it's control (right panel). Plants were harvested and analysed after a Na^+ treatment of 4 d at 10 mM, and 4 d at 20 mM. Bars represent an average of 8 plants with standard errors, except for 35S::*AtHKT1;1* control and 20 mM Na^+ are averages of 3 and 6, respectively (see text for details). A * next to a pair of means indicates a significant difference exists between the means at $P<0.05$ according to the Mann-Whitney test.

The outer background and inner background (as well as inner *AtHKT1;1*) lines appear to have some increase in FW over the WT line (Figure 6.17). Again, this could be related to the enhancer trap insertion, although this explanation seems unlikely since the insertion has also increased the Na^+ accumulation in the shoot of the outer background line. More likely is that it is again related to the different seed stocks. Additionally, the WT appears to have lost very little FW with the Na^+ stress, so whether the Na^+ stress was sufficiently large enough remains a question.

The 35S::*AtHKT1;1* line actually grows better under salt-stressed conditions. The line germinates poorly and develops very slowly compared to the other lines when

transplanted to hydroponic conditions (despite very low Na^+ presence). When salt stress is imposed the plants that have not died completely recover and end up being the same size as the other lines at harvest. One 35S::*AtHKT1;1* plant in the control tank (no added Na^+) survived and grew comparably to the other control plants, but when it was genotyped it was found to be null for *AtHKT1;1*. Thus, overexpression of *AtHKT1;1* appears to provide a strong negative effect on germination and seedling survival in a low Na^+ environment (section 6.2.4.1). The 35S::*AtHKT1;1* line is more tolerant than the WT, and this compares well with the Na^+ accumulation data, which shows that the 35S:*AtHKT1;1* line has better Na^+ exclusion than the WT.

The outer *AtHKT1;1* line is slightly smaller than the outer background line in control conditions, but it is significantly more salt tolerant than the outer background line and has a greater FW under salt stress than the outer background line. This compares well with the Na^+ accumulation data, which showed significantly better sodium exclusion in the outer *AtHKT1;1* line than in the outer background line.

The inner *AtHKT1;1* line is unchanged in FW compared to the inner background line in control and salt stressed conditions, even though the inner *AtHKT1;1* line accumulates more Na^+ in the shoot than the inner background line. This is odd since 35S::*AtHKT1;1* is more tolerant and excludes more Na^+ than WT, the outer *AtHKT1;1* line is more tolerant and excludes Na^+ more efficiently than the outer background line, but inner *AtHKT1;1* is similarly tolerant although it accumulates more Na^+ than the inner background.

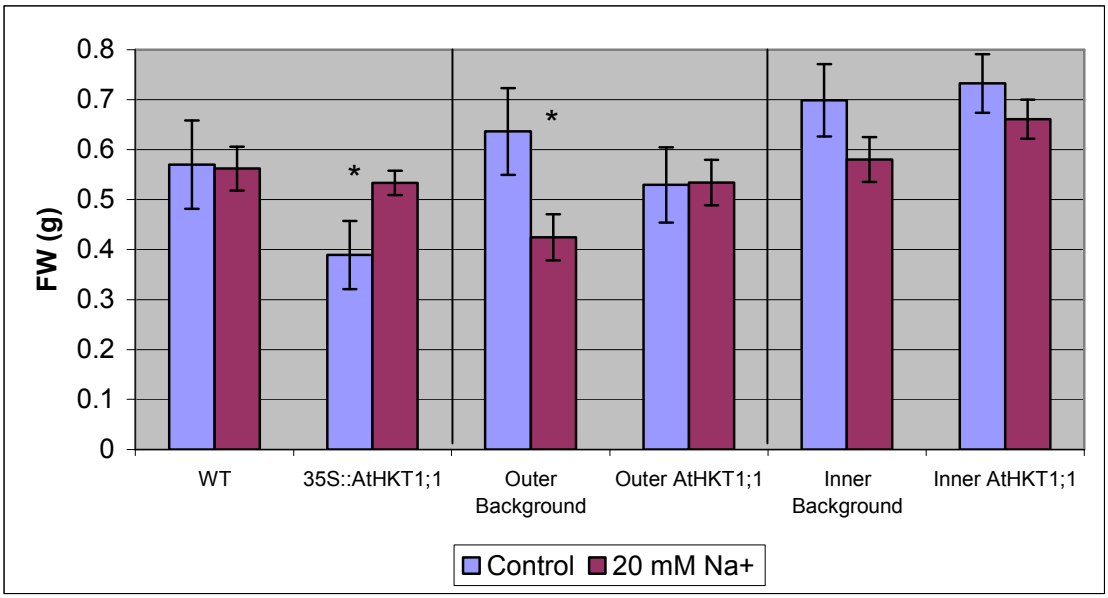

Figure 6.18: FW of roots of WT Nipponbare, 35S::*AtHKT1;1* (14-A1), Outer Background, Outer *AtHKT1;1* (2-B5), Inner Background and Inner *AtHKT1;1* (5-C4) lines. 35S::*AtHKT1;1* and Outer *AtHKT1;1* lines were more Na^+-tolerant than their control lines (right and middle panels, respectively), while Inner *AtHKT1;1* was similarly Na^+-tolerant to it's control line (right panel). Plants were harvested and analysed after a Na^+ treatment of 4 d at 10 mM, and 4 d at 20 mM. Bars represent an average of 8 plants with standard errors, except for 35S::*AtHKT1;1* control and 20 mM Na^+ are averages of 3 and 6, respectively (see text for details). A * next to a pair of means indicates a significant difference exists between the means at $P<0.05$ according to the Mann-Whitney test.

The root tolerance data is nearly identical to the shoot data. Again the outer background, inner background and inner *AtHKT1;1* lines are larger than the WT plants (Figure 6.18). There may be a similar phenomenon going on with the outer *AtHKT1;1* lines as there is with the 35S::*AtHKT1;1*. The outer *AtHKT1;1* line is smaller than the outer background line in both shoot and root FW in control conditions. It appears that the line requires some Na^+ to grow properly, but the stimulation of growth is less than in the 35S::*AtHKT1;1* line.

Interestingly, despite the overaccumulation of Na^+ in the roots of the 35S::*AtHKT1;1* plants, the roots do not seem to lose FW compared to the other lines which accumulate three times less Na^+ in their roots. However, the line is still more tolerant than the WT plants and shows the same improvement of growth with Na^+ stress. Apparently tolerance is related more closely to Na^+ accumulation in the shoots

and not that of the roots, otherwise the 35S::*AtHKT1;1* line would be much less tolerant.

The outer *AtHKT1;1* line shows similar tolerance based on root FW data as it did based on shoot FW data. The inner *AtHKT1;1* line actually appears somewhat more tolerant than the inner background line based on the root FW data. Both lines have similar root FW in control conditions, but the salt treated roots of the inner *AtHKT1;1* line are actually bigger than those of the inner background line. Once again, it is strange that this pair of lines has a different relationship between tolerance and accumulation of Na^+ than the other two pairs of lines.

6.3.4 35S::*AtHKT1;1* experiments

6.3.4.1 Seed germination and seedling growth

Further experiments were conducted to attempt to understand the germination and seedling growth deficiency observed in the T_1 line (also observed in a second independent 35S::*AtHKT1;1* line). Three groups of 35S::*AtHKT1;1* (14-A1) seeds were germinated on Petri dishes, as in all previous experiments, except one group of seeds was supplemented with 5 mM Na^+ and one with 5 mM K^+ (as well as one on RO water alone). The seeds germinated on RO water had a germination rate of 82%, while the Na^+ and K^+ treated plates had germination rates of 100% (WT seed had 100% germination in all three treatments). This shows that the germination process requires some additional Na^+ or K^+. Seedlings were transferred to 1 l beakers after 5 d on Petri dishes and 2 mM $Ca(NO_3)_2$ was added to the growth solution to ensure the plants were not completely nutrient deficient. After transfer to the beakers the seedlings were allowed to grow for a further 7 d (Figure 6.19). The proportion of seedlings which developed at a normal rate on RO water was 45% (included 2 seeds which never germinated, 4 small plants and 5 large plants), 82% on Na^+ (included 2 small plants and 9 large plants), and 64% on K^+ (included 4 small plants and 7 large plants). Apparently treatment with Na^+ and K^+ improve the germination rate of the line to the same extent, but Na^+ improves the plant growth beyond germination. The RO water treated plants which developed normally were not as the normally developed plants in the Na^+ and K^+ treatments indicating they still were deficient in Na^+ or K^+ in the shoots. The K^+ plants, while larger than the Na^+ treated plants, had extremely long

sheaths, but small blades compared to the more normal appearing Na^+ treated plants. This seems to indicate that the K^+ treatment cannot fully replace an apparent Na^+ requirement of the seedlings for growth. Of note, the Na^+ and K^+ treatments did not affect the growth of WT seedlings.

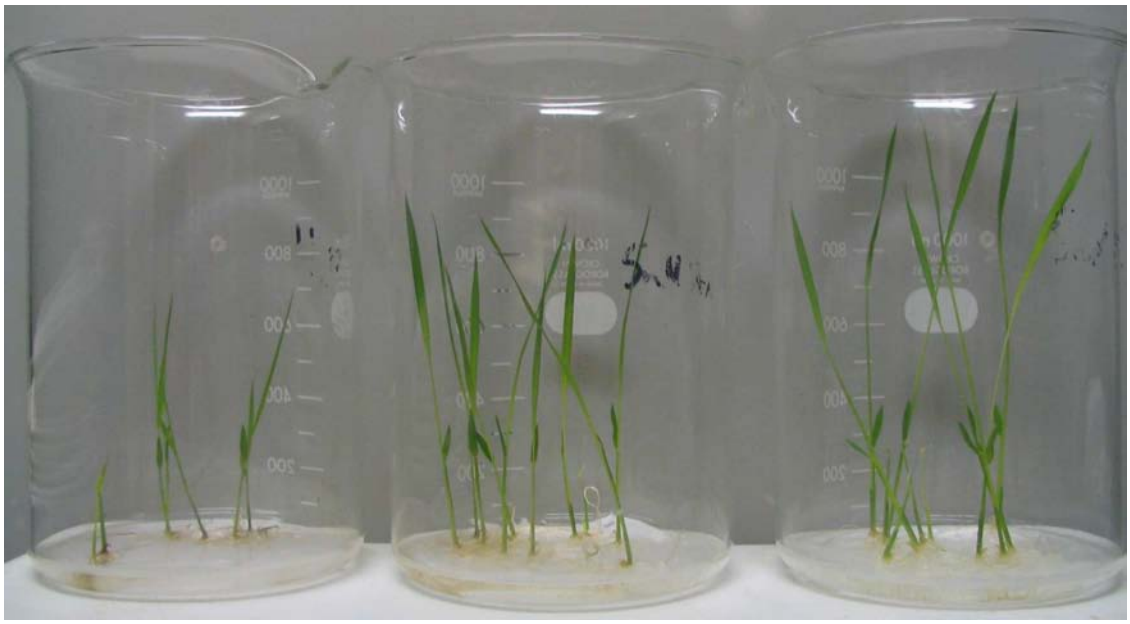

Figure 6.19: 35S::*AtHKT1;1* seedlings after 5 d growth on RO water (left), RO water + 5 mM NaCl (middle) or RO water + 5 mM KCl (right). Seedlings treated with 5 mM NaCl or 5 mM KCl were larger than seedlings treated with RO water. Seedlings were grown on Petri dishes for 5 d on the minimal solutions and transferred to beakers for an additional 7 d growth on minimal solutions supplemented with 2 mM $Ca(NO_3)_2$.

The seedlings were harvested after 7 d, separated into shoots and roots and the Na^+ and K^+ accumulation was measured using the flame photometer. The large plants were harvested individually, but the small plants were too small to analyse individually and were pooled to make one small plant root and shoot sample for each treatment.

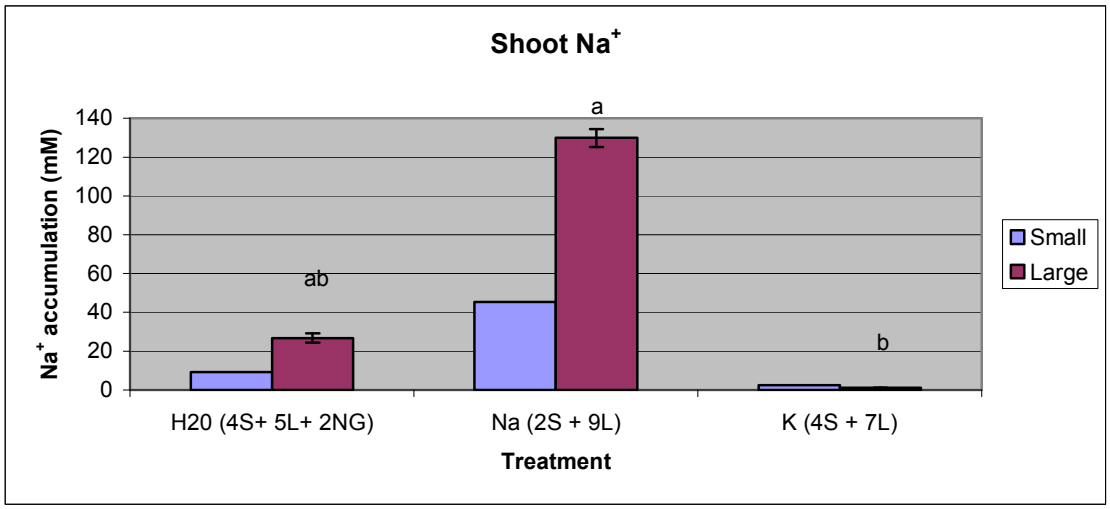
Shoot Na+
Na+ accumulation (mM)
140
120
100
80
60
40
20
0
a
ab
b
H20 (4S+ 5L+ 2NG)
Na (2S + 9L)
K (4S + 7L)
Treatment
Small
Large

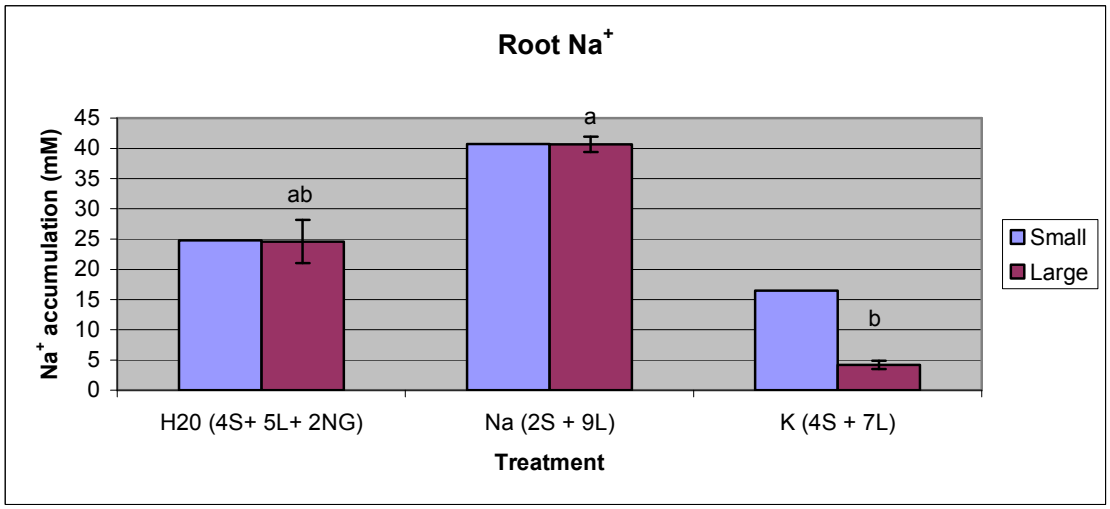
Root Na+
Na+ accumulation (mM)
45
40
35
30
25
20
15
10
5
0
a
ab
b
H20 (4S+ 5L+ 2NG)
Na (2S + 9L)
K (4S + 7L)
Treatment
Small
Large

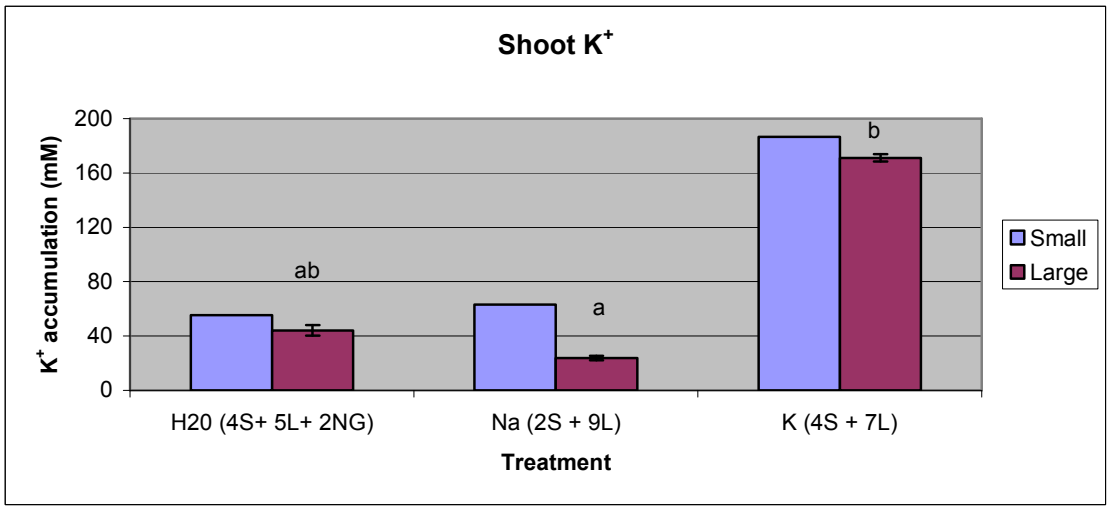
Shoot K+
K+ accumulation (mM)
200
160
120
80
40
0
b
ab
a
H20 (4S+ 5L+ 2NG)
Na (2S + 9L)
K (4S + 7L)
Treatment
Small
Large

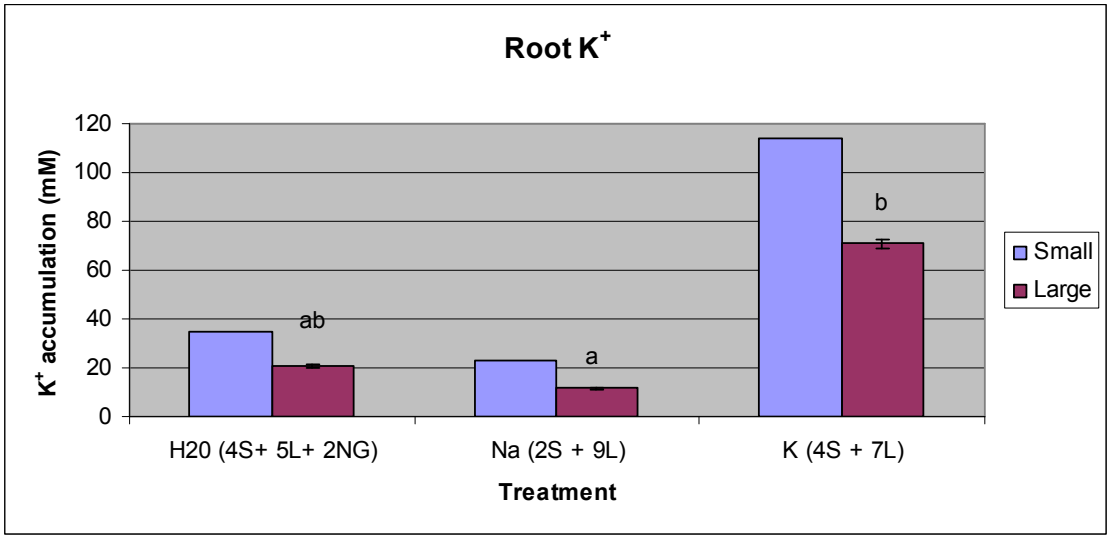

Figure 6.20: 35S::*AtHKT1;1* seedlings shown in Figure 6.19 were analysed for Na^+ and K^+ accumulation in shoots and roots after growth on RO water, RO water + 5 mM Na^+ or RO water + 5 mM KCl. Large seedlings in each treatment were analysed individually (Large), but small seedlings in each treatment were pooled into one shoot sample and one root sample (Small). In brackets, next to each treatment, is the number of small plants (S), large plants (L) and seeds that did not germinate (NG) in each treatment. The same letters above bars indicates no significant difference exists between the means at $P<0.05$ according to the Kruskal-Wallis and Dunn's Multiple Comparisons tests.

As would be expected the Na^+ treated plants had the highest root and shoot Na^+ accumulation for small or large plants in any treatment (Figure 6.20). Similarly, the K^+ treated plants had the highest root and shoot K^+ accumulation for small or large plants in any treatment. The RO water treated plants accumulated more Na^+ than the K^+ treated plants and more K^+ than the Na^+ treated plants. This Na^+ and K^+ must have originated from the seed itself, the filter paper, contamination in the RO water, or in the $Ca(NO_3)_2$. When comparing the small and large plants within a treatment, the shoots of the large RO water and Na^+ treated plants contained 3 times more Na^+ than the small plants did, while the roots contained similar amounts of Na^+. Thus, it appears that the shoot Na^+ concentration plays a large part in recovering the normal growth phenotype in the plant and that the efficiency of these plants in preventing Na^+ transfer to the shoot prevents sufficient Na^+ from reaching the shoots in the small plants. The small plants in all treatments accumulate more K^+ than the large plants, indicating that the plant may be sensing the deficiency in Na^+ in the shoot and upregulating K^+ uptake in

an attempt to combat the Na^+ deficiency. A major assumption is that the plant needs Na^+ in the shoot and K^+ can replace this deficiency, but not completely. The shoots of the large K^+ treated plants contained slightly less K^+ than the small plants, while the roots had approximately half the K^+ concentration of the small plants. It is less apparent why the K^+ treated seedlings are small or large, as there is less Na^+ and K^+ in the large K^+ treated seedlings. Interestingly, the roots of the small K^+ treated seedlings have 3.9 times the Na^+ concentration and 1.6 times the K^+ concentration of the roots of the large K^+ treated seedlings. This indicates that the small K^+ treated seedlings may be sensing a deficiency in shoot Na^+ (or K^+) and are upregulating Na^+ and K^+ uptake mechanisms to try to alleviate this deficiency. It appears that the efficiency of the 35S::*AtHKT1;1* line in preventing the movement of Na^+ to the shoots restricts sufficient movement of Na^+ to the shoot and prevents recovery of normal growth habit. Also, the K^+ treatment appears to be either blocking the ability of the seedlings to take up Na^+, or the plant is not sensing the Na^+ deficiency with the high levels of K^+ available. *OsHKT2;1* apparently functions as a Na^+ influx transporter in K^+ starved conditions to alleviate the effects of K^+ deficiency (Horie *et al.* 2007). In the K^+ deficient treatments (RO water and Na^+) the roots contain significantly more Na^+ than the K^+ treated plants indicating higher Na^+ uptake to alleviate the K^+ deficiency. The shoots also contain significant Na^+ levels which may be a result of the increased uptake or the upregulation of another transporter. The small K^+ treated plants contain more Na^+ in the roots than the large K^+ treated plants, indicating either a deficiency in sensing the shoot K^+ status and thus an attempt to upregulate *OsHKT2;1* to increase the Na^+ influx, or perhaps the regulation of *OsHKT2;1* is controlled by Na^+ balance as well and this upregulates the transporter. This is all balanced by the strong recovery of Na^+ from the xylem by the overexpression of *AtHKT1;1*, which may explain why the small plants stay small and the large plants recover in the RO water and Na treatments (also, *OsHKT1;5* may aid in recovery of Na^+ in the root, and *OsHKT1;4* could help to recover Na^+ in the sheath).

6.3.4.2 Seed elemental profile

To check whether the 35S::*AtHKT1;1* seeds (T_1) start with Na^+ or K^+ deficiency, the elemental profile of seed was analysed via ICPAES. The lines included

for comparison were 35S::*RFP* (15-C5), Outer RFP (3-A5), Inner RFP (6-A5) (all representative of the Na^+ accumulation phenotype seen in the screening of the primary transgenic lines), 35S::*AtHKT1;1* (14-A1) Outer *AtHKT1;1* (2-B5) and Inner *AtHKT1;1* (5-C4) lines. Unfortunately, no seed was available from lines grown under controlled hydroponic conditions, but, the lines chosen were treated exactly the same after tissue culture and plant regeneration. The plants were potted in soil and fertiliser was administered to the common water the pots were sitting in on the growth room bench. Thus, whether the differences observed are a factor of the genetic make-up of the plants or simply the nutrients they were individually exposed to is difficult to determine. The analysis was useful as the germination and seedling growth of the lines chosen could be compared to determine if the germination and seedling growth deficiency could be related to the seed elemental makeup or if there were further factors creating the decreased germination rate in the 35S::*AtHKT1;1* line.

Table 6.1: ICPAES analysis of the elemental profile of 35S::*RFP*, 35S::*AtHKT1;1*, Outer RFP, Outer *AtHKT1;1*, Inner RFP and Inner *AtHKT1;1* seed. Data is an average of four replicates of four seeds per line (with standard error). The same letters following mean values indicate means are not significantly different at $P<0.05$ according to the Kruskal-Wallis and Dunn's Multiple Comparisons tests.

		Fe	Mn	B	Cu	Zn	Ca	Mg	Na		K		P	S	Al
Line		mg/kg	mg/kg	mg/kg	mg/kg	mg/kg	mg/kg	mg/kg	mg/kg	stats	mg/kg	stats	mg/kg	mg/kg	mg/kg
15 C5 35S	AVG	18.1	12.4	1.2	11.3	23.3	136.7	1210	5.0	c	2350	a	2925	1100	0.7
RFP	SE	0.2	0.2	0.0	0.4	0.3	2.0	17	0.2		50		25	16	0.1
14 A1 35S	AVG	22.4	9.5	1.4	12.0	31.8	136.5	1243	1.9	a	2475	ab	3100	1123	1.1
AtHKT1;1	SE	0.4	0.3	0.1	0.4	1.1	5.6	27	0.1		48		71	30	0.6
3 A5 Outer	AVG	16.9	8.6	1.4	8.0	21.7	148.8	1065	2.2	abc	2525	ab	2600	1038	0.6
RFP	SE	0.5	0.1	0.1	0.1	0.6	5.9	31	0.2		118		71	9	0.1
2 B5 Outer	AVG	26.4	14.3	2.1	13.0	43.6	190.8	1710	3.8	bc	3925	c	4175	1355	1.5
AtHKT1;1	SE	0.9	0.4	0.1	0.6	1.9	15.0	26	0.8		206		111	24	0.5
6 A5 Inner	AVG	18.6	10.3	1.8	10.2	34.7	154.5	1448	2.1	ab	2850	abc	3550	1083	0.7
RFP	SE	0.3	0.2	0.1	0.2	0.9	5.1	34	0.1		65		96	15	0.0
5 C4 Inner	AVG	26.1	13.8	1.7	11.8	40.0	144.4	1655	2.5	abc	3325	bc	4150	1375	0.7
AtHKT1;1	SE	1.6	0.5	0.1	0.7	2.4	5.0	43	0.3		206		189	42	0.1

The analysis revealed that if a line was low in one nutrient it was likely low in all measured nutrients, which indicates the individual plant nutrient status was important (Table 6.1). For instance, the 35S line had less of all elements examined (except Cu^{3+} and Al^{3+}) than the outer and inner *AtHKT1;1* lines. Importantly, the 35S line is lowest in Na^+ accumulation and second lowest in K^+ accumulation. This may partially explain why the line germinates poorly, but the Outer RFP line has a

statistically similar level of Na^+ and K^+ in the seed and is lower or similar in accumulation of the other elements examined to the 35S line yet it germinates completely normally (as do all the other lines in this experiment). Thus, it seems that though the level of Na^+ and K^+ the 35S line starts with in the seed is low, there must be an effect of the overexpression of *AtHKT1;1* on the transport of Na^+ or K^+ within the germinating seed and later within the developing seedling to cause the poor germination and seedling establishment.

Despite all this, the requirement of Na^+ for normal germination and seedling growth of the 35S line could be quite attractive from the agricultural point-of-view since seeds would usually germinate and develop as seedlings under some level of Na^+.

6.3.5 ^{22}Na influx analysis

Analysis of the influx of Na^+ into the roots via ^{22}Na flux analysis was used to determine whether the expression of *AtHKT1;1* in various cell-types in the roots had affected the influx of Na^+ into the roots. The protocol was developed by adapting a previously used cereal protocol (see Chapter 2).

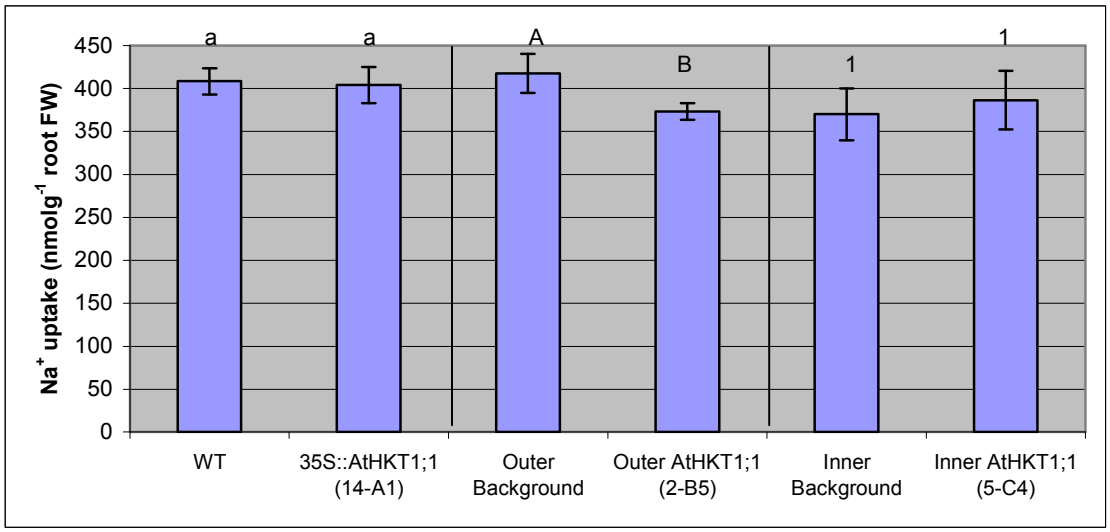

Figure 6.21: Unidirectional influx into roots of WT, 35S::*AtHKT1;1*, Outer Background, Outer *AtHKT1;1*, Inner Background and Inner *AtHKT1;1* lines measured by ^{22}Na radioactive tracer analysis of intact plants for 2 min at 30 mM Na^+ and 0.1 mM Ca^{2+} activity (see Chapter 2 for experimental details). 35S::*AtHKT1;1* and Inner *AtHKT1;1* lines had similar Na^+ uptake to their respective control lines (left and right panels, respectively), while Outer *AtHKT1;1* had lower Na^+ uptake than it's control (middle panel). Data is an average of eight replicates plus/minus standard error. The same letter or numbers above bars indicates no significant difference exists between means at $P<0.05$ according to the Mann-Whitney test.

No significant difference in influx was found between WT, outer background and inner background, though the outer background had slightly higher influx than the WT and the inner background had lower influx than the WT (Figure 6.21). Thus, it seems that the enhancer trap insertion has not affected the Na^+ influx into roots. It should be mentioned that only minor differences in Na^+ influx (assuming no change in root efflux) would be required to significantly alter the amount of Na^+ entering a plant over the course of a multi-day salt stress, and thus potentially reaching the shoot.
There was no significant difference in influx between WT and the 35S::*AtHKT1;1* line, which would indicate that the low Na^+ in the blade of the 35S::*AtHKT1;1* line is primarily due to decreased root-to-shoot transfer.

A significant decrease is observable in the influx of the outer *AtHKT1;1* line compared to that of the outer background. This is interesting since the 35S::*AtHKT1;1* line does not show this influx decrease even though it is quite likely the gene is expressed in primarily the same root cells. This indicates the low Na^+ accumulation phenotype in the blades of the outer *AtHKT1;1* line may be related to a decrease in root influx in addition to the increased root accumulation of Na^+.

The difference that exists in the root Na^+ influx between the inner background and inner *AtHKT1;1* line is not significant, but it does seem like the influx into the inner *AtHKT1;1* line has increased slightly. The slight increase in influx into this line could account for the increased Na^+ accumulation observed in the accumulation experiment.

6.3.6 X-ray microanalysis

6.3.6.1 Photographs of cell-types analysed

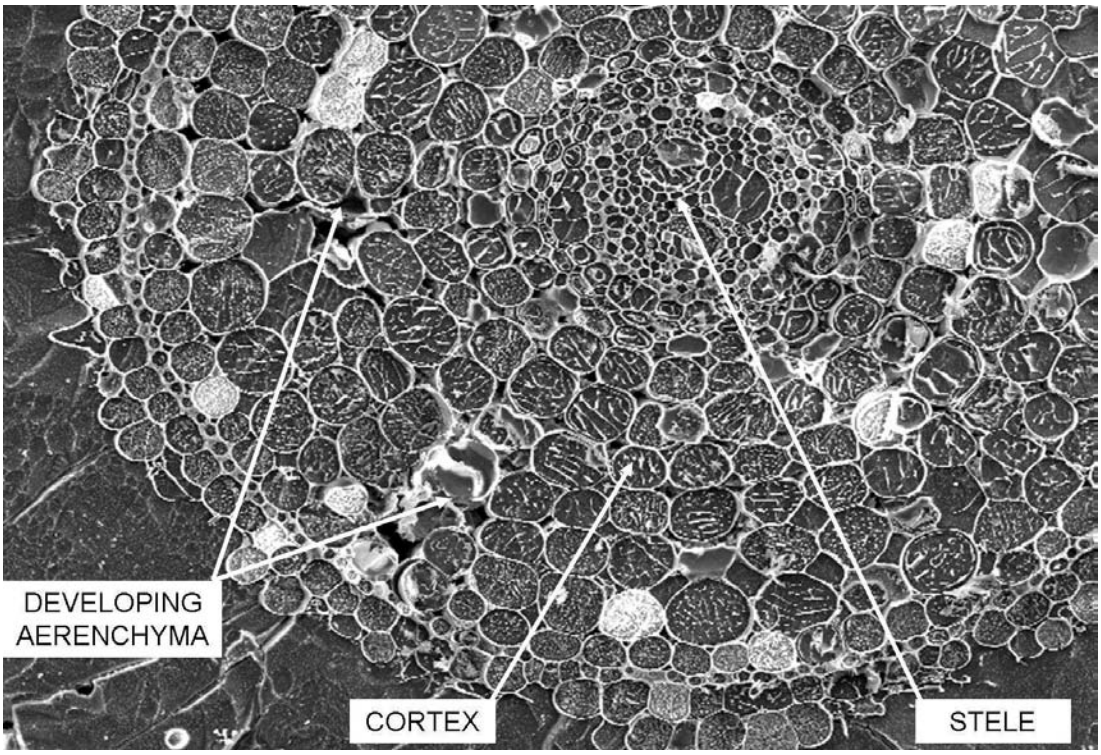

Figure 6.22: Scanning electron microscope photograph of rice root sectioned 4 mm from the root tip (see materials and methods for details) highlighting general root features.

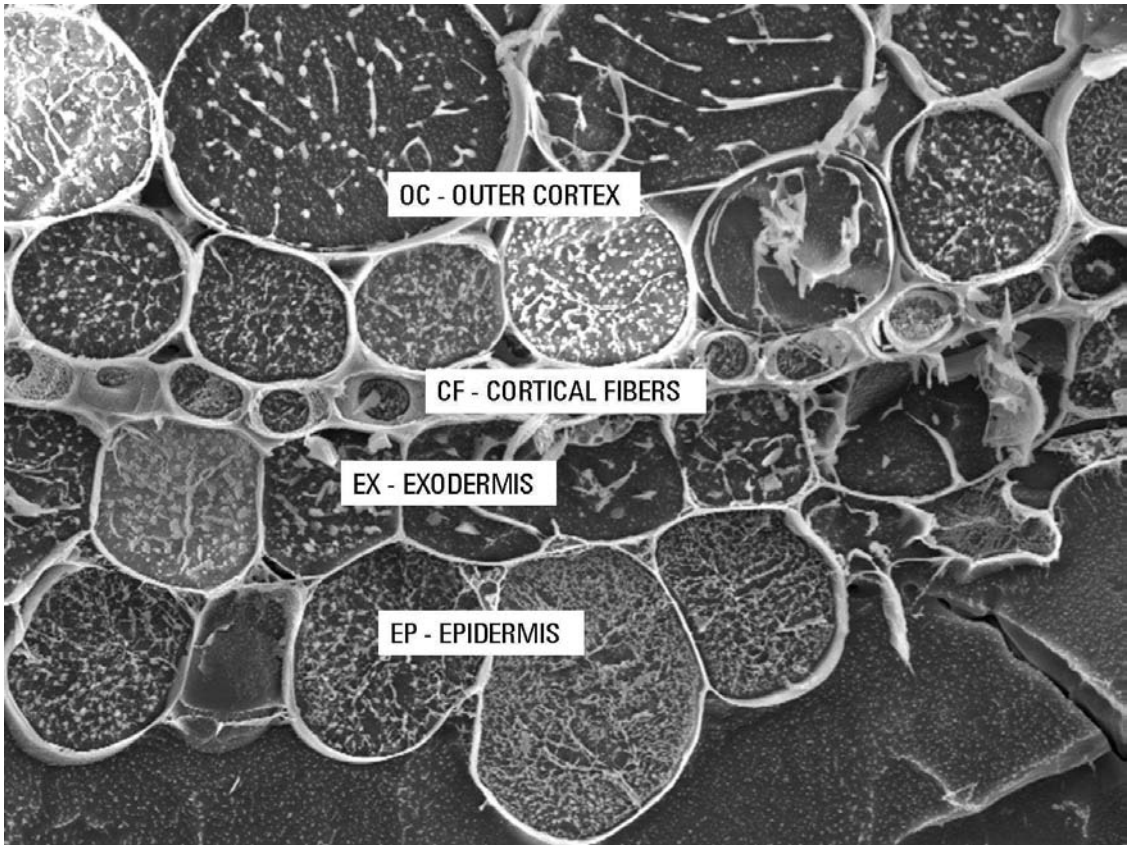

Figure 6.23: Scanning electron microscope photograph of the outer cells layers of a rice root sectioned 4 mm from the root tip (see materials and methods for details) highlighting the epidermis (EP), exodermis (EX), cortical fibres (CF) and outer cortex (OC) cells.

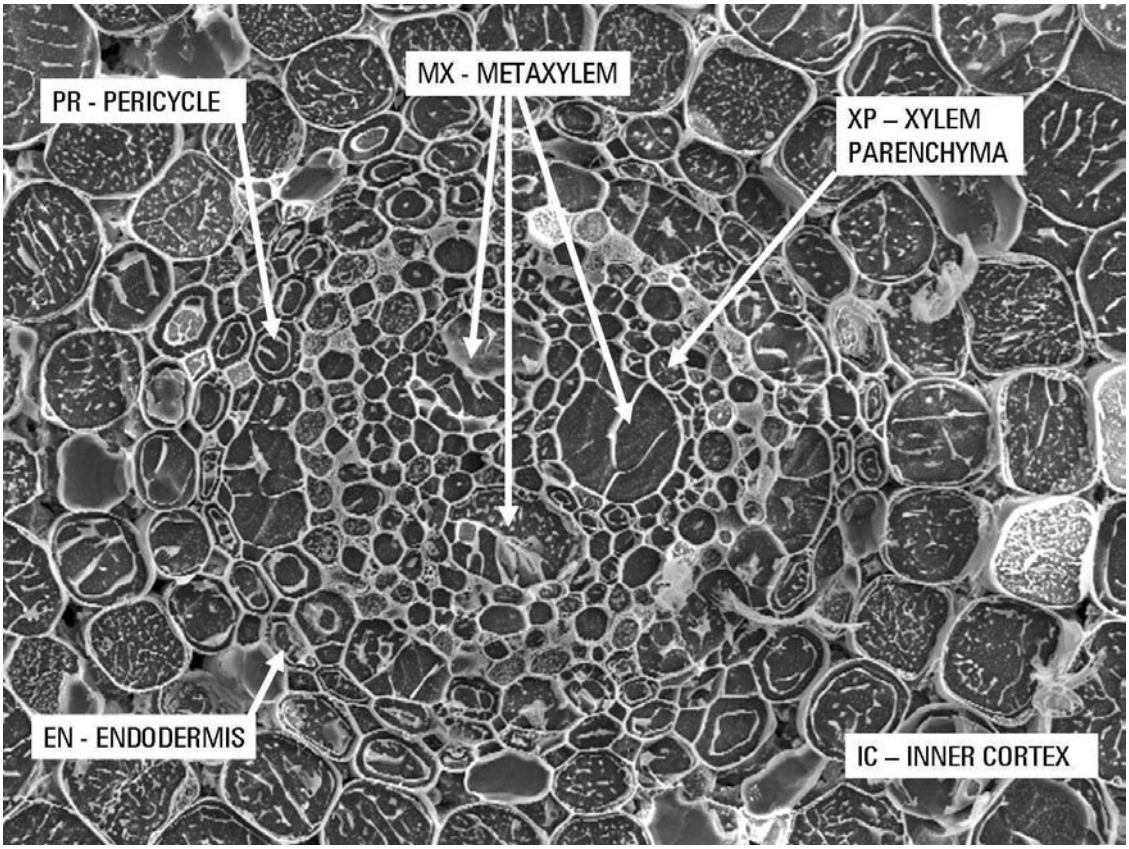

Figure 6.24: Scanning electron microscope photograph of the outer cells layers of a rice root sectioned 4 mm from the root tip (see materials and methods for details) highlighting the inner cortex (IC), endodermis (EN), pericycle (PR), xylem parenchyma (XP) and metaxylem (MX) cells.

6.3.6.2 Na^+

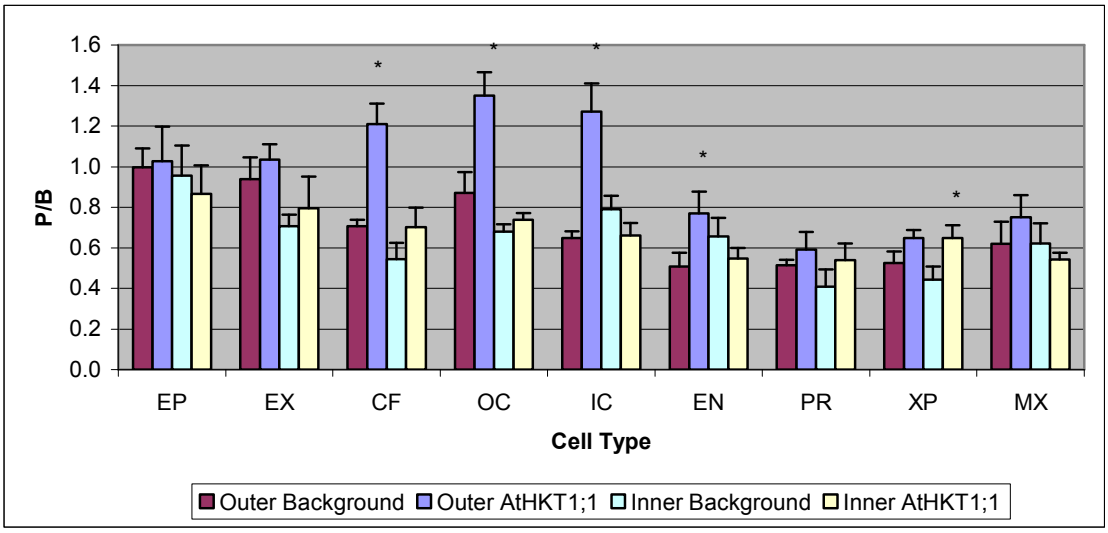

Figure 6.25: Na^+ content (P/B) measured by x-ray microanalysis in 9 root cell-types of Outer Background, Outer *AtHKT1;1*, Inner Background and Inner *AtHKT1;1* lines treated for 5 d with 50 mM Na^+ in ACPFG solution (see Methods and Materials for details). Cell-types analysed were epidermis (EP), exodermis (EX), cortical fibers (CF), outer cortex (OC), inner cortex (IC), endodermis (EN), pericycle (PR), xylem parenchyma (XP) and metaxylem (MX). Each bar represents an average of 9 individual cell measurements (3 cells from each of 3 plants) with standard errors. A * above a bar indicates that a significant difference exists between the mean and the mean of the line's respective background line at $P<0.05$ according to the Mann-Whitney test.

No large differences exist between the outer and inner background lines in Na^+ accumulation (Figure 6.25). The outer background may be slightly higher in the exodermis (EX) and outer cortex (OC), and the inner background is slightly elevated in the inner cortex (IC), but as was seen in the analysis of the whole root tissue by flame photometry, the roots are very similar in terms of Na^+ accumulation

The outer *AtHKT1;1* line accumulated significantly more Na^+ in several cell-types compared to the outer background line (Figure 6.25). The cortical fibres (CF), outer cortex (OC), inner cortex (IC) and endodermis (EN) are all higher in the outer *AtHKT1;1* line while the epidermis (EP), exodermis (EX), pericycle (PR), xylem parenchyma (XP) and metaxylem (MX) are all similar to the outer background line. Essentially, the outer *AtHKT1;1* line has higher Na^+ accumulation in the cells between the stele and the epidermis/exodermis. There is GFP fluorescence in the cortical cells

of the outer background line, so *AtHKT1;1* is expressed in these cells as well. The outer cells seem to accumulate higher Na^+, thus preventing Na^+ from being transferred up the xylem stream. These cells are highly vacuolated and are able to store significant amounts of Na^+, so it may also be that the cells in the epidermis/exodermis are accumulating the extra Na^+ and moving it to the cortical cells for storage. No change is observed in the inner root cells indicating that the expression of the transgene is specific to the outer cells. This correlates well with the whole root analysis of Na^+ accumulation, which showed the outer *AtHKT1;1* line accumulated more Na^+ in the root tissue than the outer background.

The only significant difference between the inner *AtHKT1;1* line and the inner background line is the xylem parenchyma (XP) cells of the inner *AtHKT1;1* line accumulate more Na^+ (Figure 6.25). Overall, there was very similar accumulation between the lines except in the actual cells expressing *AtHKT1;1*. This seems to indicate that expression of *AtHKT1;1* is causing the xylem parenchyma cells to accumulate extra Na^+. However, since the xylem parenchyma cells form a very small proportion of the entire root and have relatively small vacuoles, the amount of Na^+ they can accumulate is quite small compared to the outer root cells, thus the quantity of Na^+ reaching the xylem stream is almost unchanged. This is evident in the whole root accumulation data which shows the roots of the inner *AtHKT1;1* line do not accumulate extra Na^+. Possibly, the xylem parenchyma cells expressing *AtHKT1;1* draw increased amounts of Na^+ across the endodermis from the outer root, but are unable to store the extra Na^+ arriving in the stele (due to the small vacuoles), thus the extra Na^+ is transported up the xylem to the shoot (as seen in the whole plant Na^+ accumulation analysis).

6.3.6.3 K^+

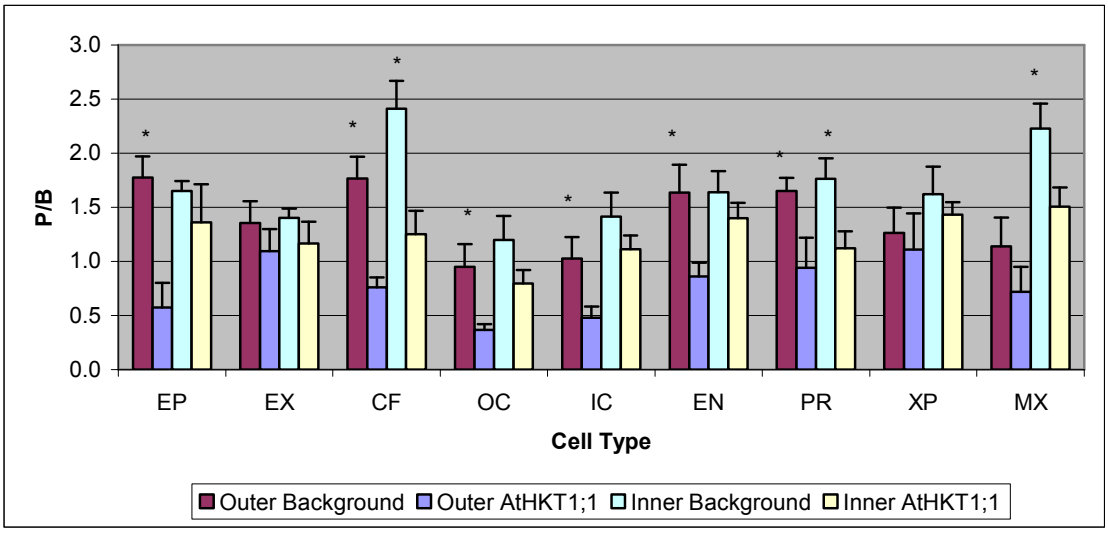

Figure 6.26: K^+ content (P/B) measured by x-ray microanalysis in 9 root cell-types of Outer Background, Outer *AtHKT1;1*, Inner Background and Inner *AtHKT1;1* lines treated for 5 d with 50 mM Na^+ in ACPFG solution (see Methods and Materials for details). Cell-types analysed were epidermis (EP), exodermis (EX), cortical fibers (CF), outer cortex (OC), inner cortex (IC), endodermis (EN), pericycle (PR), xylem parenchyma (XP) and metaxylem (MX). Each bar represents an average of 9 individual cell measurements (3 cells from each of 3 plants) with standard errors. A * above a bar indicates a significant difference exists between that mean and the mean of the respective *AtHKT1;1* line at $P<0.05$ according to the Mann-Whitney test.

There were minor differences in K^+ content between the outer and inner background lines (Figure 6.26). The cortical fibres (CF) and metaxylem (MX) of the inner background line had higher K^+ content then the outer background line. The higher content in the metaxylem (MX) may be a contamination problem as the inner background line did not show higher K^+ content in the sheath or blade in whole plant analysis which would be expected if the metaxylem (MX) actually had more K^+ in it.

Significantly higher K^+ content was observed in most of the cell-types of the outer *AtHKT1;1* line compared to the outer background (Figure 6.26). Significantly higher K^+ content was found in the epidermis (EP), cortical fibres (CF), outer cortex (OC), inner cortex (IC), endodermis (EN) and pericycle (PR) cells in the outer *AtHKT1;1* line. This is strange as it would be expected that the decreased K^+ content would only be observed in the cell-types showing increased Na^+ content. The low K^+ accumulation does show up in the whole root analysis although it does look more

severe based on x-ray microanalysis data. It could be that the specific section or root analysed in this study was more K^+ deficient compared to the root as a whole, thus not an accurate measure of root K^+ status. Alternatively, the growth conditions of these plants was slightly different since these plants were pretreated with 50 mM Na^+ for 5 d prior to analysis, thus the stress and duration of stress the plants were faced with was different from the Na^+ accumulation/Na^+ tolerance experiments. The trend is the same, thus the data seems to confirm what had been seen earlier in the whole root analysis.

Just as the outer *AtHKT1;1* line was lower in K^+ than the outer background line, the inner *AtHKT1;1* line is lower in K^+ in several cell-types than the inner background line (Figure 6.26). The inner *AtHKT1;1* line is lower in cortical fibres (CF), outer cortex (OC), inner cortex (IC), pericycle (PR) and metaxylem (MX) cell-types, but low K^+ phenotype is not as significant as it is in the outer *AtHKT1;1* line. The data from the accumulation/tolerance experiments does not show this low K^+ phenotype, possibly because the differences in individual cell-types are relatively minor in the outer cortex (OC) and inner cortex (IC), the cells which would contain the majority of the root K^+ content. Again, it may be that this section of the root does not accurately reflect the K^+ status of the whole root.

6.4 General Discussion

Functional analysis of transporters in plants is a difficult task since the phenotype of transgenic plants expressing the transporter can change dramatically depending on the expression system employed (e.g. overexpression of *AtHKT1;1* via *AtHKT1;1* native promoter vs. 35S promoter, Rus *et al.* 2001 vs. D Jha and M Tester unpublished results). Expression of transgenes via a strong constitutive promoter will result in all cell-types in the shoot and root of the plant expressing the transgene in a similar manner. This may be detrimental to whole plant transport processes which can depend on one cell-type or tissue transporting a particular nutrient or toxic element in a different manner than another tissue to achieve maximum benefit for the plant. Gene knockout mutants have been more commonly used to determine plant transporter function since the knockout may give a more discernable phenotype and may allow function to be assigned to the transporter.

Cell-type specific expression of transporters could be an important technique to aid in developing better understanding of transporter function. The GAL4-GFP enhancer trap lines in *Arabidopsis* and rice allow transgenes to be expressed in as many specific cell-types as there are cell-type specific enhancer elements trapped in the library. This method was used to control the expression of the *Arabidopsis* Na^+ transporter, *AtHKT1;1*, in rice roots in order to understand *AtHKT1;1* function more fully and to develop improved Na^+ exclusion and tolerance in rice.

Expression of *AtHKT1;1* in the outer root cells of rice resulted in better Na^+ exclusion from the shoot. The plants had significantly lower Na^+ accumulation in leaf blades and sheaths than the background enhancer trap they were derived from. There was an increase in the amount of Na^+ retained in the root of the outer *AtHKT1;1* lines, which indicates that the expression of *AtHKT1;1* in the outer cells of the root had decreased the amount of Na^+ which was reaching the xylem stream by retaining it within the root tissue. This was confirmed by x-ray microanalysis of the ion profiles of the individual cells in the root. The expression of *AtHKT1;1* in the outer cells of the root resulted in the cells expressing *AtHKT1;1* accumulating more Na^+ under Na^+ stress than the outer background line. It appears that the large cortical cells were better able to retain the Na^+ that had entered the root when they expressed *AtHKT1;1*. It may be this was an increased sequestration of Na^+ into the vacuoles of the cortical cells of symplastically transported Na^+. Alternatively, it could be that a larger proportion of Na^+ which entered the roots apoplastically was being drawn into the cortical cells (and sequestered in their large vacuoles) by the expression of *AtHKT1;1* in these cells. It is also possible that *AtHKT1;1* has been expressed in the tonoplast membrane of these cells increasing their capacity to accumulate Na^+, but this will be difficult to resolve. Regardless, a decreased amount of Na^+ crosses the endodermal Casparian band into the stele, thus less Na^+ enters the xylem and is transported up to the sheath and blade of these plants. The increased Na^+ exclusion provided by expression of *AtHKT1;1* resulted in the outer *AtHKT1;1* lines being significantly more Na^+ stress tolerant, thus this appears to be a very suitable strategy for increasing Na^+ stress tolerance in rice.

This was surprising since it was originally hypothesised that the expression of *AtHKT1;1* in the outer cells of the root would increase Na^+ into the root from the

growth media since *AtHKT1;1* retrieves Na^+ from the xylem to the xylem parenchyma in *Arabidopsis*. However, the $^{22}Na^+$ influx data shows that influx is lower in the outer *AtHKT1;1* line than in the outer background line. Potentially, the extra Na^+ that has accumulated in the cortical cells may create a decreased gradient for Na^+ influx thereby decreasing influx. Alternatively, the extra Na^+ in the cortical cells results in signalling leading to downregulation of the Na^+ influx transporters (and potentially the K^+ influx transporters, which may explain the low K^+ phenotype). Regardless, the extra Na^+ storage provided by the *AtHKT1;1* expressing cortical cells and lower Na^+ influx seem to combine to lower the amount of Na^+ being transferred to the xylem and lower shoot Na^+ accumulation. In fact, the extra storage capacity may not be able to lower the shoot Na^+ accumulation to the extent observed without a concomitant reduction in Na^+ influx.

The phenotype of the inner *AtHKT1;1* line was much more difficult to understand. In the T_0 and first T_1 experiments indications were that the line had increased Na^+ exclusion. However, the second T_1 experiment showed a completely opposite result with the line having reduced Na^+ exclusion capacity. The first possible explanation for this discrepancy is that the lines were grown in sufficiently different environments to alter the apparent phenotypes. The T_0 plants were assayed relatively quickly after they left tissue culture, thus the true Na^+ transport properties of these plants may have been masked if they were adapting to soil. The plants were stressed mildly compared to plants in the T_1 experiments, yet the accumulation of Na^+ in the leaf blades was the same between the experiments indicating the T_0 plants were under added stress after tissue culture.

The T_0 plants were potentially nutrient deficient. The plants had access to nutrients in the Jiffy Peat Pots and were given NH_4NO_3 and Osmocote, but were not growing in the complete nutrient growth solution like the T_1 plants were, which may have impacted the Na^+ transport as well. The first T_1 experiment indicated that this line was an effective Na^+ excluding line, but the second T_1 experiment indicated the line had decreased Na^+ exclusion compared to the control line. The second T_1 experiment was grown in a more favourable environment, particularly with warmer night temperature and high, stable humidity levels, thus the growth rate and

transpiration rate of the plants were likely to be quite different between the two experiments. It is difficult to determine whether this would affect the results of the two experiments, but it is apparent that the Na^+ exclusion this line displayed in early experiments is much weaker than that of the outer *AtHKT1;1* line and seems very dependent on growth conditions. Further experiments are needed to determine if the line is better under certain environmental conditions than others at excluding Na^+.

The expression of *AtHKT1;1* in the inner root cells did not have as much of an effect on ion accumulation profiles as was observed in the outer *AtHKT1;1* line. There was only a small increase in Na^+ accumulation in the xylem parenchyma cells, which is not surprising considering the capacity of the vacuoles in these cells is small, thus they would not be able to retain significant amounts of Na^+. This confirmed the whole root analysis of Na^+ accumulation which showed very little increase in root accumulation of Na^+. Thus, this strategy did not result in lower Na^+ transport to the shoot, and in fact, seems to increase the Na^+ transfer to the shoot. Potentially, the xylem parenchyma cells are drawing increased amounts of Na^+ out of the xylem and the outer root cells and are unable to store the extra Na^+, thus an increased level of Na^+ enters the xylem and is transported to the shoot. Though not statistically significant, the inner *AtHKT1;1* line does have higher root Na^+ influx then the inner background line, which may be a result of the *AtHKT1;1* expressing cells in the stele creating a slightly stronger 'pull' on Na^+ transport to the stele.

Another potential explanation for the decreased Na^+ exclusion in this line is that the overexpression in this cell-type has silenced the expression of *OsHKT1;5*, which shares significant sequence similarity with *AtHKT1;1*. *OsHKT1;5* has been shown to be expressed in the stelar cells and functions to retrieve Na^+ from the xylem. If *OsHKT1;5* was silenced, the expected phenotype would be elevated shoot Na^+ along with lower root Na^+, since xylem retrieval has been decreased. The line has increased shoot Na^+ accumulation, but the root Na^+ accumulation is unchanged. However, if the *AtHKT1;1* transgene is functioning to retrieve some Na^+ from the xylem stream, but not sufficiently to replace the silenced *OsHKT1;5*, the observed phenotype may be possible. Other *OsHKT* genes (or related transporters) may have been altered by the inner root expression of *AtHKT1;1* as well. Interestingly, even though the inner

AtHKT1;1 line accumulates more Na^+ in its shoot tissue than the inner background line it appears to have similar Na^+ tolerance. This is the opposite situation to the outer *AtHKT1;1* line which also had increased Na^+ stress tolerance, but increased Na^+ exclusion as well.

The 35S-driven overexpression of *AtHKT1;1* resulted in the majority of primary transformants having poor growth and fertility, so most of the plants did not produce seed. However, from the analysis of the T_1 plants, it is evident that the overexpression has significantly reduced the Na^+ transferred to the shoot by increasing the root accumulation (or xylem retrieval) of Na^+ and by increasing Na^+ retrieval in the sheath. The 35S::*AtHKT1;1* phenotype resembles that of the outer *AtHKT1;1* line, yet seems even stronger. Indeed, the Na^+ exclusion phenotype apparently causes the line difficulty growing without Na^+ in the growth solution. The T_1 plants were significantly larger when they were grown on Na^+ and would recover from being small, weak seedlings to being similar size as plants to the other lines. A large number of the plants grown without Na^+ died before reaching the experimental Na^+ stress and several more died while in the low Na^+ control hydroponic tank. The only plant to grow to a similar size to the other lines in the low Na^+ control treatment was genotyped and found to be a null segregant. Normal germination and plant growth was recovered with added Na^+ and additional K^+ resulted in larger plants, but the plants had a abnormal appearance with extended sheaths and shortened leaf blades. This seems to imply that K^+ could not replace some requirement for Na^+ within the plant, but could replace it to some extent. Only some C_4 plants are known to require Na^+ for normal growth to possibly aid in nitrate reductase activity (Ohta *et al.* 1988), but it appears there is a Na^+ requirement that is not being met in these plants.

Even though the T_1 seed was low in Na^+, presumably from the efficiency of the T_0 plant in restricting Na^+ transport to the shoot, several other lines had similar Na^+ levels in the seed (and lower levels of other ions) yet germinated and grew normally as seedlings without added Na^+ or K^+. This would indicate that although the 35S::*AtHKT1;1* seed has low Na^+, it is actually the restriction of Na^+ transport to the shoot that results in the poorly developed and weak seedlings. In an agricultural setting, seed likely germinates on soil with at least some Na^+ present, thus constitutive

overexpression of *AtHKT1;1* may be a useful strategy for salt tolerant cereal development.

However, there seems to be extreme variability in the 35S::*AtHKT1;1* lines based on expression level of *AtHKT1;1*. Lines expressing the transgene at high levels appear to be more likely to grow abnormally and be infertile, thus there is a fine balance between high expression and strong phenotype and too high expression and death. The expression of *AtHKT1;1* in the outer cells of the root resulted in a very significant decrease in Na^+ accumulation in the shoot, but did not create overly weak, infertile plants and thus appears it may be the better strategy toward developing Na^+ tolerant plants.

Experiments have been conducted in our lab using a similar approach in *Arabidopsis* (I Møller unpublished data; G Safwat 2006). Overexpression of *AtHKT1;1* in the epidermis and cortex or in the stele using enhancer trap lines to transactivate *AtHKT1;1* resulted in lines with enhanced Na^+ exclusion. These results in *Arabidopsis* agree with the results presented here for the outer *AtHKT1;1* expression lines, but seem to disagree with the results for the inner *AtHKT1;1* expression lines (at least in the final accumulation experiment on the T_1 lines). This difference is not surprising given there are many differences between *Arabidopsis* and rice in terms of genetics and physiology. The plant morphology is very different between *Arabidopsis* and rice. In particular, there are more cell-types in the rice root (e.g. exodermis) and more cell layers within several of the cell-types the plants have in common (e.g. cortex). The rice root has at least two Casparian bands which restrict the apoplastic influx of ions, despite apoplastic flow being an important pathway to Na^+ uptake in rice.

Arabidopsis has a very different makeup of Na^+ transporters from rice. One main difference is *Arabidopsis* has one *HKT* gene while there are nine in rice (seven expressed in Nipponbare), which are located in various cell-types (Garciadeblas *et al.* 2003). Thus, it would be expected that overexpressing a native transporter (as is the case in the *Arabidopsis* experiments) might yield different results to overexpressing the same gene in rice in terms of transport physiology, but also in terms of the impact on up- or down-regulating endogenous *HKT* genes. Also, it is undetermined exactly

which cell-type has been trapped in both *Arabidopsis* and rice, thus it may be that *AtHKT1;1* is being transactivated in subtly different cell-types in *Arabidopsis* and rice. Using a similar approach in other cereal crops, such as wheat or barley, might be expected (despite differences in apoplastic flow) to yield results resembling those in rice more than those in *Arabidopsis* since the morphology and genetic makeup of the cereals more closely resemble each other than that of *Arabidopsis*.

6.5 Future Work

There are a number of experiments that would be extremely informative towards understanding some of the phenotypes that were observed in this set of rice lines expressing *AtHKT1;1* in various ways. One important point to resolve is to determine if there is a stable phenotype of the inner *AtHKT1;1* line, and failing that to understand what environmental conditions alter the phenotype of this line. If the phenotype of this line is tied to environmental conditions it would be useful to show that two different environmental regimes are responsible for the opposing Na^+ accumulation phenotypes. Another experiment that may answer some questions about these lines is to examine the gene expression of a number of the other endogenous sodium transporters in rice roots (*OsHKT* genes, *OsSOS* genes, and *OsNHX* genes) to determine how expression of *AtHKT1;1* has altered their expression levels. Root samples were taken from all plants in the final T_1 accumulation experiment for RNA extraction, so expression of the genes mentioned could be examined in all lines in control and Na^+ stressed conditions. This may help interpret some of the Na^+ transport phenotypes that are difficult to explain with the data thus far. It may help to understand why the inner *AtHKT1;1* lines in *Arabidopsis* and rice seem to display opposing phenotypes in regards to shoot Na^+ accumulation.

Another set of data that is required is a display of cell-type specificity. Separate experiments showed that *GUS* could be transactivated in the same pattern as the original GFP fluorescence in both the epidermal and xylem parenchyma enhancer trap lines (Johnson *et al.* 2005). However, a number of experiments have been undertaken to try to show this with the *AtHKT1;1* lines including the use of laser capture microdissection to separate the outer and inner cells of the root (along the endodermis)

and extract RNA from these tissues to show the transgene is expressed within the intended cell-type. This RNA will also be used to examine expression of the *OsHKT* genes on a cell-specific basis. Root tissue has also been fixed for in *situ* hybridisation analysis of *AtHKT1;1* expression. A probe was prepared for *AtHKT1;1* analysis in *Arabidopsis*, but it was designed on the region of least homology with the *OsHKT* gene family and is being used to determine where the *AtHKT1;1* mRNA is being transcribed in the root. Attempts thus far have shown binding of the probe to all cell-types in transgenic and background lines, so either the probe is binding to similar *OsHKT* genes (unlikely) or non-specifically bound probe is not being washed off after hybridisation. Antibodies have been designed on an epitope in the first pore loop of *AtHKT1;1* (as in Sunarpi *et al.* 2005) and root tissue has been prepared for immunolabeling of the *AtHKT1;1* protein. First attempts were not successful since binding of the antibody was not specific to the plasma membrane or any particular cell structure. New root tissue has been fixed via high-pressure, low-temperature fixation to reduce the degradation of existing *AtHKT1;1* epitopes in order to improve the specificity of the binding of the *AtHKT1;1* antibody.

Since it appears that the root accumulation (and potentially xylem retrieval) of Na^+ has increased in several of the transgenic lines this could be measured using whole plant measurements of root-to-shoot transfer of ^{22}Na. It seems that while there is some variability between the lines in root influx, a more interesting difference between some of the lines may lie in the root-to-shoot transfer.

Another cell-specific experiment to do on these lines would be to actually show that *AtHKT1;1* expression in specific rice root cells has increased the Na^+ influx into those cells. Roots of transgenic plants could be protoplasted and the cells displaying GFP fluorescence (and thus, *AtHKT1;1*) could be compared for Na^+ influx currents to non-GFP cells using patch clamp electrophysiology.

CHAPTER 7: CELL-SPECIFIC EXPRESSION OF *PpENA1*

7.1 Introduction

Efficient efflux of Na^+ from roots to the soil is critical for plants to survive in high Na^+ concentrations. If the majority of the Na^+ entering the root was not returned to the soil the plant would quickly accumulate toxic levels of Na^+ (Tester and Davenport 2003). The mechanism for this efflux has not been identified. The Na^+/H^+ antiporter, SOS1, was identified by screening a mutagenised *Arabidopsis* population for root growth response on high Na^+ culture plates. *sos1* knockouts are Na^+ sensitive and accumulate increased levels of Na^+ in root and shoot tissue (Shi *et al.* 2002). SOS1 extrudes Na^+ from cells (Qui *et al.* 2002), thus it has been proposed that SOS1 is involved in Na^+ extrusion from the root to the soil (Pardo *et al.* 2006) or in Na^+ loading into the xylem (Shi *et al.* 2002). Any Na^+ extrusion function has yet to be proven for SOS1, but given the large number of cation/proton exchangers in the *Arabidopsis* genome (e.g. *CHX* and *NHX* gene families) it is likely an antiporter will be identified to be involved in Na^+ efflux from plant roots.

In addition to Na^+/H^+ antiporters (Prior *et al.* 1996), fungi express Na^+-pumping ATPases (Benito *et al.* 2002). These *ENA* genes are involved in extruding Na^+ from cells and contribute to Na^+ tolerance. Several fungal Na^+-ATPases have been identified (e.g. Banulos *et al.* 1998, Benito *et al.* 2000), but ScENA1 from yeast is likely the best characterised ENA (Garciadeblas *et al.* 1993, Weiland *et al.* 1995). Overexpression of *ScENA1* led to improved Na^+ tolerance in *S. cerevisiae* (Benito *et al.* 1997) and *Schizosaccharomyces pombe* (Banulos *et al.* 1995). *ScENA1* was expressed in tobacco cell culture and decreased Na^+ content of the cells under Na^+ stress, which may mean the expression of *ScENA1* in plants will improve Na^+ tolerance (Nakayama *et al.* 2004). The K^+ content of the cells was altered as well indicating that the ATPase may transport K^+ as well as Na^+. However, ScENA has been shown to require relatively strict levels of ATP and pH to function appropriately (Benito *et al.* 1997).

The bryophyte *Physcomitrella patens* is receiving much attention as it is tolerant to several stresses, and is potentially a source of genes to improve stress tolerance in higher plants (Nishiyama *et al.* 2003, Frank *et al.* 2005, Saavedra *et al.*

2006, Cuming *et al.* 2007). It has two Na^+-ATPases, PpENA1 and PpENA2 and heterologous expression in yeast indicated that PpENA1 was functional as it improved the growth of yeast deficient in *ScENA1* when grown on high Na^+ media (and high K^+ media) (Benito and Rodriguez-Navarro 2003). Expression of *PpENA1* is significantly upregulated by Na^+ stress (and to a lesser extent by osmotic stress), but is unaffected by other stresses (Lunde *et al.* 2007). WT plants maintained a higher K^+/Na^+ ratio and were 40% larger than an *ena1* knockout line at moderate Na^+ concentrations (100 mM), but the difference disappears at high Na^+ concentrations (Lunde *et al.* 2007).

If PpENA1 is responsible for Na^+ extrusion from *Physcomitrella patens*, it would be desirable to transfer this property to other land plants, especially crop species, to improve Na^+ tolerance. With this goal in mind, *PpENA1* was expressed specifically in the epidermis/cortex and the xylem parenchyma cells of rice roots. The GAL4-GFP enhancer trap library in rice (Johnson *et al.* 2005) contains several lines showing GFP fluorescence in specific cell-types within the root, indicating that enhancer elements have been trapped which are responsible for gene expression within those cell types. These lines can be subsequently transformed with the GAL4-UAS fused to a transgene to express the transgene in the original GFP fluorescence pattern. Hypothetically, the expression of *PpENA1* in the outer cells of the root will increase Na^+ efflux back to the soil, thereby restricting the amount of Na^+ which is transferred to the xylem and on to the shoot. On the other hand, expressing *PpENA1* in the xylem parenchyma cells may increase the Na^+ being transported to the xylem, thus increasing the amount of Na^+ reaching the shoot.

7.2 Materials and Methods

7.2.1 Plant Materials

Generation of all transgenic plant material is described in Chapter 4 (Vector Construction and Production of Transgenic Plants).

7.2.2 Quantitative-PCR (Q-PCR)

Analysis is as reported in Chapter 6 except *PpENA1* primers were used (Forward primer – AAGGCATTACCTGGGAGTGGA; Reverse primer – TCACATGTTGTAGGGAGTT; product size – 116 bp).

7.2.3 T_0 Na^+ Accumulation Analysis

T_0 plants were grown and analysed as reported in Chapter 6.

7.2.4 T_1 Growth Conditions

All T_1 experiments were carried out in parallel with T_1 experiments on *AtHKT1;1* lines, thus growth conditions are as reported in Chapter 6.

7.2.5 T_1 Na^+ Accumulation Analysis

Analysis of Na^+ accumulation was undertaken as for the *AtHKT1;1* lines in Chapter 6 except two outer *PpENA1* lines (1-B6 and 1-C1) and two inner *PpENA1* lines (4-B1 and 4-C1) were analysed for Na^+ accumulation and Na^+ tolerance levels in the T_1 generation.

7.3 Results and Discussion

7.3.1 T_0 Q-PCR vs. Na^+ Accumulation

The *PpENA1* expression level was analysed in the primary transgenic lines expressing *PpENA1* in the Outer Background, Inner Background and 35S-driven overexpression lines. Interestingly, the Outer *PpENA1* lines had approximately 10 times higher expression levels than the 35S::*PpENA1* or Inner *PpENA1* lines (Figures 7.1, 7.3 and 7.5). This contrasts with the lines expressing *AtHKT1;1* (Chapter 6) where the Outer *AtHKT1;1* had similar expression levels to the 35S::*AtHKT1;1* lines and were both higher than the Inner *AtHKT1;1*. The lines expressing transgenes in the Inner Background line would be expected to have lower transgene expression levels given the small number and size of cells expressing the transgene. However, it is difficult to determine why the Outer *PpENA1* lines would be expressing so much higher than the 35S::*PpENA1* lines. Also, the lines expressing *PpENA1* have significantly higher copy numbers than the lines expressing *AtHKT1;1* using the same expression system. This same relationship was observed among the lines expressing the two genes using the ethanol switch (Chapter 5). As mentioned previously, it may be an indication of the expression level tolerated by rice for each gene before it becomes toxic to the plant.

The T_0 plants were given a treatment of 5 mM NaCl for 13 d at which point the youngest fully emerged blade (YEB) was excised and digested to determine Na^+

concentration in the blade by flame photometry. T_0 lines expressing *RFP* were used as controls for Na^+ accumulation.

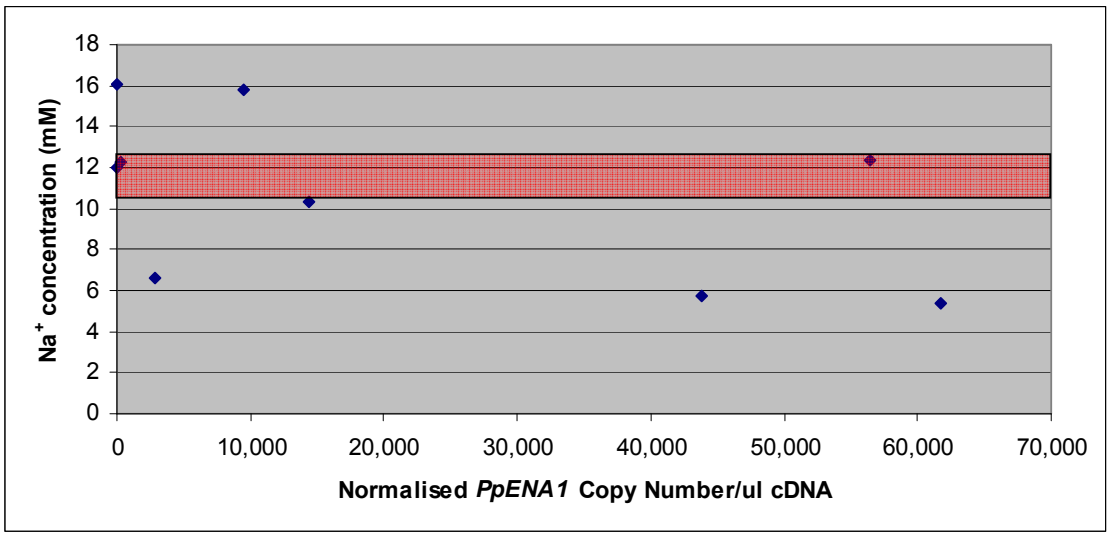

Figure 7.1: T_0 35S::*PpENA1* lines – Na^+ concentration (mM) in the YEB (after a 13 d treatment of 5 mM Na^+) versus normalised *PpENA1* copy number/µl cDNA in the root for each independent transformant. Red box indicates the average (plus and minus the standard error) Na^+ accumulation in 35S::*RFP* T_0 plant population (11.3 +/- 1.2 mM → 10.1 – 12.5 mM).

One of the 35S::*PpENA1* lines that had measurable levels of *PpENA1* expression accumulated more Na^+ than the 35S::*RFP* control lines (Figure 7.1). However, at higher expression levels (>10,000 mRNA copies/µl cDNA) all four lines accumulated similar or smaller amounts of Na^+ in their blades. Very few of the 35S::*PpENA1* lines were fertile and the individual lines were difficult to take through tissue culture. Much higher gene expression levels were measured in the blade tissue of these plants, so perhaps the expression of transporters in the shoot, as well as the root, improves the Na^+ exclusion properties of the plant, but affects the flowers or pollen of the plants sufficiently to render them sterile.

The K^+ accumulation was higher in the *PpENA1* lines than the RFP control lines, but there was no obvious correlation between gene expression level and K^+ accumulation indicating *PpENA1* expression has little or no effect on K^+ transport (Figure 7.2). It does appear that the K^+ accumulation across all *PpENA1* lines in all expression systems hovers around 250 mM (Figures 7.2, 7.4 and 7.6), thus it would

seem that 35S overexpression of *RFP* has decreased the K^+ accumulation in those plants.

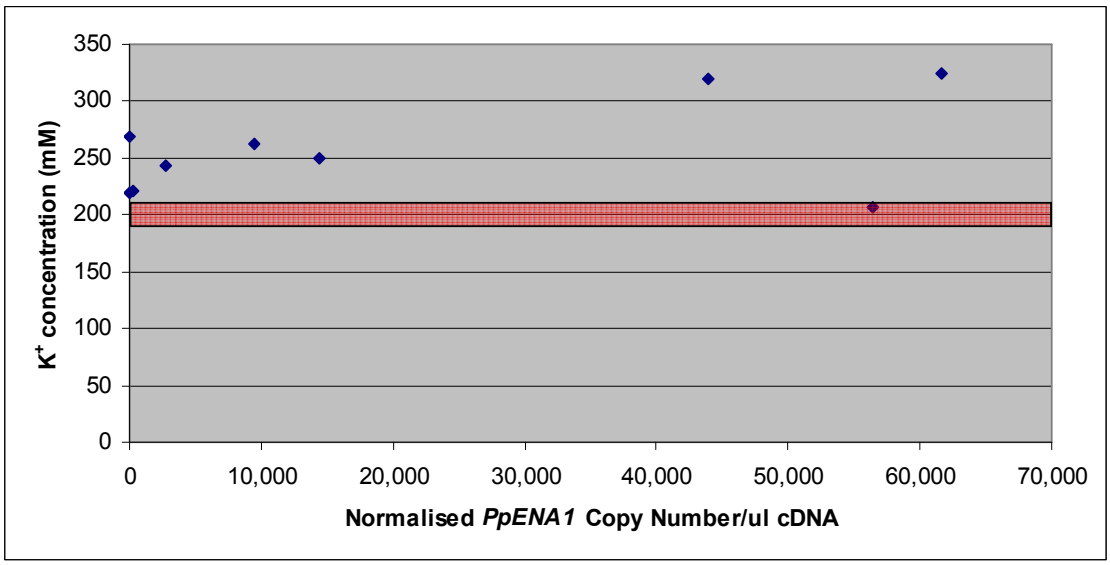

Figure 7.2: T_0 35S::*PpENA1* lines – K^+ concentration (mM) in the YEB (after a 13 d treatment of 5 mM Na^+) versus normalised *PpENA1* copy number/µl cDNA in the root for each independent transformant. Red box indicates the average (plus and minus the standard error) K^+ accumulation in 35S::*RFP* T_0 plant population (199 $^+$/- 8 mM → 191 - 207 mM).

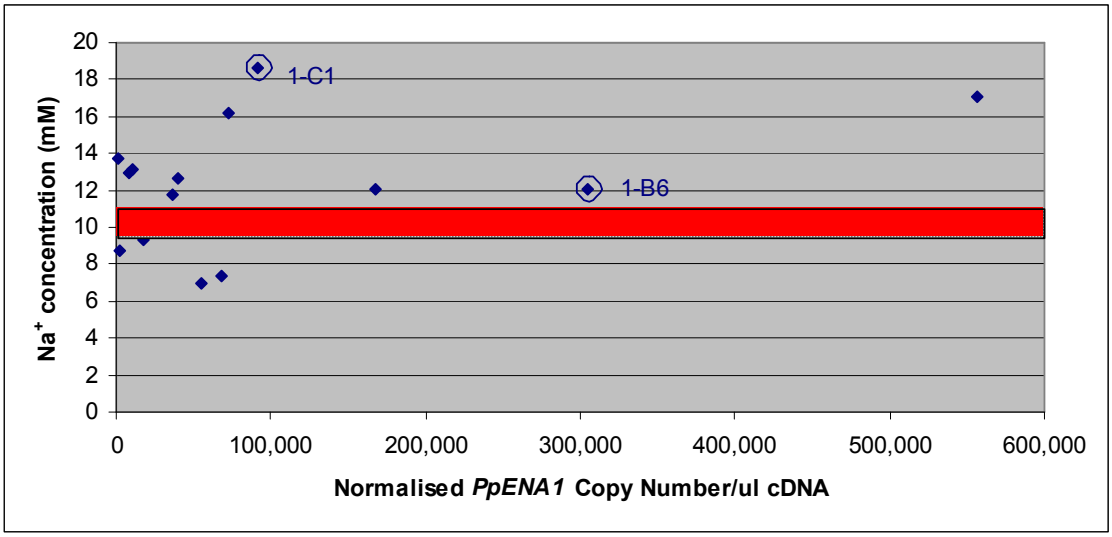

Figure 7.3: T_0 Outer *PpENA1* lines – Na^+ concentration (mM) in the YEB (after a 13 d treatment of 5 mM Na^+) versus normalised *PpENA1* copy number/µl cDNA in the root for each independent transformant. Red box indicates the average (plus and minus the standard error) Na^+ accumulation in Outer RFP T_0 plant population (10.3 $^+$/- 0.8 mM → 9.6 – 11.1 mM).

Most of the Outer *PpENA1* lines accumulated more Na^+ in the leaf blade than the Outer RFP lines (Figure 7.3). There does not appear to be a correlation between gene expression level and Na^+ accumulation, but lines expressing *PpENA1* at 100,000 copies/µl cDNA or higher all accumulated more Na^+ than the control. It seems that lines expressing *PpENA1* in the outer root cells at any level accumulate Na^+ more quickly than control lines. Two representative lines were chosen to evaluate in the T_1 generation. Line 1-C1 had moderate *PpENA1* expression and high Na^+ accumulation , while 1-B6 had medium gene expression and slightly higher Na^+ accumulation. Despite apparently aggravating Na^+ accumulation, the lines were more fertile than the 35S::*PpENA1* lines, which supports the idea that high expression level of transporters in shoot may decrease plant reproduction.

The outer *PpENA1* lines accumulated slightly less K^+ than did the Outer RFP control lines, but as with the 35S lines there is no apparent relationship between gene expression level and K^+ accumulation indicating that the gene is not actually altering K^+ transport (Figure 7.4). As mentioned above there is significant difference in K^+ accumulation between the lines expressing *RFP* in different systems, yet there is little difference in the K^+ accumulation in the lines expressing *PpENA1* in different systems.

It has been observed that RFP is toxic to cells at high expression levels (kills callus at high expression levels, strongly expressing calli rarely survive as seedlings after tissue culture) and K^+ is often a measure of plant health, so it is possible that the 35S::*RFP* lines were not as healthy due to high levels of RFP production and this showed up in the K^+ accumulation. However, why expressing *RFP* in the outer background line would result in an increased level of K^+ accumulation (or healthier plants) is a mystery. Perhaps the expression of the gene in the outer cells of the root confines RFP accumulation to the vacuoles of the cortical cells and this creates less toxicity for the plant.

It is evident that among the lines expressing either *PpENA1* or *AtHKT1;1* (Chapter 6) via the 35S promoter, or in the Outer or Inner Background that the lines expressing *PpENA1* in the outer root cells have higher K^+ accumulation in the blades. Whereas the other five lines all average approximately 250 mM K^+, the Outer *PpENA1* lines average approximately 275 mM.

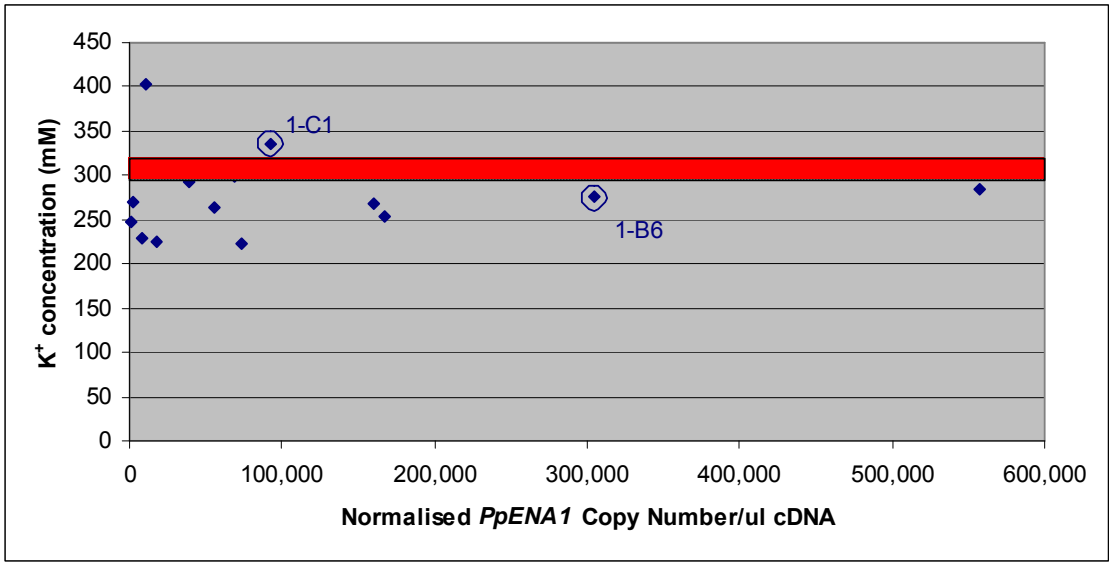

Figure 7.4: T_0 Outer *PpENA1* lines – K^+ concentration (mM) in the YEB (after a 13 d treatment of 5 mM Na^+) versus normalised *PpENA1* copy number/µl cDNA in the root for each independent transformant. Red box indicates the average (plus and minus the standard error) K^+ accumulation in Outer RFP T_0 plant population (306 $^+$/- 9 mM → 297 - 315 mM).

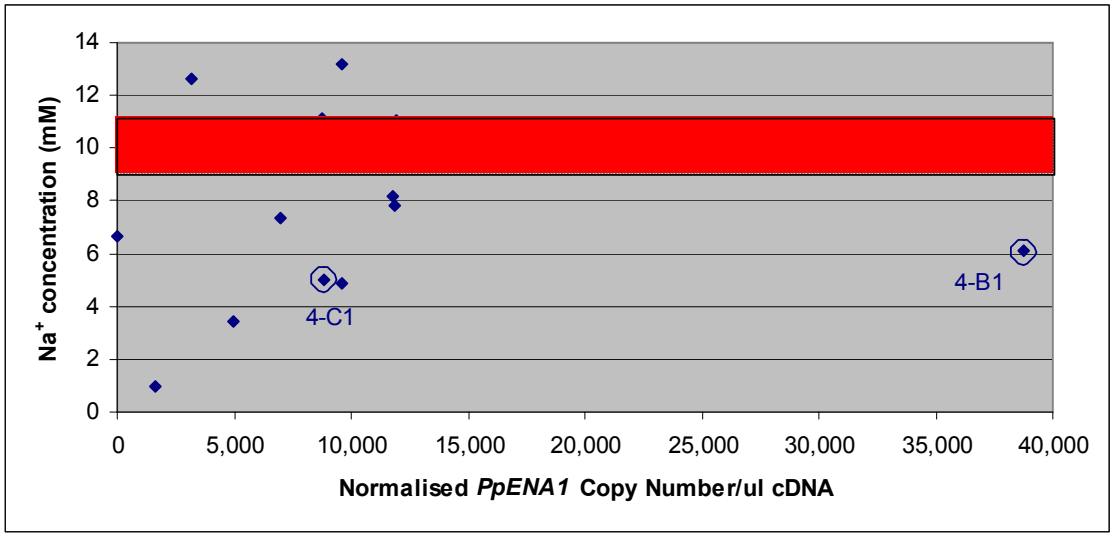

Figure 7.5: T_0 Inner *PpENA1* lines – Na^+ concentration (mM) in the YEB (after a 13 d treatment of 5 mM Na^+) versus normalised *PpENA1* copy number/µl cDNA in the root for each independent transformant. Red box indicates the average (plus and minus the standard error) Na^+ accumulation in Inner RFP T_0 plant population (10.0 +/- 1.3 mM → 8.7 – 11.3 mM).

The majority of the Inner *PpENA1* lines accumulated less Na^+ than the control RFP lines (Figure 7.5). However, there is no apparent relationship between *PpENA1* expression level and Na^+ accumulation in the blade. This would indicate that it may not be the number of PpENA1 proteins that are produced that is important to Na^+ transport, but rather it depends on some other factor like posttranslational modifications. Two lines which represented the population were chosen to examine in the T_1 generation. Line 4-B1 had high *PpENA1* expression and low Na^+ accumulation, while line 4-C1 had similar Na^+ accumulation, but 4 times lower gene expression.

Accumulation of K^+ was not altered from the level of the control lines (Figure 7.6). This may be an indication of the low toxicity of RFP production in xylem parenchyma cells (since so small a proportion of total cells are actually producing RFP). Again, there is no apparent effect of gene expression level on K^+ accumulation so it is unlikely K^+ transport is affected by expression of *PpENA1*.

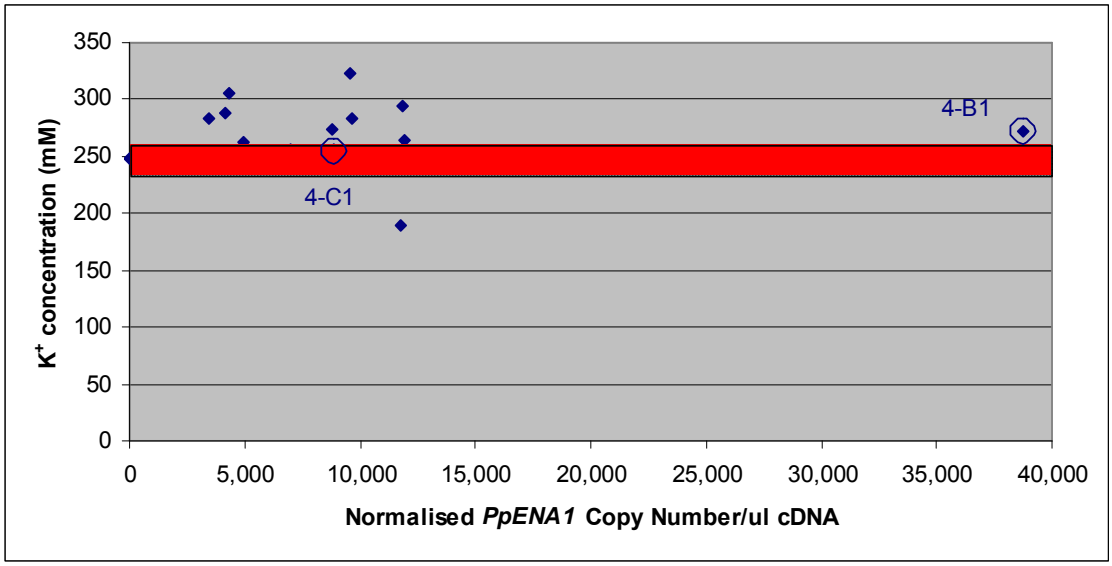

Figure 7.6: T_0 Inner *PpENA1* lines – K^+ concentration (mM) in the YEB (after a 13 d treatment of 5 mM Na^+) versus normalised *PpENA1* copy number/µl cDNA in the root for each independent transformant. Red box indicates the average (plus and minus the standard error) K^+ accumulation in Inner RFP T_0 plant population (245 +/- 10 mM → 235 - 255 mM).

7.3.2 T_1 Na^+ Accumulation

The primary transgenic lines chosen from the Q-PCR and Na^+ accumulation experiments were analysed in the T_1 generation to characterise Na^+ accumulation more completely and to discern whether the analysis of the T_0 lines was an accurate measure of the true phenotype of the line. All null segregants were removed from all further analysis. Insufficient numbers of nulls existed to use as controls, but WT or background enhancer trap lines were used as experimental controls.

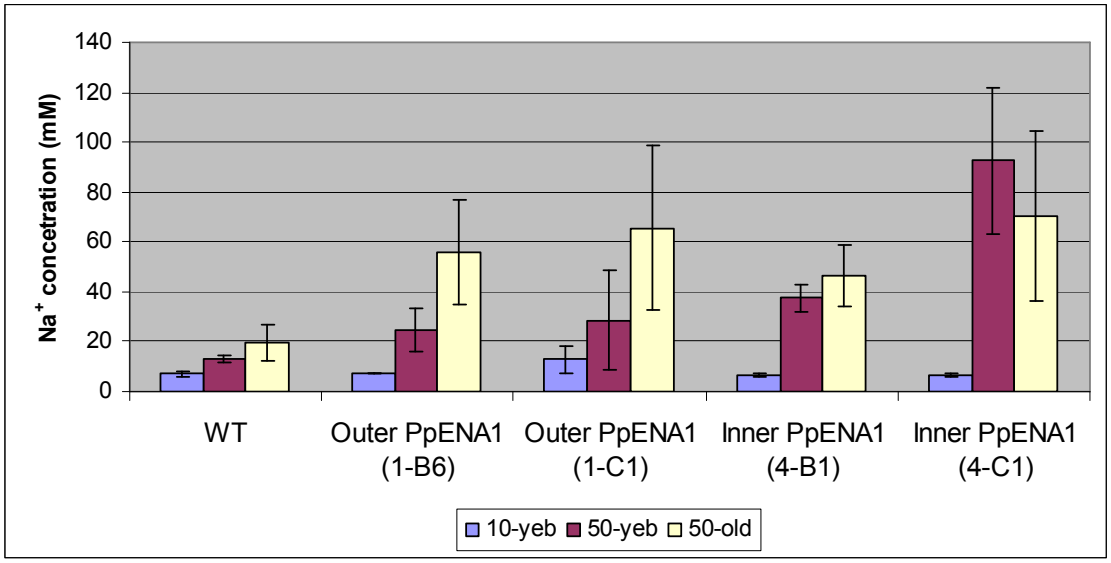

Figure 7.7: Na^+ accumulation in two Outer *PpENA1* and two Inner *PpENA1* T_1 lines selected from T_0 analysis. The YEB was analysed after 10 d of 10 mM Na^+ stress (10-yeb), then a further 50 mM Na^+ stress was imposed for 10 d and the new YEB was analysed (50-yeb) as well as the blade immediately following the 10-yeb (50-old). Bars represent an average of 3-5 plants with standard error. No significant differences at $P<0.05$ exist between means of 10-yeb, 50-yeb or 50-old of the five lines according to the Kruskal-Wallis and Dunn's Multiple Comparisons tests.

After 10 d of 10 mM Na^+-stress the YEB (10-yeb) was harvested from all plants and used to determine the Na^+ accumulation of the transgenic plants. The Outer *PpENA1* lines had both accumulated slightly more Na^+ in the YEB than the WT lines at this point. The Inner *PpENA1* lines had both accumulated slightly less Na^+ than the WT after the first 10 d. This result seemed to confirm the results seen in the T_0 experiment (Figure 7.7).

Since the differences in Na^+ accumulation were not large between the lines, the plants were grown for an additional 10 d at 50 mM Na^+. After the further 10 d the new YEB (50-yeb) was harvested as was the leaf blade immediately following the original YEB (10-yeb), which was easily distinguishable as the original excised blade was simple to identify. Root tissue was also harvested at this time for Na^+ accumulation analysis. At this point all the *PpENA1* lines had accumulated much higher levels of Na^+ in both the blades compared to the WT. This was as expected for the Outer *PpENA1* lines, based on the results from the T_0 experiment, and the 10-yeb from this experiment. The Outer *PpENA1* lines accumulated 2.5 and 3 times more Na^+ than the

WT in the 50-yeb and the 50-old, respectively. However, the apparent low Na^+ accumulation phenotype that was observed in the Inner *PpENA1* lines in the T_0 experiment and the 10-yeb in the T_1 experiment seemed to completely reverse. The Inner *PpENA1* lines accumulated 4 – 8 and 2 – 3.5 times the Na^+ than the WT in the 50-yeb and 50-old, respectively.

Although all the lines accumulated excessive amounts of Na^+, it is interesting to note that the Inner *PpENA1* lines were the only lines produced (including the *AtHKT1;1* lines) which seem to accumulate more Na^+ in the younger blades as opposed to storing the extra Na^+ in the older blades. The lines in this experiment were obviously under more stress than the WT (and the *AtHKT1;1* lines from the same experiment – see Chapter 6) as the error bars are much larger, which indicates the plants were being pushed to the limit of their ability to deal with extra Na^+. Thus, it seems the T_0 experiment was not a good measure of the true Na^+ accumulation phenotype of the Inner *PpENA1* lines, though the result for the Outer *PpENA1* lines resemble the results from the T_0 experiment. The results from the two independent lines from each genotype resemble each other quite well, thus it is likely that the phenotypes observed in the T_1 lines are an accurate measure of the entire population of T_0 lines.

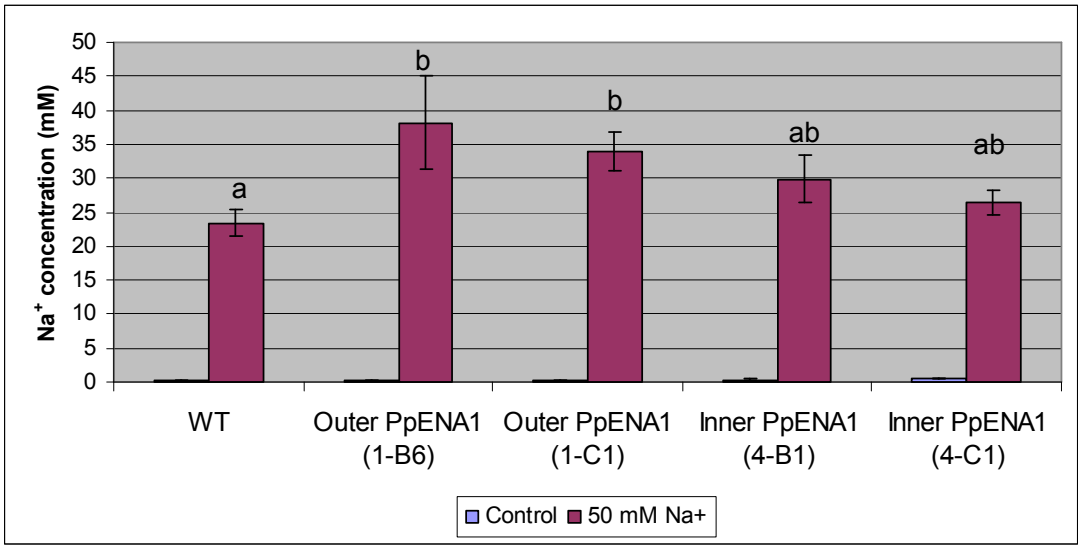

Figure 7.8: Na^+ accumulation in two Outer *PpENA1* and two Inner *PpENA1* T_1 lines selected from T_0 analysis. The roots were analysed after a 10 d 10 mM Na^+ stress and a further 10 d 50 mM Na^+ stress. Roots from plants grown in ACPFG solution without added Na^+ are presented as control. Bars represent an average of 3-5 plants with standard error. Bars with same letter(s) above are not significantly different at $P<0.05$ according to the Kruskal-Wallis and Dunn's Multiple Comparisons tests.

All four *PpENA1* lines had increased levels of Na^+ accumulation in the roots, with the inner *PpENA1* lines accumulating moderately more Na^+ than the WT and the outer *PpENA1* lines accumulating significantly more Na^+ than the WT (Figure 7.8). The shoots and roots of both the Outer and Inner *PpENA1* lines accumulated higher levels of Na^+ than the WT. Thus, it is unlikely that the shoot-to-root transfer has been altered by the expression of *PpENA1*, rather influx into the root has been increased or efflux out of the root has been decreased. Potentially, the expression of *PpENA1* in the inner root cells has increased the rate of Na^+ being loaded into the xylem, which increases the amount reaching the shoot and also creates a pull of Na^+ toward the inner root, increasing influx as a result. The expression of *PpENA1* in the outer cells of the root may increase influx into the root, thus pushing extra Na^+ toward the stele and increasing the transfer to the shoot.

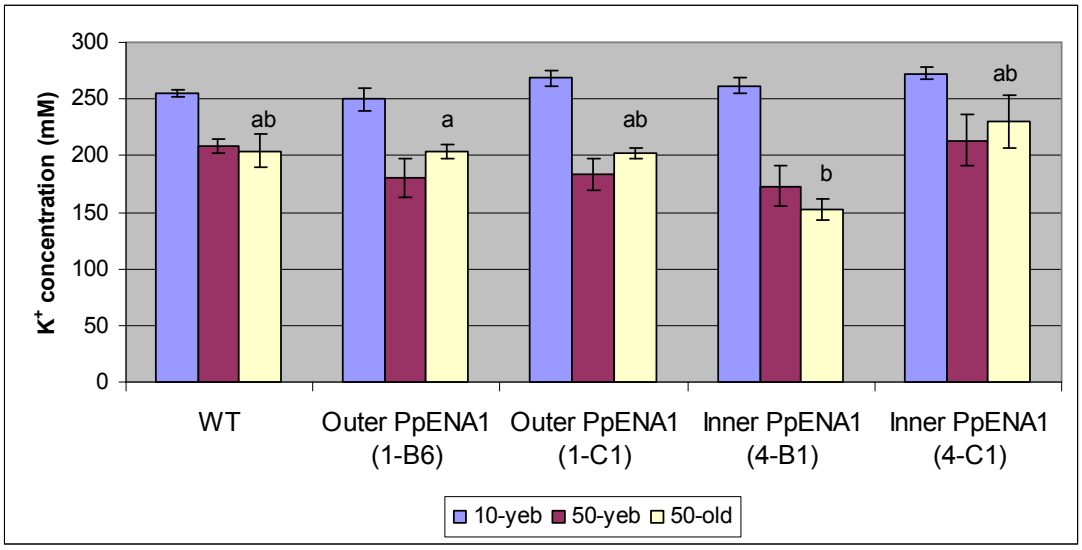

Figure 7.9: K^+ accumulation in two Outer *PpENA1* and two Inner *PpENA1* T_1 lines selected from T_0 analysis. The YEB was analysed after 10 d of 10 mM Na^+ stress (10-yeb), then a further 50 mM Na^+ stress was imposed for 10 d and the new YEB was analysed (50-yeb) as well as the blade immediately following the 10-yeb (50-old). Bars represent an average of 3-5 plants with standard error. No significant differences exist at $P<0.05$ between the means of the 10-yeb and 50-yeb measurements, while the same letters above the 50-old bars indicates a significant difference at $P<0.05$ exists between the means according to the Kruskal-Wallis and Dunn's Multiple Comparisons tests.

The K^+ accumulation in the blades of all lines decreased after the second Na^+ stress (Figure 7.9). The 4-B1 line had lower K^+ accumulation than the WT in both blades after the second Na^+ stress, while the 4-C1 line had somewhat higher K^+ accumulation in both blades than the WT. Whether this is an accurate measure of K^+ accumulation or simply related to the obvious stress the lines were challenged with is difficult to determine. Also, the 4-C1 line accumulated more Na^+ in the blades, yet has higher blade K^+, which is not the commonly observed relationship.

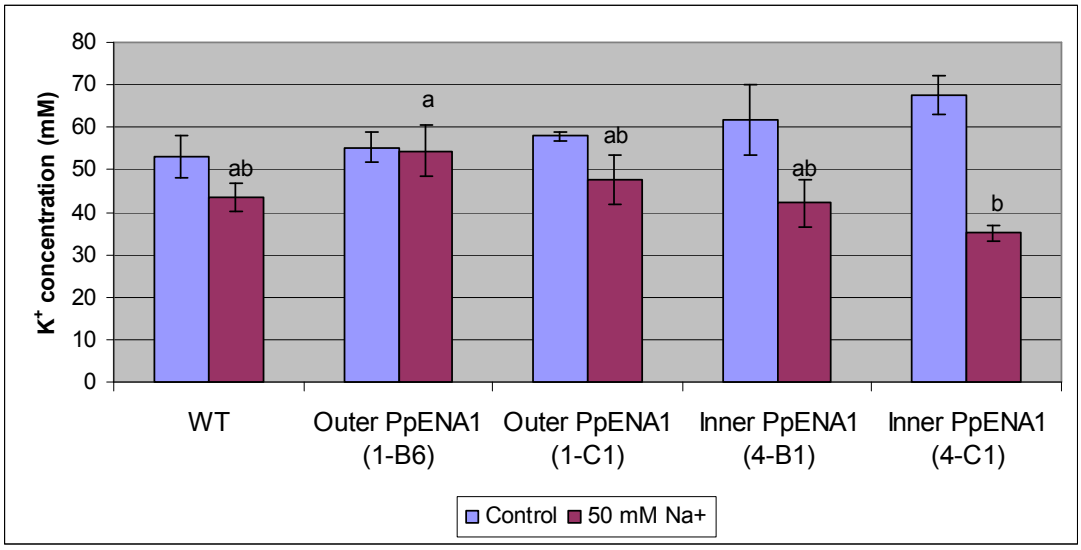

Figure 7.10: K^+ accumulation in two Outer *PpENA1* and two Inner *PpENA1* T_1 lines selected from T_0 analysis. The roots were analysed after a 10 d 10 mM Na^+ stress and a further 10 d 50 mM Na^+ stress. Roots from plants grown in ACPFG solution without added Na^+ are presented as control. Bars represent an average of 3-5 plants with standard error. No significant differences exist at $P<0.05$ between the means of the control measurements, while the same letter(s) above 50 mM Na^+ bars indicates the means are not significantly different at $P<0.05$ according to the Kruskal-Wallis and Dunn's Multiple Comparisons tests.

Interestingly, the roots of the Outer *PpENA1* had higher K^+ accumulation than WT under Na^+ stress, despite also accumulating more Na^+ in the roots. On the other hand, the Inner *PpENA1* lines accumulated lower levels of K^+ in the roots, despite having only slightly more Na^+ in the roots than the WT.

7.4 General Discussion

The sodium pumping ATPase from *Physcomitrella patens* (PpENA1) improves the Na^+ (and K^+) tolerance of yeast by extruding Na^+ (and K^+) from the yeast cells (Benito and Rodriguez-Navarro 2003). Knocking out *PpENA1* significantly decreases the Na^+ tolerance of *Physcomitrella patens* and decreases the K^+/Na^+ ratio (Lunde *et al.* 2007). Thus, it was hypothesised that expressing *PpENA1* in plants may increase Na^+ efflux and improve Na^+ tolerance. Theoretically, if *PpENA1* expression were to increase efflux Na^+ from plant cells it should be more beneficial to the plant if the pump were expressed in the outer cells of the root to efflux Na^+ back to the growth

medium. Expressing *PpENA1* in the stelar cells of the root would, in theory, have the opposite effect by pumping more Na^+ into the xylem of the root, thereby pushing more Na^+ into the shoot. It is difficult to model the effects of expressing *PpENA1* constitutively as the effects of expressing the gene in the outer and inner root cells would most likely counteract each other. Additionally, *PpENA1* would be expressed in the shoot tissue making the prediction of phenotype more difficult than in the case of cell-specific expression in the root.

Expression of *PpENA1* in the outer root cells led to an increase in the accumulation of Na^+ in the shoot. The T_0 plants accumulated more Na^+ in the YEB and this phenotype was confirmed in the analysis of the T_1 plants, which accumulated more Na^+ in the shoot and root tissue. This indicated that Na^+ was entering the root at an increased rate. Thus, it seems this line has altered influx properties, although in a completely opposite manner to the original hypothesis.

The T_0 Inner *PpENA1* plants accumulated less Na^+ than the control lines, but T_1 lines appeared to accumulate more Na^+. This may be a result of the Na^+ stress the plants were subjected to. The T_0 plants were given a 5 mM stress, whereas the T_1 plants were given a 10 mM then a 50 mM Na^+ stress. After the first 10 mM stress the T_1 plants had accumulated less Na^+ in the YEB than the control, which confirmed the T_0 result. However, after the level of stress increased, the inner *PpENA1* lines accumulated more Na^+ than the control and outer *PpENA1* lines. It is difficult to explain this reversal of phenotype. It seems that the level of Na^+ at which the Inner *PpENA1* line ceases to reduce shoot Na^+ accumulation is between 10 and 50 mM. Potentially, the phenotypes observed from expressing *PpENA1* are not robust and at increased stress levels the expression of *PpENA1* in the inner cells is insufficient to improve the Na^+ exclusion of the transgenic plants. However, it appears that both the inner and outer *PpENA1* plants move Na^+ in an extremely counter-productive manner for maintaining low shoot Na^+.

It is interesting to note that, while both outer and inner *PpENA1* lines accumulate more Na^+ than the control, they do have different phenotypes. The inner *PpENA1* lines seem to accumulate a greater proportion of Na^+ within their younger blades than the outer *PpENA1* lines, which store more Na^+ within the older blades.

Storing Na^+ in the older blades is a survival mechanism employed to keep toxic levels of Na^+ from accumulating in young, actively growing tissue to enable survival (Tester and Davenport 2003). It appears that this mechanism has been disrupted in the inner *PpENA1* line. Both the outer and inner *PpENA1* lines accumulate more Na^+ in their roots than the WT control, but the outer *PpENA1* lines seem to accumulate more than the inner *PpENA1* lines. This may reflect a greater change in influx to the root or efflux from the root has occurred in the outer *PpENA1* lines. Accumulation of K^+ in the blades of the two independent inner *PpENA1* lines were different, despite both having high Na^+ accumulation. The 4-B1 line accumulated less K^+ in the blades under Na^+ stress than the WT, while the 4-C1 line accumulated more K^+ than the WT. Interestingly, the 4-C1 line also accumulated more Na^+ in the blades than the 4-B1 line. Whether this is a true difference between the two independent transformants or if it is an experimental error will require verification. The outer *PpENA1* lines retained more K^+ in the roots than the inner *PpENA1* lines under Na^+ stress. The outer *PpENA1* lines actually retained more K^+ under Na^+ stress than the WT, while the inner *PpENA1* lines lost more K^+ than the WT under Na^+ stress. Perhaps, this is an indication there is some K^+ transporting property for *PpENA1* when expressed in plants. *PpENA1* has been shown to alter K^+ transport when expressed in yeast (Benito and Rodriguez-Navarro 2003), and *ena1* knockouts seem to have some change in K^+ transport as well (Lunde *et al.* 2007).

The precise alterations in Na^+ transport resulting from the expression of *PpENA1* in the different cell-types in rice will need further examination. The lines expressing *PpENA1* cell-type specifically will need to be analysed along side their respective background lines, which have been shown to have altered Na^+ transport properties (see Chapter 6). Given the extremely large error bars for Na^+ accumulation in the T_1 lines, it would be best to use a milder Na^+ stress in further experiments to ensure the plants are not pushed beyond a reasonable stress level. Flux analysis would show whether influx into the root has increased or whether root-to-shoot transfer has increased or both. Root tissue from the individual lines has been fixed for laser capture microdissection to extract specific root cells to determine whether *PpENA1* is being cell-type specifically expressed at the transcript level. The tissue will also be used to

determine whether there has been significant regulation of other endogenous rice Na^+ transporters (e.g. *OsSOS1*, *OsNHX1*, *OsHKTs*) in response to *PpENA1* expression. This may help to answer the question of why there has been such a dramatic alteration of Na^+ transport in these lines. Additionally, it is unknown whether *PpENA1* is being properly translated into protein as attempts thus far to develop antibodies have been unsuccessful. These results seem to indicate that expression of *PpENA1* in rice roots decreases Na^+ exclusion regardless of the cell-type in which it is expressed.

CHAPTER 8: GENERAL DISCUSSION

8.1 Summary

8.1.1 Completed Work

The purpose of this thesis was to develop techniques and technology to understand and improve Na^+ tolerance in rice. While addressing the specific aims of the project (section 1.5) a number of valuable genetic and physiological tools were developed and a significant contribution was made to current knowledge of Na^+ transport in rice.

A reliable method was developed to measure unidirectional Na^+ influx into intact rice roots using the radiotracer $^{22}Na^+$ (Chapter 2). Despite large root morphological differences with *Arabidopsis* or durum wheat, it was found that the methods were strikingly similar between the three species. Additionally, it was found that unidirectional influx differs by 30% among various rice varieties and that influx is poorly correlated with shoot Na^+ accumulation or Na^+ tolerance in general.

In an attempt to isolate Na^+-regulated enhancer elements, a population of 824 GAL4-GFP rice enhancer trap lines was screened by applying a mild Na^+ stress to the seedlings and observing changes in GFP fluorescence (Chapter 3). The screen identified that approximately 10% of the lines were regulated to some degree by Na^+, but when 18 of those lines were rescreened only 2 had reliable GFP regulation by Na^+. Both lines showed increased GFP fluorescence in roots in response to Na^+ stress, but the response was not large enough to pursue transactivation of Na^+ transporters in the lines in order to provide Na^+ stress-inducible expression of transporters.

Vectors were constructed to enable expression of transgenes (or silencing of endogenous genes) cell-specifically in the GAL4-GFP enhancer trap lines (in rice or *Arabidopsis*), but also inducibly using the ethanol gene switch (Chapter 4) (Plett *et al.* 2006). *Arabidopsis* lines were produced to inducibly overexpress *AtHKT1;1* (in ecotypes Col-0 and C24) or inducibly silence *AtHKT1;1* using artificial microRNAs (in Col-0). Rice lines were isolated that inducibly displayed RFP fluorescence specifically in the epidermis/cortex or xylem parenchyma cells of the root which indicates that the expression system is functioning appropriately (Chapter 5). The Na^+ transporters

AtHKT1;1 and *PpENA1* were also expressed in rice using this system, but it was difficult to isolate lines which were operating properly due to issues with sampling for RNA extraction. To avoid this problem a strategy was developed to cross transgenes into lines displaying RFP fluorescence cell-type specifically and inducibly.

Rice lines were produced which expressed the Na^+ transporter *AtHKT1;1* constitutively (using the CaMV35S promoter) or specifically within the epidermis/cortex or xylem parenchyma cells of the root (using GAL4-GFP enhancer trap lines) (Chapter 6). Lines expressing *AtHKT1;1* in the outer cells of the root were found to accumulate significantly less Na^+ in leaf blades and were more Na^+ tolerant than control lines. X-ray microanalysis of the ionic content of individual root cells showed that this improvement in Na^+ exclusion was the result of increased accumulation of Na^+ specifically within the cortical cells of the root. This suggests that the cortical cells expressing *AtHKT1;1* were better able to retrieve Na^+ from the apoplastic flow and sequester it within the large vacuoles found in cortical cells, thereby reducing the amount of Na^+ transferred to the stele and the shoot. However, the lines were found to have reduced unidirectional influx of Na^+ into the roots using the $^{22}Na^+$ radiotracer method developed for rice (Chapter 2).

Expression of *AtHKT1;1* specifically in the root xylem parenchyma cells increased the amount of Na^+ transported to the shoot, although it did not decrease the Na^+ tolerance of those lines (Chapter 6). It may be that the expression of *AtHKT1;1* in the xylem parenchyma cells increased the flux of Na^+ across the endodermis, but since the cells have little ability to store the extra Na^+ (given their small size and small vacuoles) the extra Na^+ may have been transported up the xylem stream.

Constitutive expression of *AtHKT1;1* using the CaMV35S promoter resulted in improved Na^+ exclusion and tolerance to the extent that the plants would not survive without some Na^+ in the growth solution (Chapter 6). It appeared that the plants had improved root sequestration of Na^+ (like the lines expressing *AtHKT1;1* in the epidermis/cortex cells) and improved retrieval of Na^+ from the xylem as sheath storage of Na^+ had been increased.

Expression of the Na^+-ATPase, *PpENA1*, specifically within the epidermis/cortex or xylem parenchyma cells of the root appeared to increase Na^+

transport to the shoot in both cases (Chapter 7). These lines warrant further examination as early indications were that the xylem parenchyma lines showed improved Na^+ exclusion and the apparent loss of Na^+ exclusion may have been related to the level of Na^+ stress that was applied to the plants. However, time constraints prevented further work on these lines during this project.

8.1.2 Future Work

This research has generated a number of questions that have been left unanswered and material that has been left unexamined to this point.

Since it was established that there is a range in unidirectional Na^+ influx in rice germplasm, but that it is not correlated to Na^+ tolerance, further experiments should be conducted to establish which component of Na^+ transport is most correlated to Na^+ exclusion and tolerance in rice. The obvious next step would be to extend the Na^+ flux protocol to explore the root-to-shoot transfer of Na^+ in the 11 lines.

The enhancer trap screening for stress-regulated genetic elements would be worth exploring further, perhaps using larger Na^+ stress or other abiotic stresses. The screen showed promise and with some alterations in experimental conditions would likely yield valuable clues to abiotic stress signaling and regulation.

The cell-type specific, ethanol-inducible lines displaying RFP fluorescence ('driver lines') will be crossed with lines transformed with an *alcA* promoter (second component of the ethanol switch) fused to a transporter of interest. This will allow ease in screening lines since it will be primarily done visually by the fluorescence of RFP. As well, an *alcA* promoter fused to a dsRNAi cassette will be crossed to the 'driver lines' to cell-type specifically and inducibly silence endogenous genes. These lines, along with the *Arabidopsis* lines in which *AtHKT1;1* has been inducibly overexpressed or silenced, will be used to determine the degree to which plants compensate for changes in transport as a result of the overexpression or silencing of a transporter. This may be best achieved through microarray analysis of gene expression changes in response to cell-type specific, ethanol-inducible expression of transgenes. Cell-type specific expression changes can be determined by microarray analysis of individual cell-types isolated via fluorescently-activated cell sorting (FACS) (A Johnson, unpublished results).

Rice lines expressing *AtHKT1;1* require further characterisation using $^{22}Na^{+}$ flux analysis to quantify changes in initial root influx and in root-to-shoot transport and sheath sequestration of Na^{+}. An attempt will be made to determine whether apoplastic or cell-to-cell transport of Na^{+} has been altered by the expression of *AtHKT1;1* by measuring the Ca^{2+} sensitivity of $^{22}Na^{+}$ fluxes. Channel-mediated Na^{+} influx is inhibited by Ca^{2+} (e.g. Davenport and Tester 2000), thus cell-to-cell transport of Na^{+} should show Ca^{2+} sensitivity, while apoplastic transport should be insensitive to Ca^{2+} concentrations. Also, analysis of *OsHKT* genes (and other Na^{+} transporters) in response to the expression of *AtHKT1;1* may shed some light on the phenotypes observed, particularly on the lines expressing *AtHKT1;1* within the root xylem parenchyma. In addition, efforts to measure the cell-type specificity of the transgene expression via laser capture microdissection and RT-PCR, *in situ* hybridization and immunolabeling need to be continued.

Rice lines expressing *PpENA1* should be examined further using the same techniques used to characterise the *AtHKT1;1* lines to determine whether the phenotypes observed for those lines are accurate and if so, why expression of *PpENA1* in two different individual root cell-types has decreased Na^{+} exclusion in both cases.

8.2 Transport studies in rice versus *Arabidopsis*

8.2.1 Will knowledge of transport in *Arabidopsis* inform research in rice?

Recent attempts to transfer knowledge gained from *Arabidopsis* studies and technology developed in *Arabidopsis* to equivalent transport studies in rice have shown that there may be significant challenges involved. For example, function of apparently homologous genes can be quite different between the two model species. Nakagawa *et al.* (2007) report different functions for the *Arabidopsis* and rice orthologous boron transporters, AtBOR1 and OsBOR1. *AtBOR1* is primarily expressed in the stele under boron deficient conditions and appears to be involved in loading boron into the xylem. *OsBOR1* is also expressed under deficient boron conditions, but is expressed in both the exodermis and endodermis of rice roots and appears to function in both boron uptake from the soil and transfer of boron to the stele.

Similarly, the results of Chapter 6 of this thesis show that successful use of technology in *Arabidopsis* does not necessarily provide similar success in rice. Cell-type specific expression of *AtHKT1;1* in the stele or the epidermis/cortex of *Arabidopsis* roots has been shown by members of our laboratory to significantly reduce the amount of Na^+ transferred to the shoot (Safwat 2006, I Møller, unpublished results). In rice, it appears that the cell-type specific expression of the same gene, using the same technology, results in reduced transfer of Na^+ to the shoot when expressed in the epidermis/cortex, but results in increased transfer of Na^+ to the shoot when expressed in the stele. The reasons for this difference remain to be elucidated.

8.2.2 What are the crucial differences between the model species concerning transport?

Together, the two examples above highlight the fact that there will be differences between the results from similar experiments in the model plant species. There are some important differences in morphology and transport between the model species that bear some consideration in interpreting past results and planning future experiments.

8.2.2.1 Rice has at least two Casparian bands

Casparian bands are primarily composed of suberin, a hydrophobic, waxy substance which functions to prevent water penetrating plant tissues. In roots, suberin is deposited in the radial and transverse cell walls of certain cell types to form so-called Casparian bands. Their function is to prevent water and nutrients from crossing particular cell layers via the apoplast. Instead, water, and the solutes dissolved therein, must traverse these cell layers through the symplast. This allows the plant to select the solutes that pass further into the root. It thus forms an important barrier to harmful solutes, but can also reduce efficient transfer of nutrients. Additionally, it could potentially inhibit the transfer of toxic ions, such as Na^+, out from inner root tissue.

Arabidopsis has a single Casparian band in the endodermal layer, while rice has at least two Casparian bands located in the exodermis and endodermis. This means that a significant proportion of nutrients must be actively transported through cell membranes at two points in rice rather than one in *Arabidopsis*. This indicates that there might be at least two sets of transporters in rice roots, and that, potentially, they

are unique sets in order to 'fine tune' the transfer of a given nutrient to the stele. In the case of toxic ions, it may mean that in order to actively transfer these toxic elements away from the stele there are two sets of active transporters. The *HKT* gene family is one of the few transporter families with significantly more members in rice than in *Arabidopsis*. Possibly, the large number of *HKT* genes in rice compared to *Arabidopsis* may be related to the extra transport barrier in rice. However, it is apparent that Casparian bands are not perfect barriers to the transfer of ions and that sufficient accumulation of certain ions on one side of a Casparian band will be relieved by leakage of the ion through the band (Ranathunge *et al.* 2005, section 8.2.2.2).

8.2.2.2 Apoplastic flow is significant in rice

Despite having at least one extra Casparian band, rice still seems particularly prone to the movement of water and ions through apoplastic space, which is less regulated than symplastic transport. For example, rice has been shown to have 10 times greater transpirational bypass flow than wheat (Garcia *et al.* 1997). Measurements of the hydraulic and osmotic conductivity using a pressure-perfusion technique indicate that the endodermal barrier in rice is potentially 30 times less permeable to water transport than the exodermal barrier (Ranathunge *et al.* 2003). As a result the movement of water and ions from the soil to the cortex may be less impeded than the transfer from the cortex to the stele. When unidirectional influx of Na^+ into the roots was measured (in Chapter 2) it was found that there is a 30% difference between rice cultivars, which implies there is genetic variation in this trait and it could be altered through breeding.

Possibly, improving the water use efficiency of rice will decrease the apoplastic flow and the associated uptake of toxic ions. This would improve the tolerance to toxic ion accumulation, but this may mean that an improvement in nutrient transport will need to accompany the improved water use efficiency to prevent nutrient deficiencies.

It may be necessary to focus efforts to improve the uptake of nutrients on increasing the transfer of these nutrients across the endodermal barrier to the stele. Conversely, the best strategy to limiting the transfer of toxic elements to the xylem may be improving the sequestration power of the cortical cells to absorb the accumulation of toxic ions on the cortical side of the endodermis. This may be the

explanation for the successful reduction of shoot Na^+ observed in the rice lines overexpressing *AtHKT1;1* in the root epidermis/cortex cells (Chapter 6). Improving the Na^+ influx capacity of the cortical cells appears to have increased the retrieval of Na^+ from the apoplastic stream and appears to prevent transfer of Na^+ across the endodermis.

8.2.2.3 Aerenchyma

Rice constitutively forms lysigenous aerenchyma in order to transfer O_2 to actively growing root meristems, which may be submerged in hypoxic conditions (Evans *et al.* 2003). This occurs due to the elimination of cortical cells (via a programmed cell death response), except for one layer of cells immediately inside the cortical fiber cell layer and one layer immediately surrounding the endodermis (Ranathunge *et al.* 2003). This process begins early as cortical cell disruption has been observed (via electron microscopy) in cells 6 h old and only a few millimeters back from the root tip. Once the cells die there is a spoke appearance to the cortex resulting from the monolayered cell walls which remain after cell death. These walls apparently allow apoplastic transfer of water and nutrients to the stele. This may help explain the large proportion of Na^+ transfer to the stele via bypass flow. Thus, there is a relatively short window of time for cell-to-cell transport across the cortex and for storage of potentially toxic ions within cortical cells.

This is difficult to resolve with the results of Chapter 6, which showed that the cortical cells retain extra Na^+, which reduces the amount of Na^+ being transferred to the xylem. If most cortical cells die and release the Na^+ they are storing relatively quickly, the extra Na^+ must be returned to the external medium or stored within newly developing cortical cells, since it is not being transferred to the xylem. Regardless of the explanation this means that cell-to-cell transport across the cortex in rice only occurs within the tips of rice roots, thus the strategies employed to alter the transport of ions are possibly best focused on the root tips. This may also help explain why the rice lines expressing *AtHKT1;1* in the stelar cells of the root increased the shoot Na^+ accumulation. The enhancer trap line used to express transgenes within the root xylem parenchyma did not show GFP fluorescence in the root tips. This would imply that *AtHKT1;1* was not being expressed at the root tip, thus it may be that it was not being

expressed in a region with functional surrounding cortical cells. If this is the case, (and assuming AtHKT1;1 was retrieving Na^+ from the xylem) there may have been no outlet for the extra Na^+ retrieved from the xylem. Thus, the cells would be drawing extra Na^+ across the endodermis, but there were no cortical cells in which to store the extra Na^+ retrieved from the xylem. This may help explain the difference in shoot Na^+ accumulation noted between *Arabidopsis* and rice when *AtHKT1;1* is transactivated in the inner cells of the root

8.2.2.4 Rice has a leaf sheath where toxic ions may be stored

Retrieval of Na^+ from the xylem stream in the leaf sheath has been shown to be an effective strategy toward excluding Na^+ from the leaf blade in durum wheat (Davenport *et al.* 2005, James *et al.* 2006). This retrieval has been linked to TmHKT1;4 (formerly known as TmHKT7 or Nax1) and its function results in significant reduction in blade Na^+ accumulation and improves Na^+ tolerance (Huang *et al.* 2006).

Rice apparently has similar sheath retrieval (likely via OsHKT1;4) as there are distinct differences in sheath Na^+ accumulation between lines with similar genotype. For example, FL478 is derived from a cross of Na^+-tolerant Pokkali and Na^+-sensitive IR29. Pokkali has high root Na^+ accumulation (likely due to xylem retrieval via an efficient allele of *OsHKT1;5*), low sheath Na^+ accumulation, and low-medium blade Na^+ accumulation. IR29 has low root Na^+ accumulation (indicating a weak *OsHKT1;5* allele), high sheath Na^+ accumulation and high blade Na^+ accumulation. FL478 has high root Na^+ accumulation (likely inherited from the Pokkali parent), medium sheath Na^+ accumulation and low blade Na^+ accumulation. In fact, FL478 has higher sheath accumulation of Na^+, lower blade Na^+ accumulation and is more Na^+-tolerant than the Na^+ tolerant parent Pokkali. This indicates that FL478 has inherited an efficient sheath Na^+ retrieval allele from IR29, thus has lower blade accumulation of Na^+ and better Na^+-tolerance than Pokkali. It seems likely this effect will be tied to OsHKT1;4.

Regardless, rice apparently has an extra line of defense toward preventing toxic accumulation of ions within its leaf blades that *Arabidopsis* does not. This may also increase the impact that phloem recirculation has on prevention of toxic ion accumulation in the shoot.

8.2.2.5 The CaMV35S promoter may not provide constitutive expression in rice

The 35S promoter has been shown to be a constitutively strong promoter in *Arabidopsis* in all organs except the hypocotyl, where expression is weak (Holtorf *et al.* 1995). On the other hand, the 35S promoter in rice provides constitutive transgene expression in roots and shoots, except in the root epidermis (Battraw and Hall 1990). Thus, with the rapid death of the cortical cells in rice roots, the only cells left expressing genes driven by the 35S promoter in the root are located in the stele. This will require consideration when comparing the results of 35S driven expression of transporter transgenes in rice to the results in *Arabidopsis*. There is also some cause for concern that the 35S promoter may provide expression of transporter transgenes at a level that is detrimental to plant health. If the expression of the transgenes among independent transformants is variable to the point where some live and some die there may be faulty expression in the surviving plants. It is known the 35S promoter is modular and the resulting transgene expression it provides could depend on insertion site and interaction with surrounding genomic elements. Thus, it appears that caution needs to be exercised in interpreting data from studies involving 35S overexpression of transporters in *Arabidopsis* and rice.

8.3 Final Remarks

A targeted molecular genetic approach was taken toward improving Na^+ exclusion and tolerance in rice. It was originally thought that specifically expressing a Na^+ influx transporter in the outer cells of the root would increase Na^+ influx from the soil to the root and this would increase Na^+ transport to the shoot and decrease Na+ tolerance. Expressing the same Na^+ transporter in the inner cells of the root was expected to increase Na^+-retrieval from the xylem, which would result in less Na+ reaching the shoot and an increase in Na^+ tolerance. Unexpectedly, the results were the complete reverse of the original hypothesis. This does not discount the validity of the approach, in fact, its usefulness was demonstrated by the development of rice lines with improved Na^+ exclusion and tolerance. However, it does clearly indicate that a

better understanding of the physiological elements involved in Na^+ transport in rice is required to underpin further efforts to improve Na^+ tolerance in rice.